INFORMATION TO USERS

This manuscript has been reproduced from the microfilm master. UMI films the text directly from the original or copy submitted. Thus, some thesis and dissertation copies are in typewriter face, while others may be from any type of computer printer.

The quality of this reproduction is dependent upon the quality of the copy submitted. Broken or indistinct print, colored or poor quality illustrations and photographs, print bleedthrough, substandard margins, and improper alignment can adversely affect reproduction.

In the unlikely event that the author did not send UMI a complete manuscript and there are missing pages, these will be noted. Also, if unauthorized copyright material had to be removed, a note will indicate the deletion.

Oversize materials (e.g., maps, drawings, charts) are reproduced by sectioning the original, beginning at the upper left-hand corner and continuing from left to right in equal sections with small overlaps. Each original is also photographed in one exposure and is included in reduced form at the back of the book.

Photographs included in the original manuscript have been reproduced xerographically in this copy. Higher quality 6" x 9" black and white photographic prints are available for any photographs or illustrations appearing in this copy for an additional charge. Contact UMI directly to order.

THE FLORIDA STATE UNIVERSITY

COLLEGE OF ARTS AND SCIENCES

VARIATIONAL ASSIMILATION OF ACOUSTIC TOMOGRAPHY

By

MING LIU

A Dissertation submitted to the
Department of Oceanography
in partial fulfillment of the
requirements for the degree of
Doctor of Philosophy

Degree Awarded:
Summer Semester, 1995

UMI Number: 9540056
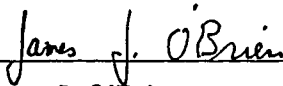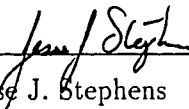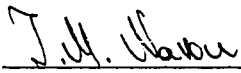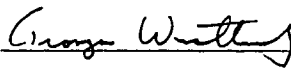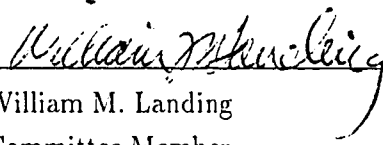
The members of the Committee approve the dissertation of Ming Liu defended on April 21, 1995.

James J. O'Brien
Professor Directing dissertation

Jesse J. Stephens
Outside Committee Member

Ionel M. Navon
Committee Member

Georges L. Weatherly
Committee Member

William M. Landing
Committee Member

ACKNOWLEDGEMENTS

It is with the deepest affection that I thank my wife, Zhenghong, for her many sacrifices, so much patience, so much support and so much love. To her I owe the greatest amount of love. I could never thank enough my father and brother for their love and encouragement. My thanks to my best friend Dr. Jiayan Yang for his friendship over ten years. Without his suggestion, my study at FSU would not have happened. Finally, I dedicate this dissertation to my late mother with all my love and wish that she could see his son with a doctoral degree.

CONTENTS

LIST OF FIGURES

ABSTRACT

For the first time an ocean model is used to assimilate oceanic tomography data in an upper ocean model of the northeast Pacific with the goal of estimating the time independent density field, and thus the slow manifold circulation structure.

The assimilation procedure works by minimizing the cost function, which generalizes the misfit between the observations and their model counterparts, in a least-squares sense, plus a penalty term. This minimization is done consistently with the constraint that the model dynamics must be exactly satisfied. The model consists of integrating the model equations forward in time over the period which data are going to be assimilated. Data misfits between the model and the observation are then calculated and the adjoint equations of the model are integrated backward using the data misfits as forcing. It is necessary to determine the gradient of the cost function with respect to the control variables (the density field). The gradient is found using the model and adjoint variables and it is used in a minimization algorithm to determine a new density field. The minimization procedure utilizes a limited memory quasi-Newton method.

The results indicate that the assimilation procedure works very well. For the twin experiments, the final estimated density recovers the Levitus density field as expected and as fast as in 10 iterations. For the experiments with the Navy layered ocean circulation model (NRLM) output, the density can be estimated through the assimilation procedures. The estimated density field improves the the Levitus climatological density data which are biased and makes the subtropical gyre stronger in the northeast Pacific region.

The proof of the identity between the discretization of the continuous adjoint equations and the adjoint equations which are from discretized model equations with the Arakawa C has been carried out.

1. INTRODUCTION

1.1 Overview of Oceanic Data Assimilation

The immensity and geometrical shape of the ocean, combined with difficulties of observation, make measurements of the ocean both expensive and a formidable technical challenge. As a result, not only are oceanic data relatively more sparse than atmospheric data, they are nonuniform. Satellites provide good coverage of the ocean surface and provide data such as sea surface temperature (SST) and sea surface height (SSH), but collection of these data was begun recently to establish climatic trends. Even much less is known about conditions below the surface. In the past, most of the oceanic data have been collected along ship tracks, from moorings, or from drifting buoys. Since the oceanic data were sparse in space and time, as well as inaccurate, or the sampling was not suited for determining oceanic variability of such phenomena as ocean currents,temperature and density, it has been exceedingly difficult to conduct so-called objective analyses which refers to procedures that are robust enough to work without human intervention and without consuming an inordinate amount of computer time (Daley, 1991 and Thiebaux, 1987).

Nevertheless, the body of data available does contain some information about the climatology of ocean. To make use of this information, there is a need to extract the maximum amount of information from a measurement and to combine it with the time evolution of the data analysis system based on past observations. In addition to observations, the laws of physics provide a basis for numerical models used to simulate the ocean circulation. Such numerical models can be useful tools for providing the dynamic predications and carrying temporal information forward.

1

Those ocean models can play on important role in reconstructing a realistic picture of ocean circulation. The technique for extracting and filtering the information from data has become known as data assimilation. Data assimilation provides an output analysis which is better than the model alone or just an analysis using the data. In addition, data assimilation is one way to test and, improve a model. Like other fields of physical oceanography, oceanic data assimilation has been greatly influenced by the work of meteorologists. There has been extensive development of data assimilation methods in meteorology and increasing application of those in oceanography. The methods of data assimilation are now comprehensively described by Ghil and Malanotte-Rizzoli (1991) and Daley (1991). More recently, Bennett (1992) has summarized the rapid development of inverse methods and data assimilation in physical oceanography over the last decade. The methods of data assimilation will be discussed in the next section and in chapter 2 in more detail.

1.2 Ocean Circulation and Modeling

There is both observational evidence and theoretical confirmation that the time-mean, direct wind-driven circulation over most of the ocean is restricted to the mixed layer and the upper thermocline of the oceans. However, since density surfaces in the oceans come in contact with the atmosphere somewhere on the globe, the density of the ocean water and stratification are determined by air-sea interaction processes. The deep circulation is forced by either the time-dependent eddy mixing processes that receive their energy from the time-mean wind driven circulation by the effects of the deep convections that are forced by the combined effects of intensive buoyancy loss and wind mixing in the surface layers when the thermocline is eroded.

Although modeling global ocean and climate will undoubtedly require sophisticated ocean models, physical intuition about the ocean circulation may be gained from simpler models. Consider the classical example of a homogeneous ocean

($\rho = \rho_o = constant$) of uniform depth H driven at its surface by wind stress. In this idealized setting, after appropriate simplification of the equations of motion, the steady response of the ocean to the applied stress can be determined directly.

The development of increasingly sophisticated and efficient models is a great challenge; however, it may not be the single greatest constraint on future progress. In order to be able to apply and validate the increasingly realistic models of the future, an increasingly comprehensive observational description of the ocean circulation itself, including its variability, and the exchange of momentum with the atmosphere will be required. This will remain a problem for oceanographers, as already noted above for the following reasons. First, data sets are difficult to collect and are sparse and inhomogeneous. Furthermore, the great bulk of the ocean will continue to be incompletely (even poorly) observed, unless efficient acoustic means of observing the oceanic interior can be developed (Munk and Forbes 1989, see the next section).

One idea which is being intensively explored in regional and basin-scale ocean models, and which may ultimately prove practical for application to global models as well, is the application of optimal and suboptimal methods for combinations of prognostic model-data synthesis. Several alternative approaches are under evaluation. One family of approaches, broadly practiced in meteorology, is the systematic combination of dynamical (usually model-produced) and observational information to produce increasingly accurate representations (usually predictions) of large and meso-scale motions (Ghil and Malonotte-Rizzoli 1991). Assimilative techniques from the atmospheric sciences, appropriately adapted for the ocean case, are being used with simulated data to explore the impact of assimilation on steady and transient ocean response. Of particular interest is the determination of which space/time scales of oceanic motion are effectively "constrained" by assimilation of different kinds of data.

Another approach that is complementary to the combined analysis of oceanic models and observations is the formulation of an optimal control or inverse problem. Formulated in this way, poorly-known model parameters, along with some estimate of how well their values are constrained by the data, can be explicitly calculated. The computational requirements associated with the optimal control approach can be severe and expensive. Nonetheless, efficient implementations of the optimization approach are possible (e.g., based on adjoint equation techniques). Applied to simple ocean models, the resulting formulation allows the optimal estimation of parameters, such as the bottom friction and forcing functions such as the wind stress, and provides a particularly attractive approach (Yu and O'Brien, 1991).

1.3   Acoustic Monitoring of Global Ocean Climate

The oceans play a major role in the dynamics of climate through their large capacity for the transport and storage of heat, moisture, and CO_2. The oceans are driven by the atmosphere, and their response to changes in atmospheric forcing represents one of the most important couplings within the complex system of climate feedbacks. The ocean-atmosphere coupling has a strong impact both on the response characteristics of the climate system of external forcing and on internal natural climatic variability.

Detecting climate changes expected as a consequence of the increase of atmospheric greenhouse gases has become increasingly important. Several attempts have been made to analyze historical data records and to compare them with the expected signal in both ocean surface and air temperature and ocean hydrographic data. Munk and Forbes (1989) have proposed measuring the changes in travel times of long-distance acoustic transmissions from Heard Island in the southern Indian Ocean to receivers scattered around other ocean basins. The change in travel times

over a period years would be used as a climate change detection strategy since they are primarily a measure of the average temperature change along the acoustic ray paths. The "acoustic thermometer" (Spiesberger, 1983) has the advantage of producing integrated quantities, which significantly reduce the noise level from measurement at individual locations and , thus, minimize the higher-frequency noise problems. Spiesberger and Metzger (1991) have demonstrated the practical feasibility of this method across the basin scale (3000 km).

1.4 Thermohaline Circulation

The oceans carry heat from the tropics to polar latitudes and carry cold water from the poles towards the equator. The details of these transport processes, which are restricted to certain depth ranges, are hidden in the Sverdrup circulation. They have to be resolved if the ocean's role in climate variability and climate change is to be understood.

It is known that the ocean carries about as much heat towards the poles as the atmosphere does, but since its time scales are so much larger, the ocean has a larger capacity to act as a damping mechanism for rapid fluctuations in our climate. Conversely, much of the long-term variability of the climate may be related to the ocean as it slowly releases heat stored from earlier rapid climate changes.

The radiative heating of the atmosphere causes motion because it leads to density differences. Perhaps this can be said in a less tutorial manner; also, it is customary to define symbols as they are used, e.g. $g\rho$ that are important. These density changes are proportional to the depths of the ocean by turbulent diffusion, subduction, and convective mixing. As a result of this, a pressure field and associated thermohaline circulation develops in the world ocean.

The quantity $-g\rho$ is called the buoyancy, the minus sign being used because a particle is said to be the more buoyant when it has less weight. The ocean moves

because of buoyancy contrasts, but these are due to differences in temperature and salinity. These differences are created by the fluxes of heat and water at the ocean surface. For example, evaporation decreases buoyancy in two ways: by cooling and by increasing salinity. Temperature differences generally make greater contributions to density differences than salinity differences in the ocean. The circulation that is driven by the buoyancy flux is called the thermohaline circulation. The complete ocean circulation consists of both wind-driven circulation and thermohaline circulation.

The thermohaline forcing, like the mechanical wind-driven ones, is external, but the pressure field formed by these factors is internal. The largest contribution to the development of thermohaline circulation is due to thermal processes; the heating and cooling of ocean waters.

The general circulation of the world ocean, especially below the surface layer, is intimately linked with the distribution of oceanographic characteristics such as density, temperature, etc.. These characteristics have long been used as indicators, or tracers of motion, although they show only the qualitative aspect of the circulation. This is because the world ocean is filled with inhomogeneous waters whose characteristics vary continuously within the world ocean. On the other hand, the distribution of these characteristics is rather regular and is mainly the result of advection and diffusion of the properties. Thus, by fixing the water characteristics at the source of water masses formation and tracing changes in these characteristics in space, objective qualitative conclusions can be drawn about the spread of these water masses.

An interesting feature of a surface-driven thermohaline circulation is the extreme asymmetry between rising and sinking regions. Whenever conditions produce surface water dense enough to sink to the bottom, it does so and spreads over the bottom.

Thermohaline circulation and its role in the general dynamics of currents were investigated at the early stages of development of oceanography. The following question was energetically posed at the time: What type of circulation, wind-driven or thermohaline, plays the dominant role in the total circulation? Now, it is known that both types are important and that they are related to each other. This makes the analysis of ocean currents more complicated that that of atmospheric motions.

The observed effects of thermohaline forcing (which directly governs the density of the ocean waters) and mechanical forcing lead to formation of the resultant field of density of the world ocean. The density field, thus formed, determines the pressure field. However, it is impossible to divide the ocean circulation into wind-driven and thermohaline since the motion components are generated by different, but interdependent, factors. The resultant currents cannot be represented by a simple linear superposition of thermohaline and wind-driven currents even if they could be separately determined by some method. The interaction of wind-driven and thermohaline forcing in the generation and maintenance of the ocean currents has not been investigated sufficiently.

1.5 Objectives

In considering the thermohaline circulation, it is natural that the advection of heat and salt by the circulation or their combined effect, density changes, is central to the problem and cannot be neglected. Therefore, the model used must be sophisticated enough to account for active thermodynamics and the salinity structure. Examples of this are the Ocean General Circulation Model (OGCM) and the U.S. Navy layered ocean model for which tremendous computational effort and hence huge quantities of supercomputer time are needed. An alternative way to study the thermohaline structure is as follows:

Formulate and modify a model from a nonlinear, reduced gravity model which has been used successfully to study two preferential cyclonic ocean eddy generation sites along the California coasts (Liu and O'Brien, 1995) and to investigate the variations in the thermocline depth of the northeast Pacific ocean during 1970-1989 (Meyers *et al.* 1995). In contrast with the models which assume a constant density in a layer, horizontal variations in the upper layer density are considered. This assumption instantaneously leads to the thermohaline forcing which is not included in the above mentioned models. On the other hand, oceanic tomography data imply both wind-driven and thermohaline information. In this study, an effort is made to develop a method to estimate the density field as well as the thermohaline structure in the upper Northeast Pacific ocean, from a simple model associated with acoustic tomography data, using variational data assimilation.

2. DATA ASSIMILATION

With respect to the problem of assimilating observations into numerical ocean models, a variety of different methods already exist, most of them originally developed in meteorology. An extensive review of these methods can be found in Ghil and Malanotte-Rizzoli (1991) and Le Dimet and Navon (1988). Data assimilation methods can be classified as (a) function fitting methods (b) statistical interpolation methods (c) nudging data assimilation and (d) variational (adjoint) methods. The latter method is described in detail in the following section, but first, the other methods are introduced.

In function fitting methods (a), which are the early data assimilation methods, the idea is to expand the data misfit in terms of some interpolating functions. The observations and the first-guess are weighted with prescribed weights that decrease with distance from the observation (Bergthorsson and Doos, 1955). Cressman filters are a commonly used meteorological assimilation technique. Neither knowledge of the statistical property of the data nor a numerical model is used. Comprehensive studies of these methods, together with their historical perspective, are provided by Thiebaux and Pedder (1987), and Daley (1991).

The statistical interpolation methods in (b) include both optimal interpolation (OI) methods and Kalman filter methods. The OI methods, which combine the model field and the observed data to estimate the correct field in a way consistent with the estimated accuracy of each of the two, are the most commonly used methods in major forecasting centers. The OI scheme requires knowledge of spatial error covariances for the model field and the observations. since the weights needed to minimize analysis error depend on these covariances (Gandin 1963; Lorenc 1981. 1986).

The Kalman filter represents a sequential assimilation procedure. It is based on the statistical concept of optimal interpolation. That is, at each observation time, the Kalman filter (Kalman 1960, 1961) optimally interpolates between the model forecast and the observations to obtain a new state vector with reduced error covariance. This state is subsequently used as the initial state for the model to compute a forecast for the next observation time. By repeating this assimilation cycle and keeping track of the error covariance of the model state in a sequential manner, the model absorbs the information of the sequence of observations step-by-step (Cohn, 1982; Ghil et al., 1981). The crucial point is that for this technique to be optimal, the time evolution of the covariance matrix of the model errors must be computed. Neither the forecast error covariance matrix nor the observation error covariance matrix are known. It is the corresponding computational cost which, for present purposes, rules out the use of the Kalman filter.

In (c), nudging data assimilation (NDA) (Anthes 1974), which is called optimal nudging data assimilation in the work of Zou *et al.* (1992c) and Wang (1993) combines the aforementioned data assimilation schemes in an efficient way. The original idea of optimal nudging data assimilation was put forward by Le Dimet. A parameter-estimation approach is used in the framework of the variational data assimilation algorithm to simultaneously determine the best initial conditions for numerical weather prediction (NWP) and optimal coefficients for the NDA scheme. The goal is to find the best initial conditions and optimal nudging coefficients which best assimilate the given observations.

2.1 Optimal Control: Theory and Application

The data assimilation problem can be stated in a general sense as the determination of the model evolution which is the closest solution to the observation. This is equivalent to looking for the parameters which optimally fit to the observation.

2.2 History and Background of Variational Calculus

The development of variational calculus in the seventeenth and eighteenth centuries was motivated by the need to find the minima or maxima of rapidly varying quantities. Many early applications of this calculus were to the problems of classical mechanics where they provide attractive alternatives to Leibniz and Newton. The appeal of variational procedures is that they consider a system as a whole and do not deal explicitly with the individual components of the system. Thus, it is possible to derive the behavior of a system without the details of all the interactions among its various subcomponents.

2.2.1 A formal definition of optimal control

A system which is defined by some variable X is conidered . The system also has some input described by a variable U. The output of the model, which can be observed, is defined by O. It is assumed that, once the input has been fixed, the state of the system is uniquely defined through a relation:

$$F(X, U) = 0 \qquad (2.1)$$

from which the output is given by another function

$$G(X, O) = 0 \qquad (2.2)$$

Therefore, O is an implicit function of U through X thanks to [Eq. (2.1)] and [Eq. (2.2)]. O_d is a given state belonging to the spaces of the model output, O. We may state the problem as follows:

How can U (the control variable) be acted on in such way that the resulting output O will be as close as possible to O_d, an estimation of the proximity between O and O_d as some cost functional J. The problem of optimal control is to determine the U^* leading to the best adjustment of a solution of the model to the observation. If such a controlled U^* exists, then it will said to be optimal.

In order to solve this problem, most of the time a scheme of the following form will be used:

- Frame the problem in an adequate mathematical context, especially if the state of the system belongs to an infinite dimensional space.

- Characterize the optimal control U^*.

- Derive numerical algorithms to implement the optimal control.

2.2.2 Variational method

As one of the most classic and elegant methods in physical and mathematical sciences and as a powerful tool of optimization and numerical analysis, variational calculus has been employed in many areas of the geosciences, including meteorology, oceanography, hydrology and geophysics within the last few decades to interpret and assimilate geophysical data and to simulate geophysical phenomena.

The theoretical aspect of variational calculus is comprehensively described in the book by Courant and Hilbert (1953) and in other mathematical physics books and it is not repeated here.

The variational approach consists minimizing the distance between a model solution and available data, usually to be distributed in space and time. The measure of the distance is called the cost function. Sasaki (1969, 1970a, b) first introduced a number of variational techniques whereby the imposed constraints are satisfied only approximately, not exactly. In particular, a cost function can be defined so that the solution does not have to obey the dynamics of the model exactly by adding a term that measures the model error as in the representer method (Bennett, 1992). The minimization of the cost function gives rise to the weak constraint minimization problem. When the solution is required to satisfy the model exactly, it is referred to as strong constraint minimization. By integrating a nonlinear model forward

in time, followed by a backward integration of an (non-homogeneous) adjoint linearized system forced by the observations, the cost function can be reduced. By defining the cost function as an inner product, Lions (1971) showed that the result of the backward integration of the adjoint model to initial time, is the gradient of the cost function with respect to the control variables, e.g. the initial conditions in his case. He also pointed out that a descent method can be used to iterate toward the minimum of the cost function.

The first application of variational methods in meteorology was pioneered by Sasaki (1955, 1958). Stephens (1966, 1968), Sasaki (1969, 1970a, 1970b, 1970c) and others have given a great impetus towards the development of variational methods in meteorology.

In the strong constraint case, control theory has been used to develop a computationally efficient method called the adjoint method. Control theory is a branch of mathematics developed to solve optimization problems of functionals such as those arising from the variational formulation.

The optimal control methods may be mathematically described by

$$\min_{U} \ J(U) \tag{2.3}$$

$$F(U, X) = 0 \tag{2.4}$$

where $F(U, X)$ is the dynamical constraint; the cost function $J(U)$ is defined as

$$J(U) = \int_{\Sigma} W \| O(X) - O_d \|^2 d\Sigma \tag{2.5}$$

where X denotes the various prognostic fields, O the output, O_d the local observations of O over Σ. $O(X)$ in [Eq. (2.5)] is equivalent to the implicit function, $G(X, O) = 0$ in [Eq. (2.2)]

The classical variational approach of $\delta J = 0$ leads to the Euler-Lagrange equations which also depend on the constraint F(U,X) or the model equations. In a series

of basic papers Sasaki generalized the application of variational methods with either the strong or the weak constraint formalism in meteorology to include time variations and dynamical equations in order to filter high-frequency noise and to obtain dynamically acceptable initial values in data void areas. In all these applications, the Euler-Lagrange equations were used to calculate the optimal state. Stephens (1970) derived the general form of Euler-Lagrange equations with a coupled PDE system of a mixed type of well-posed initial-boundary value problems. There are also so-called Augmented Lagrangian methods which consider both a strong constraint and a weak one (Navon and de Villiers, 1983) to prevent numerical instabilities.

Variational data assimilation solves the Euler-Lagrange equations by directly minimizing a cost function measuring the misfit between the model solution and the observations with respect to the control variables.

It is well-known that solving the above constraint problem [Eq. (2.1) and Eq. (2.2)] is very difficult or sometimes impossible. Introducing an inner product $(.,.)$ compatible with the norm $\| . \|$ into the function space, one defines the Lagrangian functional (Le Dimet and Talagrand, 1986b)

$$L(U, \Lambda) = J(U) + (\Lambda, F(U, X)) \qquad (2.6)$$

where Λ is the Lagrangian multiplier. as the so-called the adjoint method, and reduces a constrained minimization problem to an unconstrained one. The advantage is that Euler-Lagrange equations can be solved numerically by classical descent algorithms which are a popular topic in the mathematical optimization literature.

2.3 Parameter Estimation

Parameter estimation is an aspect of data assimilation. It assimilates the observation into an atmospheric or oceanic model in order to obtain an estimate of a

designated model control parameter and, at the same time, to obtain an optimal state of the atmosphere or the ocean. This process is able to provide an exact consistency between the analysis and dynamics using various kinds of available data sets.

The unknown parameters of the model can be deduced simultaneously by minimizing a cost function that measures the distance between the model results and observation in which the model parameters are the control variables. The systematic application of the variational adjoint methods to parameter estimation problems in oceanography proceeded with O'Brien and his colleagues. For example, the barotropic gravity-wave speed in a two dimensional reduced-gravity, linear-transport model for the equatorial Pacific Ocean was used as a control variable (Smedstad and O'Brien, 1991). Recently, Kamachi and O'Brien (1995) used a similar model to assimilate the trajectories of drifting buoys. In the work of Panchang and O'Brien (1988), the friction coefficient for a one-dimension tidal-flow model was the parameter to be estimated from the observations. Yu and O'Brien (1991) sought to use measurements of the upper ocean currents to determine the eddy mixing coefficients in the Ekman layer together with the surface drag coefficient.

A general question with any kind of numerical modeling concerns the sensitivity of the results to the input parameters of the model. A numerical model can be described as a process which starts from a set of input parameters and produces a set of output parameters. In the case of meteorological or oceanic models, which integrate the equations governing the temporal evolution of ocean circulation, the input parameters could be the initial and boundary conditions which, in this study, is the upper layer density. The output parameters are the geofluid fields produced at successive times by the integration and also the various quantities which can be computed from these fields such as energy and potential vorticity.

The determination of the uncertainty of the model's output results from the uncertainty of the input. For instance, the uncertainty on the horizontal transport U, V and the upper layer thickness h is due to the uncertainty of the density which is the control variable in this study.

2.4   Uniqueness, Identifiablity, and Stability

It is widely recognized that, whereas there are situations in which the inverse problem defined below has no solution, there also are many circumstances under which a meaningful solution is possible, albeit in a limited sense. The important thing is to recognize the circumstances that may or may not allow solution of the problem and, if a solution is possible, to impose on it the proper limitations so as to make it mathematically well-posed and physically meaningful. Achieving this goal requires clear definitions of the terms uniqueness, identifiability, and stability. In addition, one must understand how each of these aspects affects the behavior of the inverse solution and how their adverse effects can be mitigated.

The inverse problem can be defined as follows: let a functional relationship, $X = F(\rho)$, be given between parameters ρ which in this case is the density field and X which represents the state variables of our problem, $(U, V, h)^T$. The inverse problem will be to determine the parameter ρ on the basis of X and the inverse relationship $\rho = R(X)$. The problem is said to be well-posed if (1) for every X there corresponds a solution ρ (*i.e.*, a solution exists); (2) the solution is unique for any given X; and (3) the solution depends continuously on X (*i.e.*, the solution is stable). If the inverse problem fails to satisfy one or more of these three requirements, it is said to be ill-posed.

Uniqueness can be defined in the following way. If $X_1 = F(\rho_1)$ and $X_2 = F(\rho_2)$ are two solutions of the inverse problem, then

$$\|X_1 - X_2\| = 0 \Leftrightarrow \|\rho_1 - \rho_2\| = 0 \qquad (2.7)$$

where $\| \cdot \|$ represents a norm over the appropriate space. In a practical problem, X is only given at discrete points in space and in time and R represents a minimization of a functional J as given in the previous subsection.

While uniqueness refers to the inverse problem, R, identifiability refers to the forward problem, F. If two sets of parameters lead to the same function X, the parameters are said to be unidentifiable. Uniqueness, on the other hand, is concerned with the problem whether different parameters may be found for a given X. If so, the parameters are non-unique.

Stability can be defined in the following way. For every $\epsilon \leq 0$ there exists a δ such that for $\rho_1 = R(X_1)$ and $\rho_2 = R(X_2)$ one has

$$\|X_1 - X_2\| < \delta \Leftrightarrow \|\rho_1 - \rho_2\| < \epsilon \tag{2.8}$$

[Eq. (2.8)] states that small errors in the variables must not lead to large changes in the computed parameters.

2.5 Adjoint Method

Adjoint equations, also called backward or top-down differentiation, are the tools of the theory of optimal control for solving a number of optimization and sensitivity problems which arise in the general context of numerical modeling of atmospheric and oceanic circulation. It has been developed in the last twenty years and generally deals with questions of how to "control" the input parameters of a numerical process in order to "optimize" its output parameters. The idea of applying adjoint equations to meteorological problems is by no means new and it was first suggested by J. Lions.

In many situations, one is led to consider a problem whose solution requires, in one form or another, the explicit determination of a number of output parameters with respect to a number of input parameters. Among such situations, we can mention the following ones in particular.

(1) One wants to solve an inverse problem, i.e. to determine values of the input parameters corresponding to given (e.g., observed) values of output parameters. Such inverse problems will normally be solved as an optimization problem, i.e. one which will determine the values of the input parameters which minimize a prescribed scalar function of the output parameter of the model (e.g., a function which measures the fit of the output parameter to observed quantities). A typical example of such an inverse problem is an assimilation of observations which will be described below.

(2) One wants to determine which of the input parameters was at the origin of some observed feature in the output parameters. A typical example might be a situation in which a numerical weather forecast has been erroneous in some respect and one wants to determine what, in the model physical parameters or in predicting the rapid deepening of a depression was the cause for the error.

In some situations, one will be interested in the sensitivities of a large number of output parameters with respect to a large number of input parameters such as the density field of the upper ocean of the northeast Pacific in this study. In situations where one wants to determine the gradient of one output parameter with respect to a large number of input parameters the method of adjoint equations is powerful.

2.6 Numerical Optimal Algorithms

The useful implementation of data assimilation depends crucially upon the fast convergence of a large-scale unconstrained minimization algorithm. The aim of the application of variational optimization for this study is to iteratively search for the set of the parameters that minimizes the cost function, using the knowledge of its gradient with respect to the control variable.

Since problems in oceanography often contain many degrees of freedom $O(10^6)$. Conjugate-Gradient (C-G) methods (Navon and Legler, 1987) and Limited Memory Quasi-Newton (LMQN) methods are the only ones under consideration due to the

fact that only information from the first few iterations can be saved due to huge memory requirements. For experience and details concerning various algorithms, see a recent review paper by Zou et al. (1993c).

Shanno and Phua (1980) proposed an extension of the (C-G) method which requires more vectors of storage and resembles a Quasi-Newton (QN) method and is a LMQN method. The LMQN method of Shanno and Phua is a two-step LMQN like the CG method which incorporates Beale restarts. Only seven vectors of storage are necessary.

LMQN algorithms use the following procedure for minimizing $J(X), X \in \Re^n$:

(1) Choose an initial guess X_0, and H_0, a symmetric and positive definite initial approximation to the inverse Hessian matrix (H_0 may be chosen as the unit matrix).

(2) Compute

$$g_0 = g(X_0) = \nabla J(X_0) \qquad (2.9)$$

and set

$$d_0 = -H_0 g_0 \qquad (2.10)$$

(3) For $k = 0, 1, \cdots, n + 1$, set

$$X_{k+1} = X_k + \alpha_k d_k \qquad (2.11)$$

where α_k is the step-size obtained by a line search to satisfy a sufficient decrease.

(4) Compute

$$g_{k+1} = \nabla J(X_{k+1}) \qquad (2.12)$$

(5) Check if a restart is needed (see the discussion below).

(6) Generate a new search direction, d_{k+1}, by setting

$$d_{k+1} = -H_{k+1} g_{k+1}, \qquad (2.13)$$

(7) Check for convergence: if

$$\|g_{k+1}\| \le \epsilon max\{1, \|X_{k+1}\|\} \qquad (2.14)$$

then stop, where $\epsilon = 10^{-5}$. Otherwise continue from step 3.

Step-sizes are obtained by using Davidon's (1959) cubic interpolation method to satisfy the following conditions of Wolfe (1968):

$$J(X_k + \alpha_k d_k) \leq J(X_k) + \beta' \alpha_k g_k^T d_k, \tag{2.15}$$

$$\left| \frac{\nabla J(X_k + \alpha_k d_k)^T d_k}{g_k^T d_k} \right| \leq \beta \tag{2.16}$$

where $\beta' = 0.0001$, and $\beta = 0.9$.

The following restart criterion is used:

$$|g_{k+1}^T g_k| \geq 0.2\|g_{k+1}\|^2. \tag{2.17}$$

The new search direction d_{k+1}, defined by Eq. (2.19), is obtained by setting (in the BFGS Q-N update of rank-2)

$$H_{k+1} = \hat{H}_k - \frac{p_k q_k^T \hat{H}_k + \hat{H}_k q_k p_k^T}{p_k^T q_k} + (1 + \frac{q_k^T \hat{H}_k q_k}{p_k^T q_k}) \frac{p_k p_k^T}{p_k^T q_k} \tag{2.18}$$

If a restart is required, Eq. (2.13) is changed to

$$d_{k+1} = -\hat{H}_k g_{k+1}, \tag{2.19}$$

where $p_k = X_{k+1} - X_k$ and $q_k = g_{k+1} - g_k$,

$$\hat{H}_k = \gamma_t(I - \frac{p_t q_t^T + q_t p_t^T}{p_t^T q_t} + \frac{q_t^T q_t}{p_t^T q_t} \frac{p_t p_t^T}{p_t^T q_t}) + \frac{p_t p_t^T}{p_t^T q_t} \tag{2.20}$$

Here the subscript t represents the last step of the previous cycle for which a line search was made. The parameter $\gamma_t = p_t^T q_t / q_t^T q_t$ is obtained by minimizing the condition number $H_t^{-1} H_{t+1}$.

Shanno and Phua's method implemented in CONMIN uses two pairs of vectors, q and p, to build its current approximation of the Hessian matrix. The advantage

of CONMIN is that it generates descent directions automatically without requiring exact line-searches as long as (q_k, p_k) are positive at each iteration. This can be ensured by satisfying Wolfe second condition in the line search. The CONMIN algorithm is globally convergent with inexact line searches on strong constraint problems.

3. ESTIMATION OF THE TIME INDEPENDENT DENSITY FIELD

IN THE UPPER NEP OCEAN

3.1 Oceanic Model

In this study, we use a nonlinear, reduced gravity model to simulate the northeast Pacific Ocean. Due to the large latitudinal extent, spherical coordinates are used with ϕ (longitude) increasing toward the east and θ (latitude) increasing toward the north. The domain for this model is as shown in Fig. 3.1. The actual configuration of the northeast Pacific Ocean and its topography used is from $18°N$ to $50°$ N and from the west coast of North America to $155°W$, the longitude of Hawaii, with $\frac{1}{12}°$ C-grid spacing in both horizontal directions. In the reduced gravity model driven by observational winds, the ocean is assumed to consist of two layers of slightly different density (ρ, ρ_2), with the interface as the thermocline. Similar models have been successfully used to simulate the ocean circulation of the northeast Pacific Ocean (e.g., Pares-Sierra and O'Brien, 1989; Johnson and O'Brien, 1989). After modifying the local phase speed and including the bottom topography in the above models, Liu and O'Brien (1995) studied the eddy formation sites and eddy migration in the same area. In another study with same model, Meyers (et al., 1995) investigated the interannal variations in the thermocline depth of the northeast Pacific ocean during 1970-1989.

The simple models for the wind-driven circulation described above assume that buoyancy variation plays little or only a passive role in the dynamics. This type of ocean model is quite successful in representing the basic pattern of the upper ocean circulation and provides the underpinning of much of the theory of the ocean

circulation. For climate applications, however, it is the spatial and temporal variations of the temperature and salinity distribution of the ocean and its capacity for heat storage and transport that are of primary concern. A fuller understanding of the wind and thermal forcings of the oceanic flows has gradually emerged only through a number of studies that either invoke some theoretical approximation to allow analytical solutions or utilize numerical methods.

It is difficult to determine the thermohaline driven circulation resulting from the joint effects of heat and salt on buoyancy and the reciprocal effects of the circulation on the distribution of water mass properties for several reasons. First and foremost is the essential nonlinearity of the system. In considering the thermohaline circulation, it is natural that the advection of heat and salt by the circulation or their combined effect, density, is central to the problem and cannot be neglected. Additional complications in modeling the thermohaline circulation arise from the nonlinear equation of the state of sea water and the presence of double-diffusive phenomena. Therefore, this requires that the model which is used would be sophisticated enough to account for active thermodynamics and the salinity structure. Examples of this are the Ocean General Circulation Model (OGCM) and the Navy layered ocean model for which tremendous effort and huge quantities of supercomputer time are needed. An alternative way to study the thermohaline structure is as follows:

We use mass continuity and the momentum equations as the the governing equations for the numerical model. In contrast with most layer models which assume a constant density in a layer, we allow horizontal variations in the upper layer density $[\rho = \rho(\phi, \theta)]$ which are treated as model parameters that can be estimated through tomographic assimilation using the variational adjoint method. This assumption instantaneously leads to the thermohaline forcing which is not included in the above mentioned models (the detailed derivation is in *Appendix A*).

The fluid is of the *Boussinesq* type, which allows the neglect of density variations in the momentum equations except when coupled with gravitational acceleration, and to assume the fluctuations in the density are the result of thermal effects (Spiegel and Veronis, 1960).

The variables $U = uh$ and $V = vh$ are the transports in the east and north directions, respectively, where $(u(\theta, \phi, t), v(\theta, \phi, t))$ are the depth-independent velocity components in the upper layer and $h(\theta, \phi, t)$ is the upper layer thickness (ULT).

The model equations are:

$$E_u = \frac{\partial U}{\partial t} + \frac{1}{a\cos\theta}\frac{\partial}{\partial \phi}\left(\frac{U^2}{h}\right) + \frac{1}{a}\frac{\partial}{\partial \theta}\left(\frac{UV}{h}\right) - \frac{2\tan\theta}{a}\left(\frac{UV}{h}\right) - 2\Omega\sin\theta V$$

$$-A\left[\Delta(U) + \frac{1 - \tan^2\theta}{a^2}U - \frac{2\tan\theta}{a^2\cos\theta}\frac{\partial V}{\partial \phi}\right]$$

$$-\frac{\tau^\phi}{\rho_o} + \frac{g}{2a\cos\theta\rho_o}\frac{\partial}{\partial \phi}\left[(\rho_2 - \rho_1(\phi,\theta))h^2\right] = 0 \tag{3.21}$$

$$E_v = \frac{\partial V}{\partial t} + \frac{1}{a\cos\theta}\frac{\partial}{\partial \phi}\left(\frac{UV}{h}\right) + \frac{1}{a}\frac{\partial}{\partial \theta}\left(\frac{V^2}{h}\right) + \frac{\tan\theta}{a}\left(\frac{U^2 - V^2}{h}\right) + 2\Omega\sin\theta U$$

$$-A\left[\Delta(V) + \frac{1 - \tan^2\theta}{a^2}V + \frac{2\tan\theta}{a^2\cos\theta}\frac{\partial U}{\partial \phi}\right]$$

$$-\frac{\tau^\theta}{\rho_o} + \frac{g}{2a\rho_o}\frac{\partial}{\partial \theta}\left[(\rho_2 - \rho_1(\phi,\theta))h^2\right] = 0 \tag{3.22}$$

$$E_h = \frac{\partial h}{\partial t} + \frac{1}{a\cos\theta}\left[\frac{\partial U}{\partial \phi} + \frac{\partial}{\partial \theta}(V\cos\theta)\right] = 0 \tag{3.23}$$

where

$$A\Delta(\cdot) = \frac{A}{a^2}\left(\frac{\partial^2}{\partial \theta^2} + \frac{1}{\cos^2\theta}\frac{\partial^2}{\partial \phi^2} - \tan\theta\frac{\partial}{\partial \theta}\right) \tag{3.24}$$

A is an eddy viscosity coefficient, a is the radius of the Earth, and Ω is the Earth's rotation rate. The wind stress is $\tau(\phi, \theta, t) = (\tau^\phi(\phi, \theta, t), \tau^\theta(\phi, \theta, t)) = C_d\rho_a\|\mathbf{u}_w\|\mathbf{u}_w$, where $\mathbf{u}_w(\phi, \theta, t)$ is the surface wind, C_d is a drag coefficient and ρ_a is the air density. Monthly average pseudo-stress was obtained from COADS monthly mean climatological winds and interpolated to the model grid. A linear temporal interpolation

was used between each monthly value. Define

$$c = g' \frac{(H - h)h}{H} \qquad (3.25)$$

where $H = H(\phi, \theta)$ is the total depth of the ocean and g' the reduced gravity which is equal to $g\Delta\rho/\rho_2$ (Liu and O'Brien, 1995). c is the local phase speed of the *baroclinic* mode.

The major physical features of this ocean model are:

- Reduced-gravity

- Linear as well as non-linear primitive equations

- Realistic spherical coordinates, including geometrical terms

- Irregular coastline and topographic geometry

3.2 Oceanic Tomography Data and Climate Modeling

It takes a research vessel roughly a month to map a 1000 by 1000 square km region with mesoscale resolution using conventional means such as CTDs and XBTs. Previous studies indicate that data from available hydrographic stations are insufficient for estimating the change in a large-scale temperature field.

However, it seems that oceanic acoustic tomography offers an alternative solution. Sound travels at about 1500m/s and is effectively transmitted through the oceans. Since the travel time of sound rays is a function of the ocean temperature, one has, in principle, a method of remotely observing the ocean. Ocean acoustic tomography was first proposed by Munk and Wunsch (1979) to apply geophysical inverse techniques to map temperature in the interior of the ocean from the travel

times of acoustic pulses measured between source and receivers below the ocean's surface.

Sound speed C in the ocean is controlled by density ρ which is a function of temperature Θ, salinity S and pressure P, but the dominant variable in the upper ocean is temperature. However, we use a layered model without salinity structure or thermodynamics and cannot directly yield an estimate of C. This handicap of the isopycnal model was addressed by Roed [personal communication, 1994], who provided a means to estimate variations in c as a function $C(H)$. The essence of his argument is reproduced below (also see Meyers et al. 1995).

Consider a tomography section of acoustic pulses between a source S and a receiver R. The velocity component of the current in the vertical plane along S - R is u. The acoustic ray i projected from S to R has a travel time,

$$
\begin{aligned}
T_i &= \int_i \frac{ds}{C+u} = \int_i \frac{ds}{C_o + \delta C + u} \\
&\approx \int_i \frac{ds}{C_o} - \int_i \frac{\delta C + u}{C_o^2} ds \\
&\approx \int_i \frac{ds}{C_o} - \int_i \frac{\delta C}{C_o^2} ds
\end{aligned}
\tag{3.26}
$$

The integral is along the geodesic acoustic path of ray i. The sound speed C in an instantaneous ocean realization is decomposed into an "unperturbed" sound speed C_o, the climatological sound speed profile characteristic of the region, plus a perturbation δC. Here $C_o \sim 1500 ms^{-1}$. Using a *Taylor* expansion, neglect $u/C_o^2 \ll \delta C/C_o^2$. The "unperturbed" travel time is

$$
T_{io} = \int_{\Gamma_{io}} \frac{ds}{C_o}
\tag{3.27}
$$

This is the travel time of the acoustic ray Γ_{io} when traversing the unperturbed, climatological ocean defined by C_o. By tracing the acoustic rays through C_o, T_{io} can be directly evaluated . Thus, the data used are the differential travel time

$$
T_i \approx T_{io} - \int_{\Gamma_i} \frac{\delta C}{C_o^2} ds
\tag{3.28}
$$

The above equation defines "density" tomography as being proportional to the sound-speed perturbation δC along the section which is proportional to the temperature perturbation. The data measured in the tomography experiment are the travel times of different acoustic rays reaching the receiver. The measured travel times are coupled to the reference travel times with the unperturbed ocean defined by C_o. For each ray the reference travel times are defined by [Eq. (3.27)].

Propagation of sound is due to the pressure differences in the incompressible media and the speed of sound in the sea water, C, is defined by the formula,

$$C^2 = \left(\frac{\partial P}{\partial \rho}\right)_A \tag{3.29}$$

where A indicates an adiabatic process, ρ density and P pressure. Thus, C depends on pressure p, temperature, Θ, and salinity S, viz., $C = C(p, \Theta, S)$ and may be written

$$C = C_o + \beta(\Theta - \Theta_o) + \gamma(p - p_o) + \kappa(S - S_o) + H.O.T. \tag{3.30}$$

where the subscript o denotes the corresponding reference state. It should also be noted that the first two terms are by far the most significant ones. A good approximation to C may be written as

$$C = C_o + \beta(\Theta - \Theta_o) \tag{3.31}$$

In the mid-latitude ocean, the density is commonly assumed to be a function of temperature to first order only, viz.

$$\rho = \rho_o - \alpha(\Theta - \Theta_o) \tag{3.32}$$

where α is an expansion coefficient.

However, use a layered model without thermodynamics which cannot directly give an estimate of travel time or sound speed. Therefore, have to find a means to estimate the travel time in terms of the model variables in order to construct the

data misfit to be minimized. The connection to the layered model is now introduced. There is evidence that in many regions of the ocean variations in the thermocline depth are related to variations in temperature, then density. In the context of a layered ocean, Roed [personal communication, 1994] finds the following relation between the upper layer thickness h and speed of sound [Eq. (3.23)]

$$\rho = \rho_o - \frac{\Delta\rho}{D}(h - h_o) \tag{3.33}$$

in which h_o is the reference upper layer thickness (ULT), $\Delta\rho = \rho_2 - \rho_o$, the density difference between the upper and lower layer, and D is a measure of the shape of the (vertical) density profile and is set to a constant 1000 m, though this value has no effect on the essential results.

Given that the choice of a reference state is arbitrary, [Eq. (3.33)] and [Eq. (3.32)] can be combined to give

$$\Theta = \Theta_o + \frac{\Delta\rho}{\alpha D}(h - h_o) \tag{3.34}$$

Further, invoking [Eq. (3.31)] gives finally

$$\begin{aligned}
\delta C &= C - C_o \\
&= \frac{\beta\Delta\rho}{\alpha D}(h - h_o) \tag{3.35}
\end{aligned}$$

In summary, the travel time at $t = t_j$, due to anomalies in ULT [Eq. (3.33)], is

$$\begin{aligned}
T_{i,j} &\approx T_{io} - \int_i \frac{\delta C}{C_o^2} ds \\
&= T_{io} - \frac{1}{C_o^2}\frac{\beta\Delta\rho}{\alpha D}\int_i (h - h_o)ds \\
&= T_{io} - C_T \int_i (h - h_o)ds \\
&= \int_i [\frac{T_{io}}{\Gamma i} - C_T(h - h_o)]ds \\
&= T_i[t_j] \tag{3.36}
\end{aligned}$$

where $C_T = \frac{1}{C_o^2}\frac{\beta\Delta\rho}{\alpha D}$, $\Gamma i = \int_i ds$, the arc length of the ray i, Σ_s indicates the space domain, as before.

Downwelling raises ocean temperature anomalies and increases δC, reducing $T_{i,j}$. The opposite effect occurs for upwelling. This dependence of temperature anomalies on thermocline depth variations is well known in the tropics where a strong permanent thermocline exists. It does not necessarily hold for SST anomalies in mid-latitudes where the seasonal thermocline cycle has a significant effect on SST.

Unfortunately there will be no ocean tomography data available until at least late 1995, but can use the so-called "*identical twin*" experiment and pseudo-tomographic experiments as an initial effort to solve this problem. The idea is the following:

(1) for the "*identical twin*" experiment, given a density distribution, ρ_o, such as climatologic data, run the model with ρ_o and produce the travel time "data" with [Eq. (3.36)], then start the initial density guesses, ρ obtained by adding ρ_o and a perturbed $\delta\rho$;

(2) for pseudo-tomographic experiments, the "travel time" is calculated with the outputs from the Navy layered ocean circulation model (additional details are provided in the next chapter), use the Levitus climatological density as the initial guess of control variables, the density field, instead of the perturbed density field in the case of the "twin experiments"

We carry out the minimization scheme; which will be described below, and anticipate that ρ_o can be successfully recovered in the "*identical twin*" experiments. The improved ρ can be estimated in the experiments with NRL model outputs.

3.3 Identical Twin Experiments

The assimilation procedure finds the solution to the model equations that best fit, in the generalized least-squares sense, all observations made within some specified space-time interval. The first kind of experiments are of the "identical twin" type:

synthetic data are generated by sampling the observable fields produced by a control run of the model, then the data are assimilated using the same model initiated with some error. The sequence of numerical experiments serves two purposes: (1) to demonstrate the performance of the assimilation procedure in the context of a full 3-dimensional, time-varying northeast Pacific ocean model and (2) to examine the utility of specified data sets, in particular, observations of tomography, in estimating the density field or thermohaline circulation structure of the northeast Pacific ocean.

A cost function must be defined which measures the distance between the observation and the corresponding model outputs in the frame work of optimal control method. In this study, the oceanic *tomography* data will be used. The density field $\rho(\phi, \theta)$ in the upper layer is treated as a model parameter, which will be determined by the variational data assimilation process. For an efficient implementation of such a method, it is necessary to determine the gradient of this cost function with respect to the control parameters, namely the density field. In terms of the language of optimal control theory, such parameter forms the control variable. This gradient can be determined in a computational efficient way by using the adjoint of the model.

The first step is to choose the cost function:

$$J(T, \rho) = \|T - T^o\|_T + \|\rho(\mathbf{x}) - \tilde{\rho}(\mathbf{x})\|_\rho \tag{3.37}$$

Two different sets of information are available for this use. The data are the travel time T^o which were produced by the model control run. Two different sets of information are available for this use. Second, the Levitus density $\tilde{\rho}$ is chosen as the "first guess". It is interesting to take into account the background as it allows an increase in the number of available pieces of information and, therefore, the number of equations to solve, without an increase in the number of unknown factors. Thus, it makes the optimization calculation more stable. Besides, taking into account the guess allows the use of a relaxation term toward the parameters. Therefore, it avoids

obtaining local parameters that would not be too different from what we want and would not be physically realistic.

3.4 Adjoint Model and the Variational Procedure

The cost function J (also see Eq. (2.5)) is taken to be

$$
\begin{aligned}
J(T,\rho) &= \frac{K_T}{2}\sum_i \int_0^\tau \left[(T_{i,j} - T_{i,j}^o)\right]^2 dt + \tau \int_{\Sigma_s} \frac{K_\rho}{2}[\rho(\mathbf{x}) - \tilde{\rho}(\mathbf{x})]^2 d\sigma \\
&= \frac{K_T}{2}\sum_i \int_0^\tau \left[\int_{\Sigma_s} \left(C_T(h - h_o) + [\frac{T_{i,j}^o - T_{io}}{\Gamma i}]\right) \Delta^i(\mathbf{x})d\sigma\right]^2 dt \\
&\quad + \tau \int_{\Sigma_s} \frac{K_\rho}{2}[\rho(\mathbf{x}) - \tilde{\rho}(\mathbf{x})]^2 d\sigma
\end{aligned}
\tag{3.38}
$$

where the subscript i denotes a section between the i th pair between a source and a receiver, the superscript 'o' the observed data, T_i^o corresponds to T_i [Eq. (3.36)] and T_{io} [Eq. (3.27)], and the tilde $\tilde{}$ is the estimated values. K_T is the inverse covariance matrix of the observational *rms* error. If the errors in the data are uncorrelated and equally weighted, K_ρ is the computational weight.

The momentum equations [Eq. (3.21) and Eq. (3.22)] and the conservation of mass [Eq. (3.23)], which are the strong constraints, can be enforced simultaneously by introducing the *Lagrange* multipliers. Referring to [Eq. (2.6) and Eq. (3.38)] this leads to the formulation of the associated Lagrange function:

$$
L(S,\Lambda,\rho) = J(T,\rho) + \int_\Sigma \Lambda^T E(S,\mathbf{x},t,\rho)d\sigma
\tag{3.39}
$$

where

$$
\begin{aligned}
S(\mathbf{x},t) &= (U,V,h)^T \\
\Lambda &= (\lambda_u, \lambda_v, \lambda_h)^T \\
E(S,\mathbf{x},t,\rho) &= (E_u, E_v, E_h)^T
\end{aligned}
$$

λ_u, λ_v, and λ_h are the *Lagrange* multipliers for the strong constraints, E_u, E_v and E_v respectively [Eq. (3.21), Eq. (3.22) and Eq. (3.23)].

The first variations of L [Eq. (3.39)] with respect to λs yield the original model equations [Eq. (3.21), Eq. (3.22) and Eq. (3.23)]. Letting the first variations of L [Eq. (3.39)] with respect to U, V, and h vanish, yields the adjoint equations

$$
\begin{aligned}
& -\frac{\partial \lambda_u}{\partial t} - \frac{1}{h}\left[\frac{2U}{a\cos\theta}\frac{\partial \lambda_u}{\partial \phi} + \frac{V}{a}\frac{\partial \lambda_u}{\partial \theta} + \frac{\tan\theta V}{a}\lambda_u \right. \\
& \left. -\frac{2\tan\theta U}{a}\lambda_v + \frac{V}{a\cos\theta}\frac{\partial \lambda_v}{\partial \phi}\right] + 2\Omega\sin\theta\lambda_v \\
& = \frac{1}{a\cos\theta}\frac{\partial \lambda_h}{\partial \phi} + A\left[\Delta(\lambda_u) + \frac{1-\tan^2\theta}{a^2}\lambda_u - \frac{2\tan\theta}{a^2\cos\theta}\frac{\partial \lambda_v}{\partial \phi}\right]
\end{aligned}
\tag{3.40}
$$

$$
\begin{aligned}
& -\frac{\partial \lambda_v}{\partial t} - \frac{1}{h}\left[\frac{U}{a\cos\theta}\frac{\partial \lambda_v}{\partial \phi} + \frac{2V}{a}\frac{\partial \lambda_v}{\partial \theta} + \frac{U}{a}\frac{\partial \lambda_u}{\partial \theta} + \frac{\tan\theta U}{a}\lambda_u\right] - 2\Omega\sin\theta\lambda_u \\
& = \frac{1}{a}\frac{\partial \lambda_h}{\partial \theta} + A\left[\Delta(\lambda_v) + \frac{1-\tan^2\theta}{a^2}\lambda_v + \frac{2\tan\theta}{a^2\cos\theta}\frac{\partial \lambda_u}{\partial \phi}\right]
\end{aligned}
\tag{3.41}
$$

$$
\begin{aligned}
& -\frac{\partial \lambda_h}{\partial t} + \frac{g(\rho_2 - \rho_1(\phi,\theta))h}{a\cos\theta\rho_o}\frac{\partial \lambda_u}{\partial \phi} + \frac{g(\rho_2 - \rho_1(\phi,\theta))h}{a\rho_o}\frac{\partial \lambda_v}{\partial \theta} \\
& +\frac{1}{ah^2}\left[\frac{U}{\cos\theta}\left(U\frac{\partial \lambda_u}{\partial \phi} + V\frac{\partial \lambda_v}{\partial \phi}\right) + V\left(U\frac{\partial \lambda_u}{\partial \theta} + V\frac{\partial \lambda_v}{\partial \theta}\right) + U\tan\theta\left(V\lambda_u - U\lambda_v\right)\right] \\
& = K_T C_T \sum_i \left[\left(C_T(h - h_o) + [\frac{T_i^o - T_{io}}{\Gamma i}]\right)\Delta^i(\mathbf{x})\right]
\end{aligned}
\tag{3.42}
$$

The details of the derivation of the [Eq. (3.40), Eq. (3.41), Eq. (3.42)] are given in Appendix B. Comparing [Eq. (3.21)], [Eq. (3.22)] and [Eq. (3.23)] with [Eq. (3.40)], [Eq. (3.41)] and [Eq. (3.42)] respectively, we find that the adjoint equations have similar forms to the corresponding model equations, except that the diffusion terms in the adjoint equations have signs opposite to those in the corresponding model equations and the adjoint equations correspond to evolution backward in time with forcing by the misfit of the model to the data. The *Lagrange* multipliers serve to collect information from the data and to propagate it back to the initial time.

After computing the integration of the model forward and the integration of the adjoint model backward in time, the gradient of cost function J with respect to the control variable ρ vanishes, and we have:

$$\nabla_\rho J = K_\rho[\rho(\mathbf{x}) - \tilde{\rho}(\mathbf{x})] + \frac{gh^2}{2a\cos\theta\rho_o}\left[\frac{\partial\lambda_u}{\partial\phi} + \frac{\partial}{\partial\theta}(\lambda_v\cos\theta)\right] \qquad (3.43)$$

The aim of the application of variational optimization for this study is to find the set of the parameters that minimizes the cost function, using availability of the gradient with respect to the control variable. For this study, an algorithm based on the two-step LMQN like the CG method is used. A detailed description of this algorithm is in 2.6 or can be found in Zou et al. (1993c). At each iteration computation of the gradient with respect to the control variable is required.

In order to obtain the optimal distribution of ρ, the model equations and corresponding adjoint equations can be performed iteratively with the descent algorithm which uses Eq. (3.43), by performing the following operations:

- The model "travel time" is computed with the Levitus climatological density $\rho_o(\mathbf{x})$.

- Choose $\rho_o(\mathbf{x}) + \delta\rho(\mathbf{x})$ as the initial density.

- Integrate the model equations forward in time from the initial density to obtain and store the outputs, $0 \leq t \leq \tau$.

- Integrate the adjoint equations backward from $t = \tau$ to $t = 0$ using the outputs stored in step 3, starting with the $\lambda s = 0$ at $t = \tau$.

- Check if the optimal solution has been found by satisfying an 'a priori' chosen convergence criterion. If not, compute a new distribution of ρ

which minimizes the the cost function by using LMQN. At last, $\rho_o(\mathbf{x})$ should be recovered.

3.5 Correctness for Discretization of the Continuous Adjoint Equations

One controversy has been around in the data assimilation community for a quite while. That is if you discretize the continuous adjoint equations, it only gives an approximation, which means the gradient of cost will be misleading. With a large amount of algebric effort, I have proven the identity between the discretization of the continuous adjoint equations and the adjoint equations which are derived from the discretized model equations with the Arakawa C grid scheme. This result is fundamentally important to this study. The details of the derivation are provided in Appendix C and D.
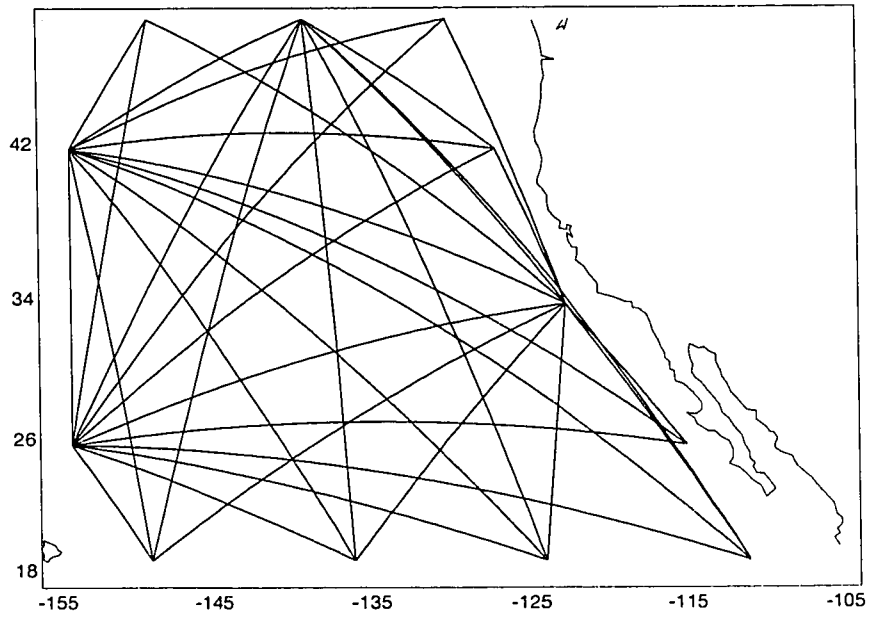
Figure 3.1: Model domain and the configuration of acoustic tomography

4. EXPERIMENTS AND DISCUSSIONS

4.1 Ocean Acoustic Tomographic Experiments

Ocean acoustic tomography was first proposed as a viable method to observe the ocean by Munk and Wunsch in 1979. The basic principle of acoustic tomography relies on the fact that the ocean is essentially transparent to acoustic radiation. That is, sound waves can travel very long distances in the ocean without substantial decay. Since the sound speed is dependent on density and pressure, distortions in the temperature, salinity, etc, are reflected as changes in the sound speed. Since the concept of acoustic tomography was proposed, some experiments by the Ocean Tomography Group (OTG) have been performed to assess its capabilities. These experiments have focused on the study of mesoscale variability in particularly well-observed areas of the ocean.

More recent experiments (Spiesberger and Metzger, 1991 and Global Acoustic Mapping of Ocean Temperatures (GAMOT)), have shown its capabilities with long-range networks of sources and receivers and have proved its potential for studying and monitoring mean properties of the gyre-scale and even global-scale circulation. They speculate that the variations in travel time are related to basin scale temperature changes occurring when El Nino (and similar) signals pass from the equator to higher latitudes as coastal Kelvin waves and radiate offshore as Rossby waves. Rossby waves modify the vertical distribution of temperature. Significant horizontal modifications in the thermal structure persist for several years as the waves propagate westward. Rossby waves are important for understanding the changes in acoustic travel time. A set of recent numerical model experiments (Shriver et al., 1991; Meyers et al., 1995; Liu and O'Brien, 1995) include the relevant physics.

36

Those model results explain most of the variability found in records of temperature measured at 300m across the eastern Pacific basin.

GAMOT's task is to determine whether these changes can account for the expected warming and travel time differences. As a part of the GAMOT task, this study is attempting to estimate the density field or thermohaline structure through tomographic data assimilation using the variational adjoint method.

4.2 Assimilation Experiments

In the last chapter, we described in some detail the construction of a nonlinear, reduced Northeast Pacific ocean model and a procedure for assimilating acoustic tomography data into that model. The development of the combined model and assimilation system was motivated by the need to establish the state of the Northeast Pacific and to forecast its evolution in time, a perceived prerequisite for estimating thermohaline structure. Numerical simulation offers the best hope for successful oceanic representation, but requires both a validated numerical model and relevant density field, and these requirements can, in turn, only be met by reference to acoustic tomographic observation. Unfortunately, no real tomography data are currently available, and it is important to be able to check the performance of the data assimilation algorithm. No test to check how well it performed was possible, but, consistent with the practice in meteorology, identical twin experiments and pseudo-tomographic assimilation experiments were conducted, and the "observations" were obtained from the models. The variational data assimilation procedure finds the solutions to the model equations that best fit, in the generalized least-squares sense, all "observations" made within some specified space-time interval (window of assimilations).

To examine the assimilation scheme, we have conducted a sequence of numerical experiments in which the tomographic "observations" are produced either from this

model or from the Navy layered ocean model. In each case, the data are extracted from a control run of this model, and successful results are measured by the extent to which the assimilation process is able to retrieve the control and to retrieve the control variables. For all experiments, we have assumed that wind stress is the COADS climatological wind stress for the twin experiments and the Hellerman-Rosenstein monthly wind-stress climatology for the NRL-model output assimilation experiments, known everywhere over the assimilation interval. Attention is then focused entirely on the effect of tomographic data on the recovery of the model state.

To maximize the conditioning of a simple inverse problem (Barth and Wunsch, 1990; Bennett, 1992), the configuration of acoustic paths is designed over the region (Fig. 3.1) for both types of experiments. Acoustic travel times are determined for various paths.

4.3   Identical Twin Experiments

The twin experiments are devised as follows. The model was run for a spin-up a period of 12 years with the COADS climatological wind stress and the Levitus upper ocean climatological density (Fig. 4.2a) being inserted. The model was essentially in a seasonal, periodic state at the end of this spin-up period and exhibited flow patterns that were similar in distribution and magnitude to those observed in the Northeast Pacific, such as the realistic subtropic gyre and California current, etc. (see Fig. 4.3). We then used the last year of this spin up period as a control run, extracting a general set of synthetic model "travel time" from this run. That is, the model "travel time"is calculated with [Eq. (3.36)] as the observation at three-hour intervals.

The sum (Fig. 4.5a) of the perturbed density anomaly field (Fig. 4.2b) and the Levitus density field are then used as the initial guess of control variables, i.e..

the density field. The time-length of the assimilation window is 3 hours which, in turn, involves 18 time steps of 10 minutes each. The model equations are integrated forward in time with the perturbed density and the wind mentioned above. The U, V and h fields are saved only once a day for the whole domain because of the huge memory required. A linear temporal interpolation was used between each day value for the adjoint-variable and the gradient of the cost function calculation.

The adjoint model equations [Eq. (3.40), Eq. (3.41) and Eq. (3.42)] are forced by the difference between the model "travel time" and its model counterpart (or the data misfit) and integrated backward in time, using the outputs stored above starting with the $\lambda s = 0$ at $t = \tau$. The time step in the adjoint model is the same as in the forward model, 10 minutes. Similarly, the λ_u, λ_v and λ_h fields are saved every day. h, λ_u and λ_v are used when the gradient of L with respect to ρ is calculated by [Eq. (3.43)] at each iteration by solving the adjoint model equations [Eq. (3.40), Eq. (3.41) and Eq. (3.42)]. These equations, derived from those defining the reduced ocean model itself, propagate the influence of the model/data misfits for any given model state backward from the time of the latest observation to the initial time of the model run and yield the desired cost function gradient. The adjoint model is similar in size and complexity to the ocean model itself and requires about the same computing effort to solve. One iteration of the data assimilation procedure involves, at minimum, one forward run of the ocean model from current initial conditions, to establish the current cost function gradient.

The variation data assimilation with the penalty term is implemented by starting from a model ocean with a perturbed density field and minimizing the cost function defined in [Eq. (3.38)]. When a prescribed convergence criterion is met, the minimization process was stopped. In all the experiments, we employed the CONMIN, a limited memory quasi-Newton method (the details are in Chapter 2). We expect that ρ_o can be finally recovered.

The results of the iterative process are shown in Fig. 4.4a and Fig. 4.4b. The iteration procedure converges rapidly (Fig. 4.5b - Fig. 4.8b), only requiring about 9 iterations to recover the Levitus density field (Fig. 4.9b). This is indicated by the rapid reduction in the cost function. The evolution of the cost function, normalized by that of the first iteration during the iterative process, is shown in Fig. 4.4 a. There is rapid decrease during the first 3 iterations. The values do not decrease much during the next couple of iterations. Then, they drop very fast and converge during the final 3 iterations. In Fig. 4.4 b, the normalized value of the gradient of the cost function is shown. The gradient also experiences a rapid decrease at the beginning and the ending, just as the cost function itself.

4.4 Pseudo-Tomography Assimilation Experiments

The Navy layered ocean circulation model (NRLM) is assumed to represent the ocean. The model has the following features: (1) 6 vertical layers with free surfaces, (2) nonlinear primitive equations, (3) hydrodynamic, i.e., isopycnal, (4) semi-implicit time difference scheme, and (5) Full-scale bottom topography in lowest layer and arbitrary coastline geometry. The horizontal resolution is 0.125^o by 0.176^o (latitude, longitude) for each variable or about 15 km at mid latitudes.

The pseudo-tomographic measurements were taken from NRLM model outputs. Starting from rest, the NRLM was spun up to statistical equilibrium at 1/4 degree resolution using the Hellerman-Rosenstein monthly wind-stress climatology, and then continued another 15 years at 1/8 degree resolution. Fig. 4.10 shows the basic features of upper ocean circulation in the Northeast Pacific. The subtropical gyre and the California current are clearly evident. The NRLM outputs of a 3 day average were interpolated to the model grid. A linear temporal interpolation was used between 3-day values.

Only take the sum of heights of layer 1 and layer 2 from NRLM as the counterpart of the upper layer thickness of the reduced gravity. Similarl to the "twin experiments", pseudo-tomographic "travel time" is calculated with [Eq. (3.36)] as the "observation" at three-hour intervals. Only use the Levitus climatological density as the initial guess of the control variable, where the density field is used instead of the perturbed density field in the case of the "twin experiments". All the other assimilation procedures are similar to those used in the "twin experiments" except that the penalty term in [Eq. (3.38)] is weighted inversely proportional to the square of the number of iteration. We anticipate that ρ_o, can be estimated through the assimilation procedures.

The results of the iterative process are shown in Fig. 4.11a and Fig. 4.11b. The iteration procedure converges rapidly (Fig. 4.12 - Fig. 4.16), only requiring about 10 iterations to achieve a decrease of 4 orders of magnitude and to reach the final density field (Fig. 4.16b) which improves the initial guess, the Levitus density field (Fig. 4.2a or Fig. 4.9b). The 3-D density surface is very rough during beginning iterations, especially along the ray paths (see Fig. 3.1). The reason is the ray paths are covered where the data misfits are located. Those disturbances propagate westward as the number of iteration increases and finally exit out of the domain. The entire procedure is also characterized by a rapid reduction in the cost function which was close to zero after 10 iterations, but never attain zero because the "observation" was from the NRLM. In Fig. 4.11 b, the normalized value of the gradient of the cost function is shown. The gradient behaves differently from that in the "twin experiment". It increases during the first 5 iterations prior to dropping very rapidly to zero.

The density field can be estimated by using NRLM output assimilation and improving the Levitus density by checking the difference between them (Fig. 4.17). The estimated density field (Fig. 4.16b) decreases the Levitus density by approx-

imately 0.3 $kg\ m^{-3}$. Their differences creat the meridional density shear which is about 0.1 $kg\ m^{-3}$ over 20 degrees of latitude (Fig. 4.17a). The shear can produce additional eastward transport of about $2 - 5$ Sverdrups and enhance subtropical gyre. The above is as expected. The reason for the enhanced transport is that the Levitus climatological density field is calculated with historical hydrographic data, obtained from various cruises which are biased due to the fact that the data were not uniformly distributed in time and space (i.e. lack of data during winters). As we know, the purely thermal circulation in the upper ocean is represented by a single large anticyclonic gyre with a typical westward displacement of the center. Therefore, it is natural that the estimated density makes the subtropical gyre stronger in the northeast Pacific region.

Both assimilation procedures find that solution to the model equations is best fits, in the generalized least-squares sense. All experiments are of the "identical twin" and pseudo-tomographic assimilation types; synthetic data are generated by sampling the observable fields produced by control runs of the models; then the data are assimilated using the same model. The sequence of numerical experiments serves two purposes: to demonstrate the performance of the assimilation procedure in the context of a fully-nonlinear, time-varying, reduced-gravity ocean model; and to examine the utility of data sets, in particular, observations of tomography, in estimating the density field or thermohaline circulation structure of the northeast Pacific ocean. The results indicate that the assimilation procedure works very well.

Finally, the data assimilation scheme demonstrated here seems to offer a powerful tool for analyzing a large, complex, tomography data set.
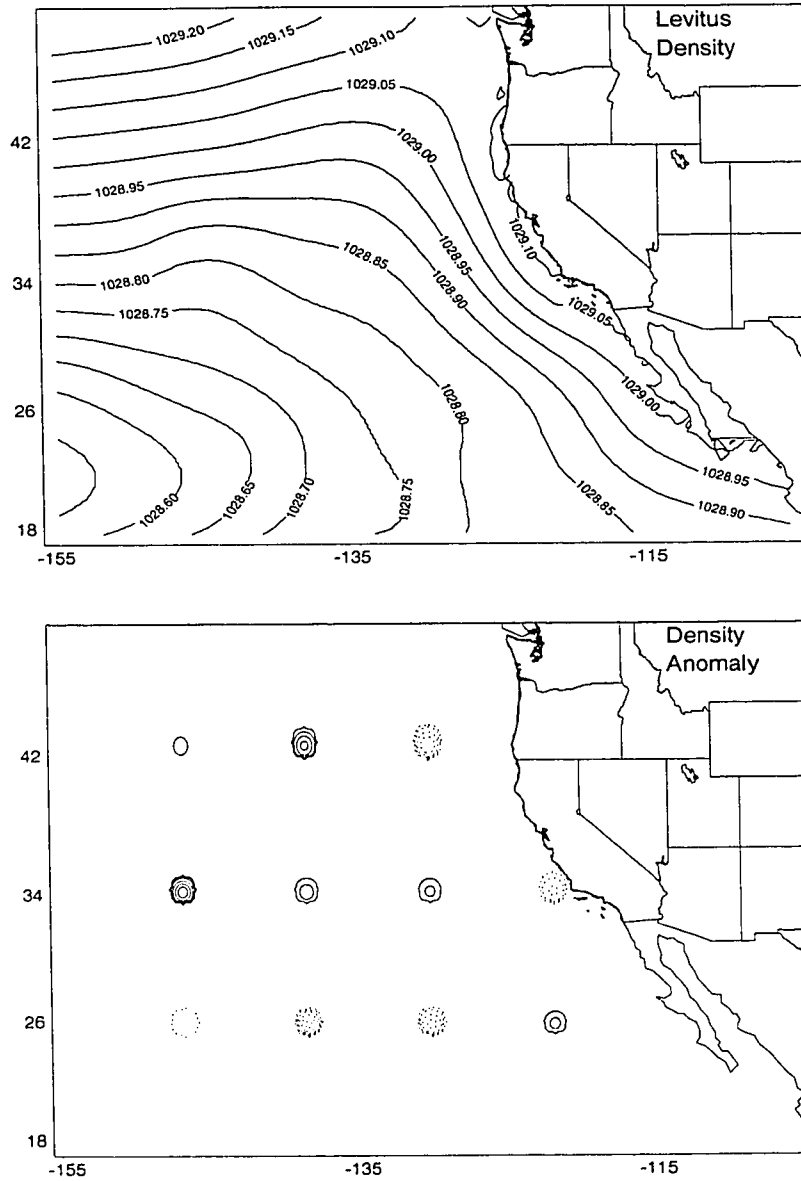
Figure 4.2: (a) The climatological Levitus density field. (b) The perturbed density anomaly field. Contour interval is 0.01 kg/m³ and dashed lines indicate negative values.
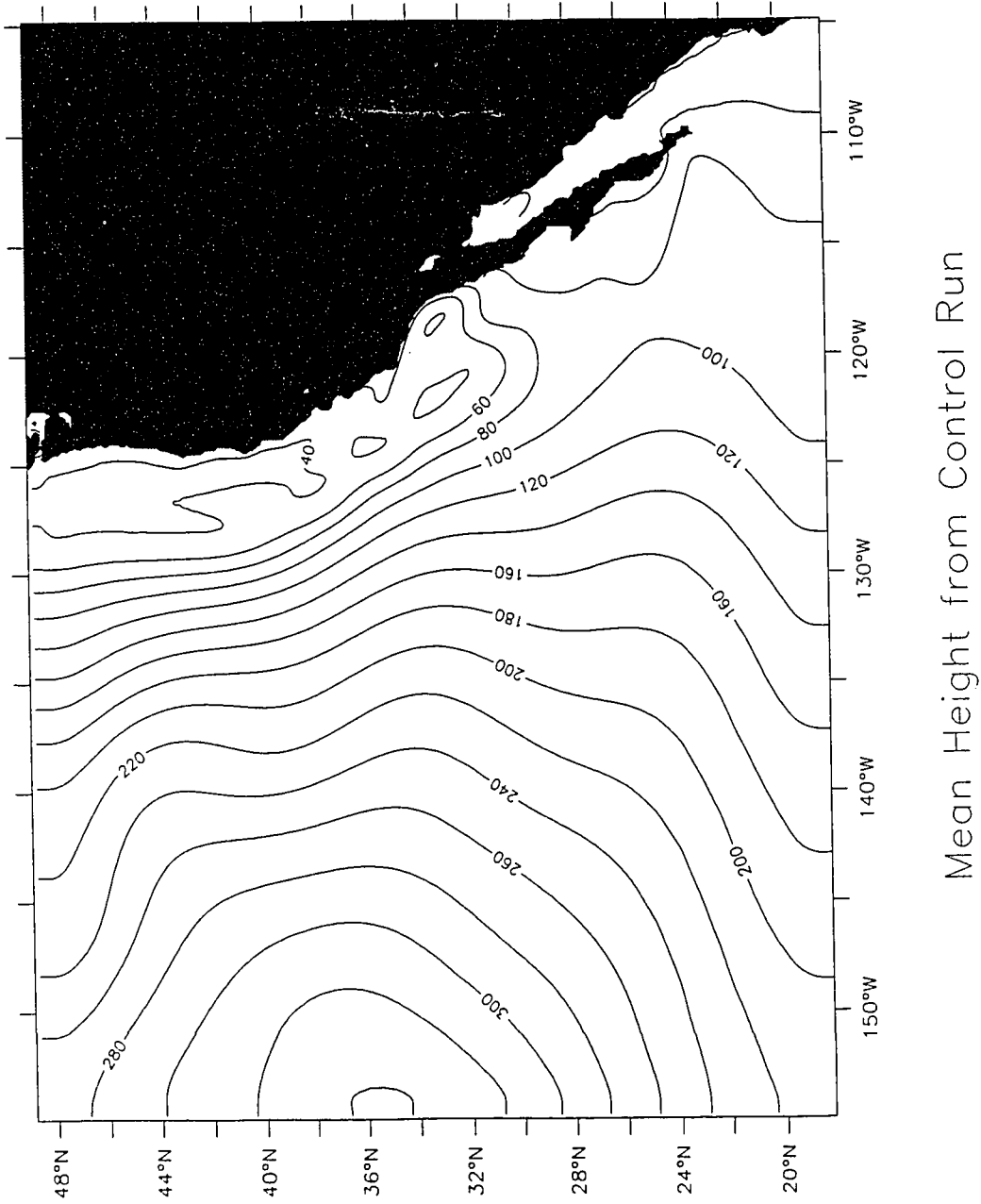
Figure 4.3: Mean upper layer thickness from the control run. Contour interval is 20 m.
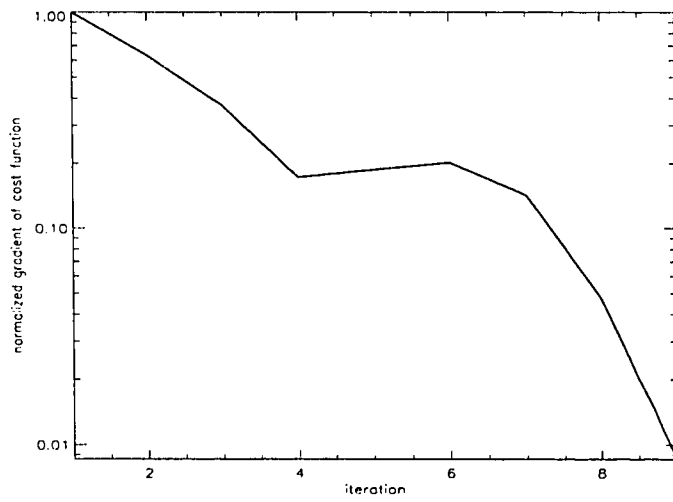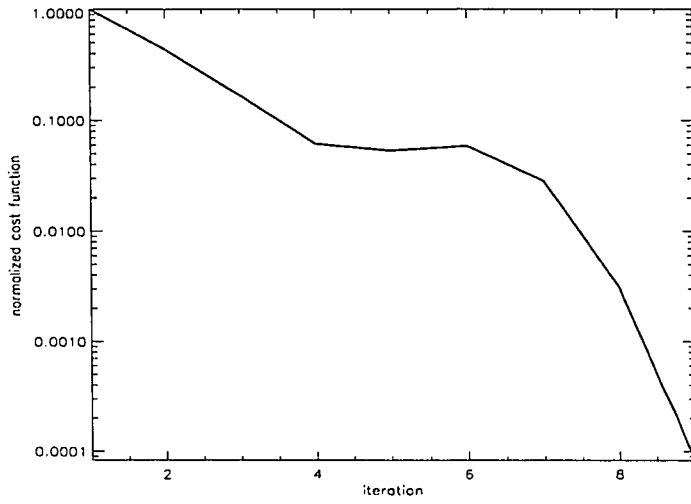
Figure 4.4: (a) The evolution of the cost function normalized by that of the first iteration during the iterative process. Twin experiments. (b) Same as (a) except for gradient of the cost function.
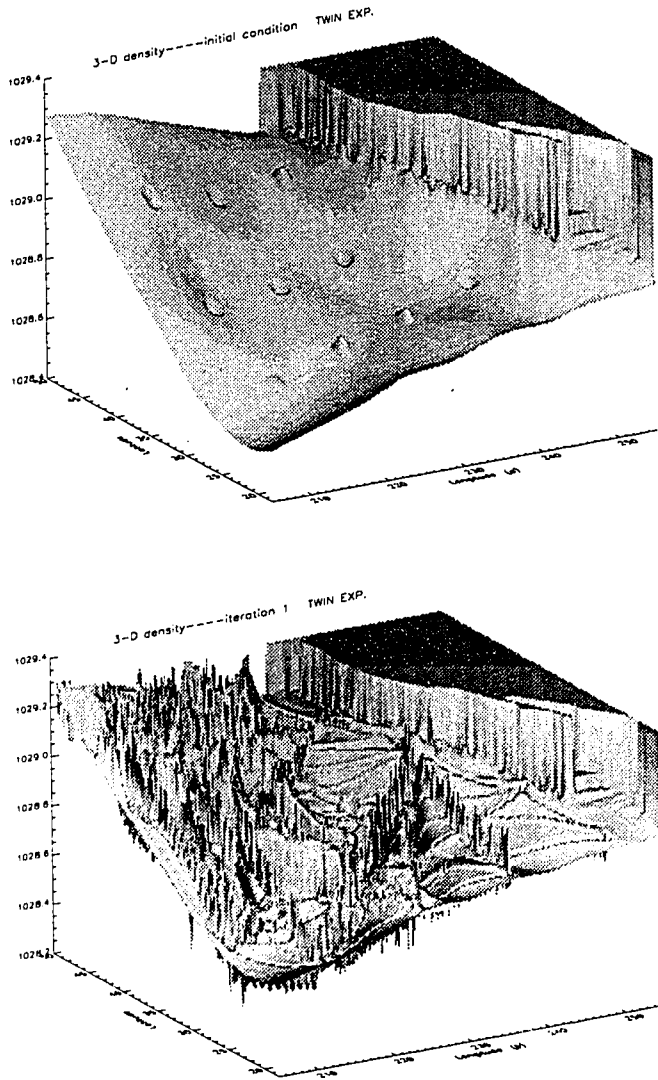
Figure 4.5: (a) The 3-D surface of initial density guess prior to iterative process. (b) The 3-D surface of density after 1 iteration.
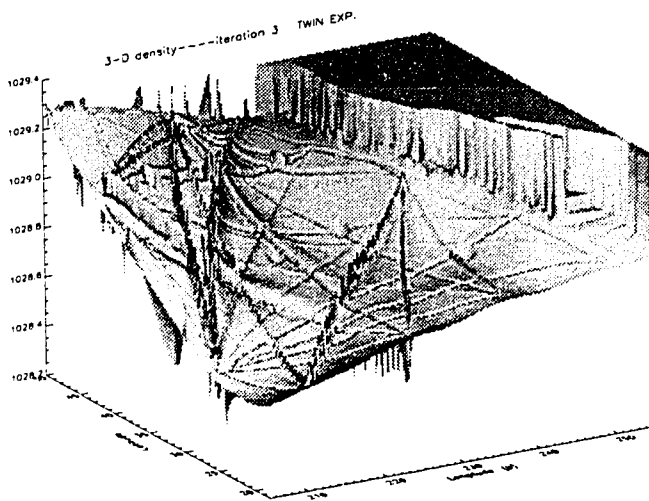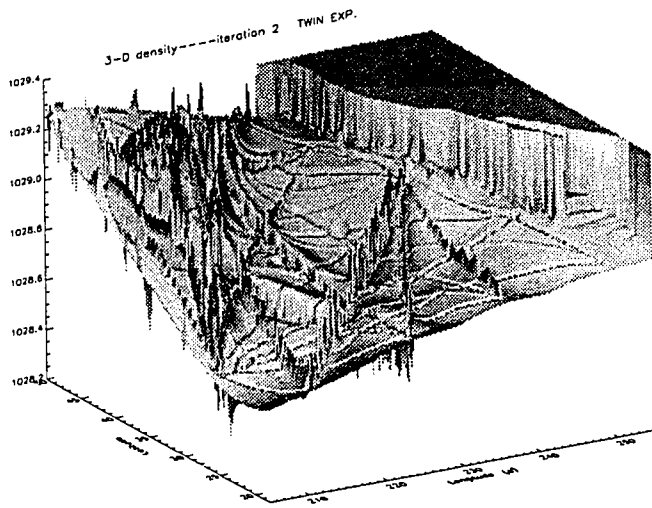
Figure 4.6: (a) The 3-D surface of density after 2 iterations. (b) The 3-D surface of density after 3 iterations.
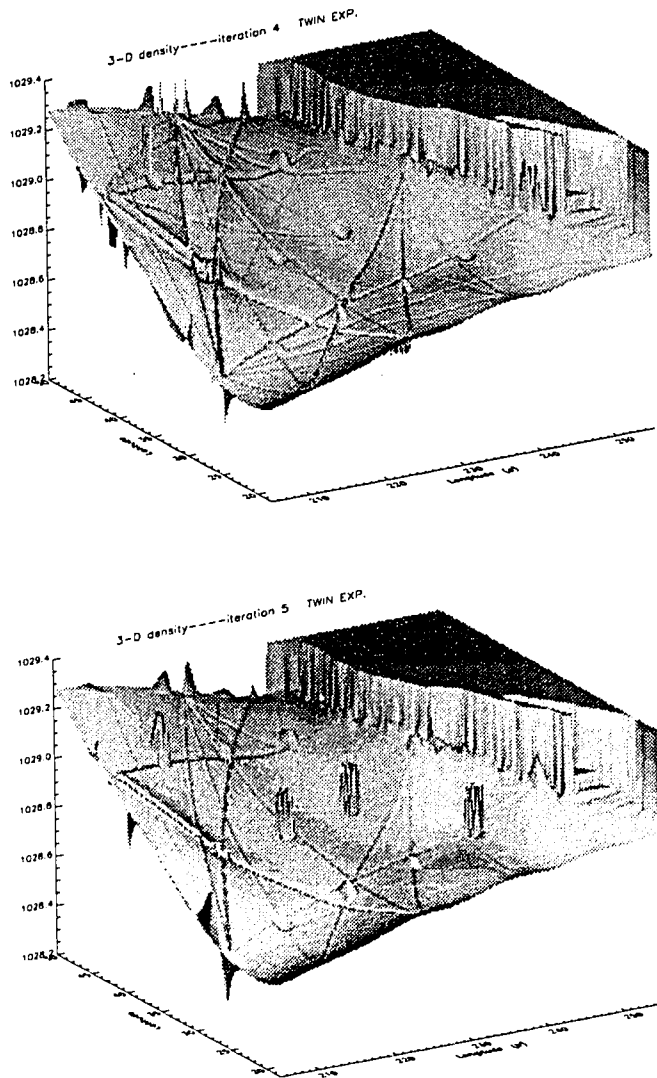
Figure 4.7: (a) The 3-D surface of density after 4 iterations. (b) The 3-D surface of density after 5 iterations.
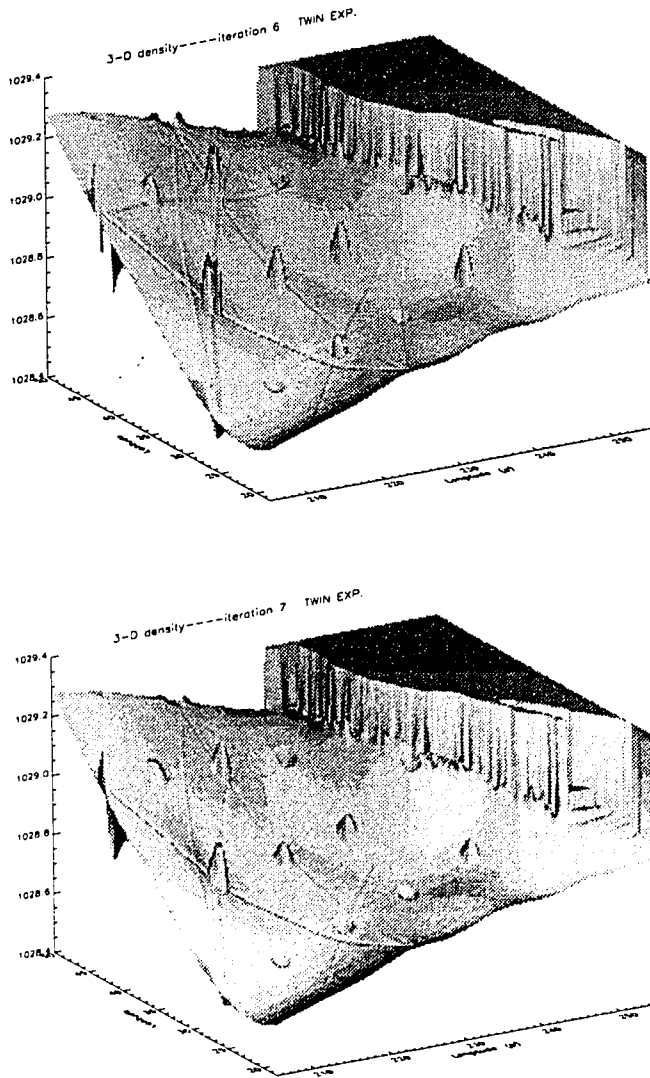
Figure 4.8: (a) The 3-D surface of density after 6 iterations.(b) The 3-D surface of density after 7 iterations.
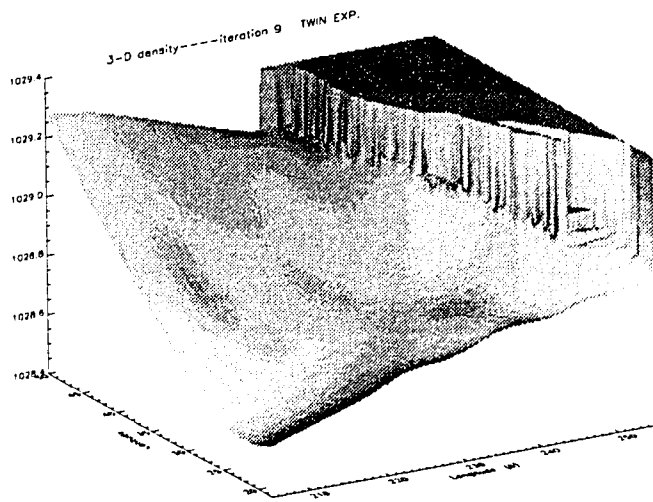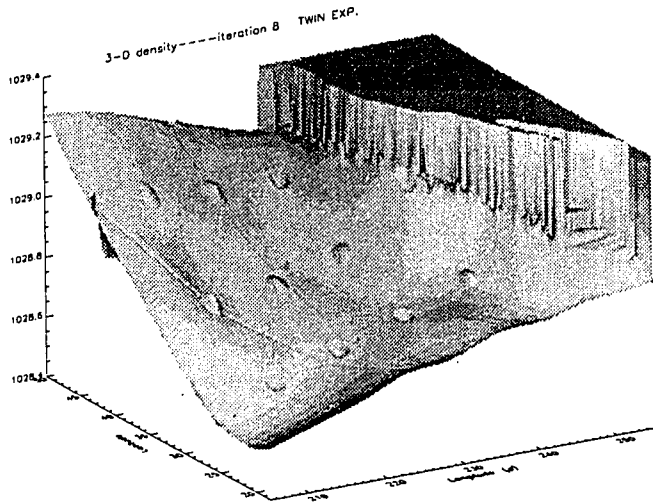
Figure 4.9: (a) The 3-D surface of density after 8 iterations.(b) The 3-D surface of density after 9 iterations.
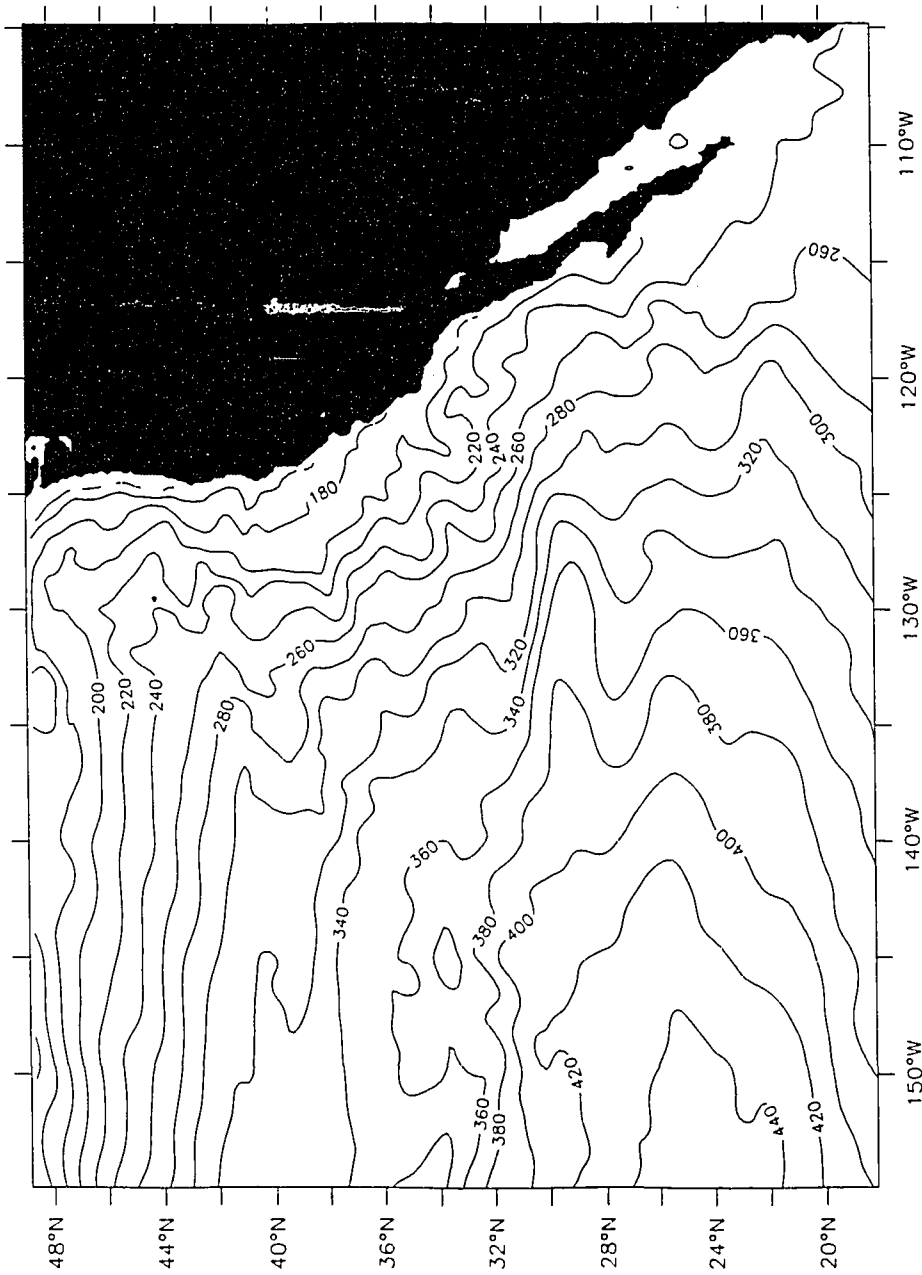
Figure 4.10: Mean height of layer 1 plus layer 2 from NRL model. Contour interval is 20 m.
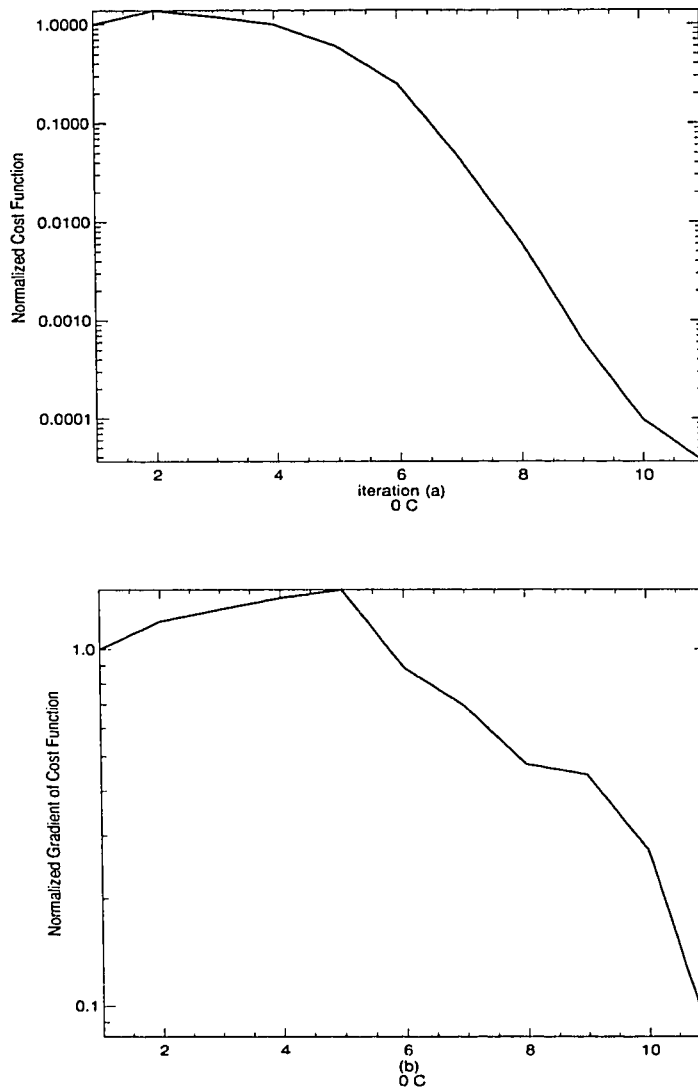
Figure 4.11: (a) The evolution of the cost function normalized by that of the first iteration during the iterative process. Experiments with NRL data. (b) Same as (a) except for gradient of the cost function.
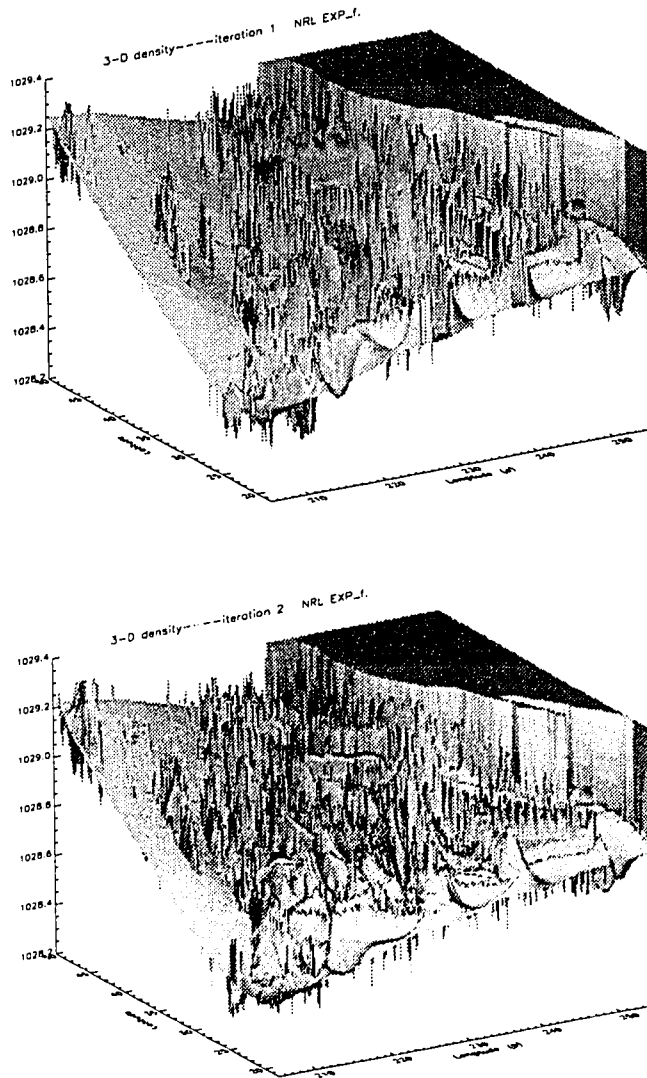
Figure 4.12: (a) The 3-D surface of density after 1 iteration. Experiments with NRL data. (b) after 2 iterations.
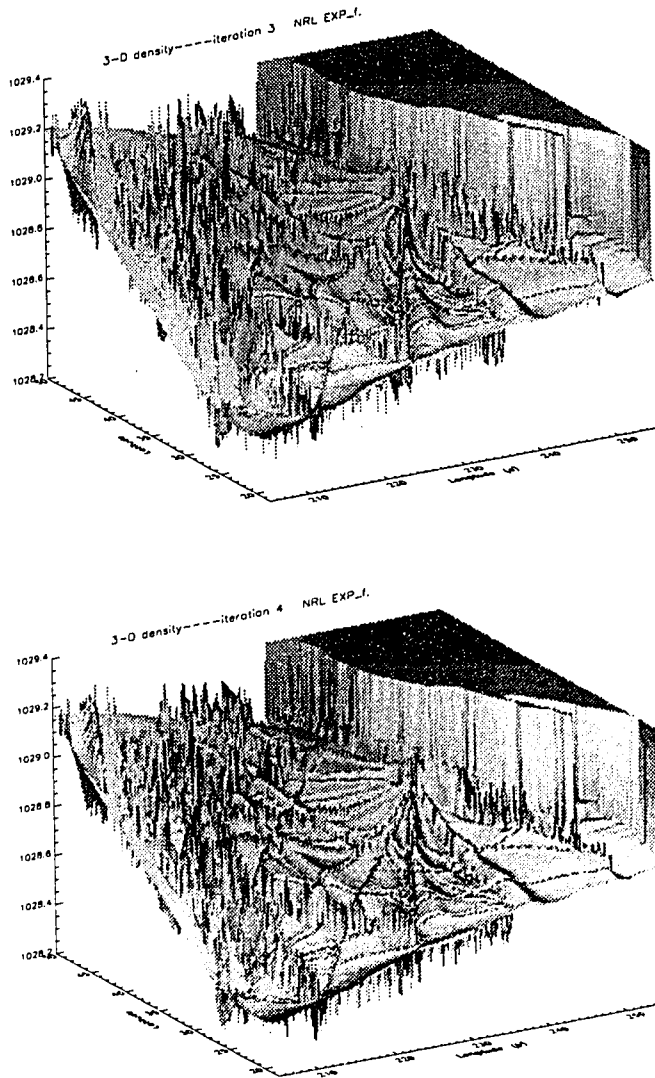
Figure 4.13: (a) The 3-D surface of density after 3 iterations. Experiments with NRL data. (b) The 3-D surface of density after 4 iterations.
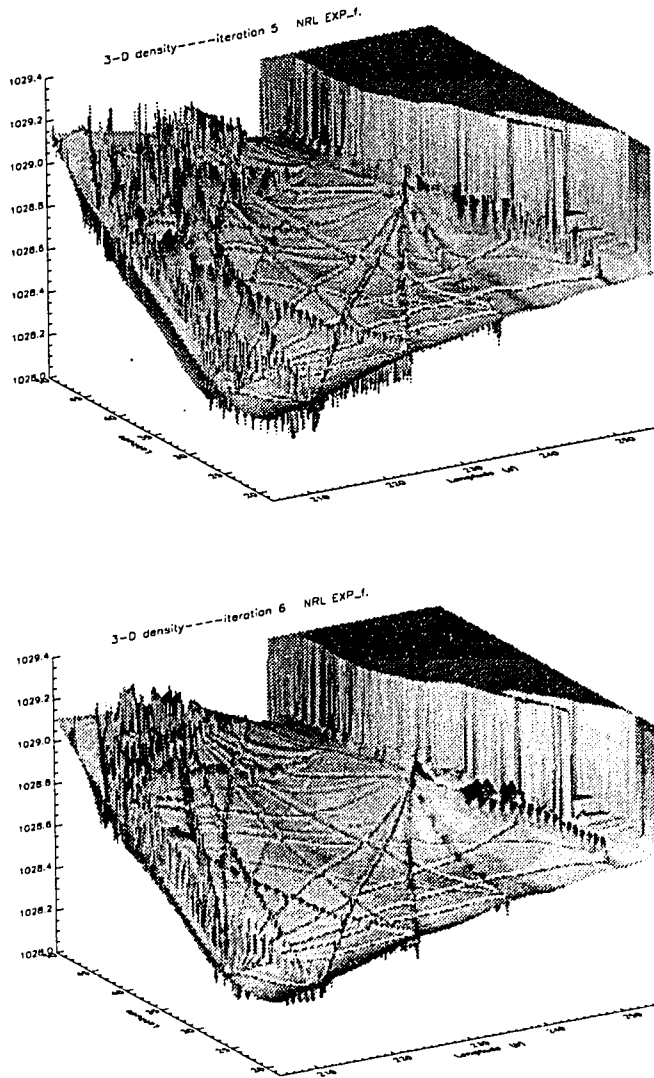
Figure 4.14: (a) The 3-D surface of density after 5 iterations. Experiments with NRL data. (b) The 3-D surface of density after 6 iterations.
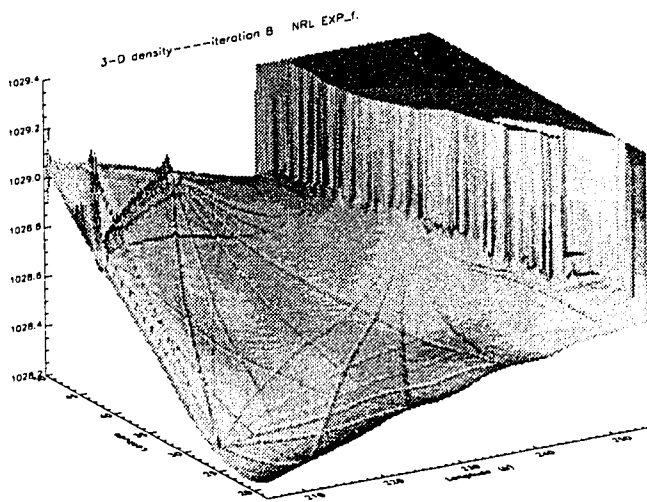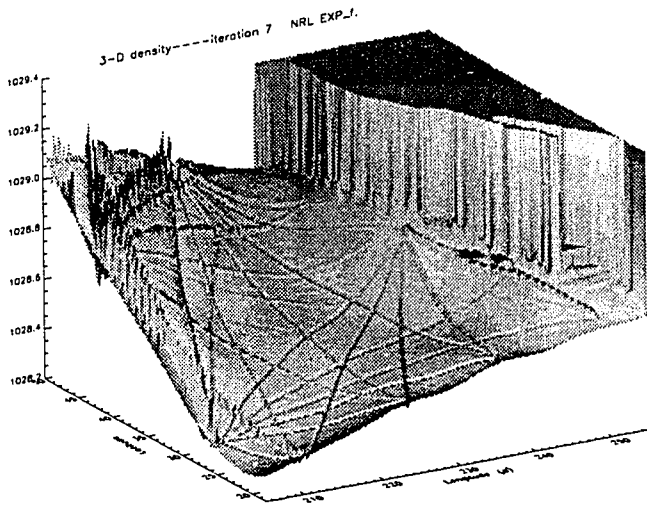
Figure 4.15: (a) The 3-D surface of density after 7 iterations. Experiments with NRL data. (b) The 3-D surface of density after 8 iterations.
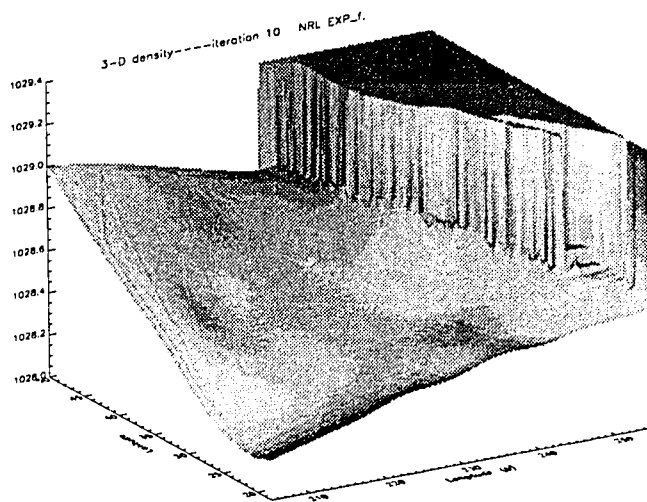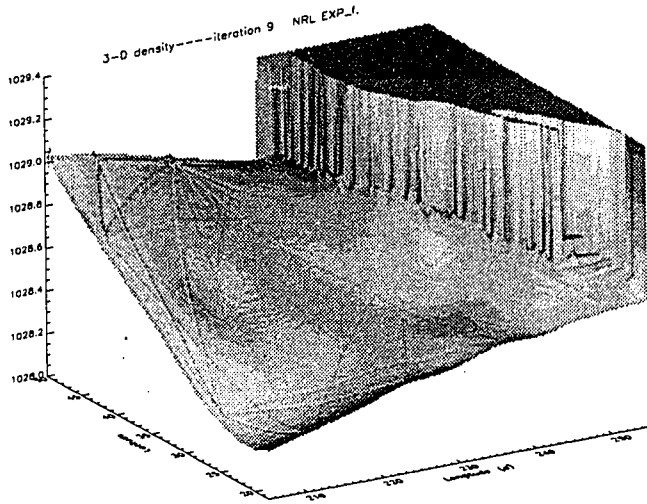
Figure 4.16: (a) The 3-D surface of density after 9 iterations. Experiments with NRL data. (b) The 3-D surface of density after 10 iterations.
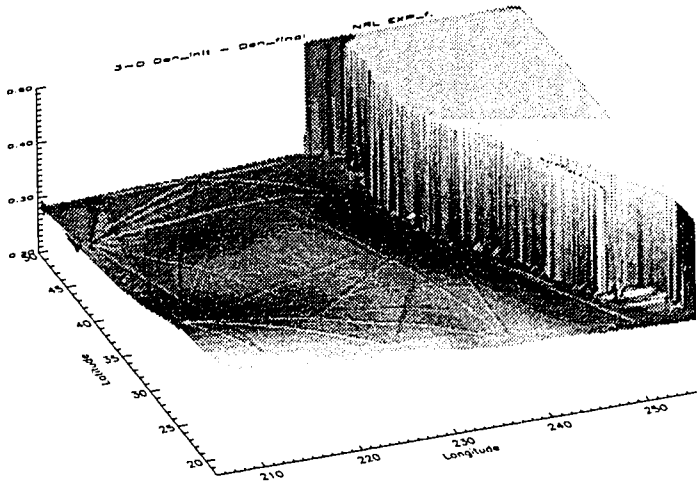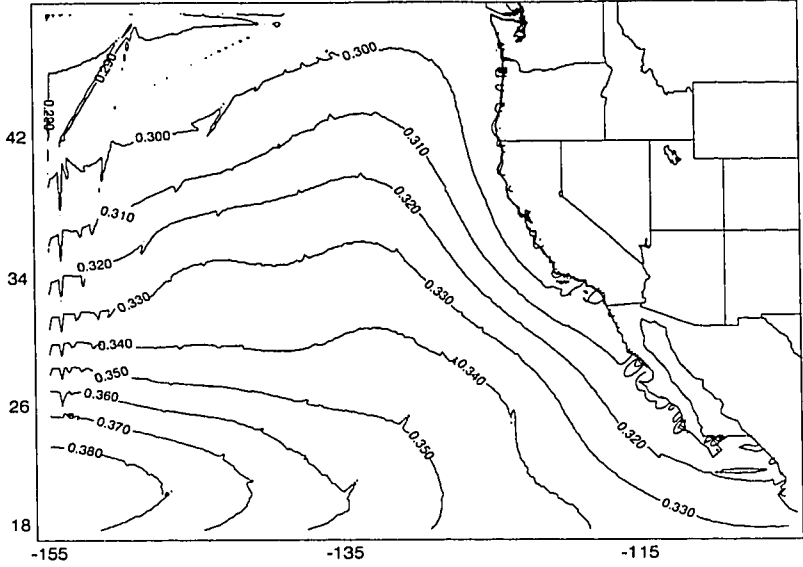
Figure 4.17: (a) The initial dendity (Levitus) minus the final density. The contour levels are in $kg\ m^{-3}$. (b) The 3-D surface of the density difference.

5. SUMMARY AND CONCLUSIONS

An optimal control method is developed to assimilate tomographic data in an upper ocean model of the northeast Pacific with the goal of estimating the time-independent density field and thus the thermohaline structure. The horizontal density field serves as the control variable.

The assimilation procedure works by minimizing the cost function which consists of the misfit between observations and their model counterparts, in a least-squares sense, plus a penalty term. This minimization is carried out consistently while satisfying the constraint that the model dynamics must be satisfied exactly. The variational data assimilation consists of integrating the model equations forward in time over the period which data are to be assimilated. Data misfits between the model and the observation are then calculated and the adjoint equations of the model are integrated backward using the data misfits as forcing. It is necessary to determine the gradient of the cost function with respect to the control variables (the density field). The gradient can be found using the model and adjoint variables and it is used in a minimization algorithm to determine a new density field. The minimization procedure utilized a large-sacle unconstrained minimization code, a limited memory quasi-Newton method (Navon and Legler, 1987; Zou et al., 1993c).

Several identical twin experiments and experiments with NRL model outputs were performed. In identical twin experiments, the Levitus density data is perturbed as the initial density field and the estimated acoustic tomography from the control runs is assimilated into the model. The final estimated density recovers the Levitus density field as expected as fast as in 10 iterations. In the experiments with NRL model outputs, the Levitus density serves as the initial guess, and the density is

estimated by using NRLM output assimilation. The estimated density makes the subtropical gyre stronger in the northeast Pacific region. The results indicate that the variational assimilation procedure works very well.

It can be reasoned that the thermohaline circulation has the same direction as wind-driven circulation in the northeast Pacific region. Therefore, the thermohaline structure may be estimated since the acoustic tomographic data contains information of both the winddriven circulation and, also, the thermohaline circulation.

The total number of control parameters, consisting of the upper ocean density field, in this study is very large, $O(10^5)$. We perform the descent algorithm efficiently by applying the technique of scaling to improve conditioning of the Hessian (the second derivative matrix of the cost function w.r.t. control variables). Scaling transforms the variables from units that typically reflect the physical nature of the problem to units that display certain desirable properties of the optimization. The basic rule of variable scaling is to make all the variables in the scaled problem to be of order unity so that each variable has a similar weight during the optimization. By scaling the variables, the derivatives of the cost function are scaled implicitly. Experiments have shown that an initial well-scaled functional leads to a significant improvement in the performance of the descent algorithm (see Yang, et. al, 1995).

In variational analysis, the solution of a problem is sought by minimizing the cost function. The use of *a priori* information, the Levitus density data, is investigated in the formulation of the cost function to obtain meaningful control variables. Experimental evidence has verified that adding *a priori* information or a penalty term can increase the probability that the solution will be unique due to convexification of the Hessian which is positive definite. Also, *a priori* information plays the role of bogus data. It serves not only to compensate for the shortage of observations, but to improve the conditioning of the Hessian matrix. Hence, the practical benefit

of adding *a priori* information is to precondition the Hessian and to accelerate the convergence of the descent algorithm.

The ocean is modeled with the FSU nonlinear, reduced-gravity model at high resolution, assuming horizontal variations in the upper layer density $[\rho = \rho(\phi, \theta)]$, which can be estimated through tomographic data assimilation. The model successfully reproduces many features of the circulation such as the realistic subtropical gyre and the California current, particularly at large scales. Changes in acoustic travel time are estimated from these non-thermodynamic model runs by assuming vertical displacements of the layer leading to adiabatic changes of sound speed speed and temperature.

The proof of the identity between the discretization of the continuous adjoint equations and the adjoint equations which are from discretized model equations with the Arakawa C has been carried out. This result will be very useful for this kind of assimilation in the future.

The results from this research are very promising. It provides a way for estimating the density field and extracting thermohaline information from oceanic acoustic tomographic data. As many applications have made clear, the adjoint method is so versatile and powerful that it can adjust to any model parameter or field as long as there are sufficient observational data available.

APPENDIX A

DERIVATION OF THE PRESSURE GRADIENT IN THE UPPER

LAYER

The hydrostatic approximation will be made first. The means of describing the situation is shown in Fig. 1. Subscript 1 is used for the upper layer whose density is $\rho_1(x, y)$ and whose equilibrium depth is H_1. The free surface, whose equilibrium position is $z = 0$, has the perturbed position $z = \eta$. The interface displacement (upward) is ς. It follows from the hydrostatic equation

$$\frac{\partial p}{\partial z} = -\rho g \tag{A.1}$$

and the surface condition $p = 0$, that the pressure p_1 in the upper layer is given by

$$p_1 = \rho_1 g(\eta - z), -H_1 + \varsigma < z < \eta \tag{A.2}$$

Similarly, for the lower layer, denoted by subscript 2, the pressure p_2, obtained by integrating [Eq. (A.1)] and using continuity of pressure at the interface, is

$$p_2 = \rho_1 g(\eta + H_1 - \varsigma) - \rho_2 g(z + H_1 - \varsigma), z < -H_1 + \varsigma \tag{A.3}$$

Because of the stagnation of the lower layer, $\nabla p_2 = 0$ [Eq. (A.3)] leads to

$$\nabla \eta = \frac{1}{\rho_2} [(\rho_2 - \rho_1)\nabla h - h\nabla \rho_1] \tag{A.4}$$

where $h = H_1 + \eta - \varsigma$

Therefore, from Eq. (A.2) we have

$$
\begin{aligned}
\nabla p_1 &= g \left(\overline{(\eta - z)}\nabla \rho_1 + \frac{\rho_1}{\rho_2} [(\rho_2 - \rho_1)\nabla h - h\nabla \rho_1] \right) \\
&= g \left(\left[\overline{(\eta - z)} - \frac{\rho_1}{\rho_2}h \right] \nabla \rho_1 + \frac{\rho_1}{\rho_2}(\rho_2 - \rho_1)\nabla h \right)
\end{aligned} \tag{A.5}
$$

However

$$
\begin{aligned}
\overline{(\eta - z)} - \frac{\rho_1}{\rho_2}h &= \frac{1}{h}\int_{-H_1+\varsigma}^{\eta}(\eta - z)dz - \frac{\rho_1}{\rho_2}h \\
&= \frac{h}{2} - \frac{\rho_1}{\rho_2}h \\
&= \frac{1}{2\rho_2}\left[(\rho_2 - \rho_1) - \rho_1\right]h \\
&= \frac{1}{2\rho_2}(\Delta\rho - \rho_1)h \\
&\approx -\frac{\rho_1}{2\rho_2}h
\end{aligned}
\tag{A.6}
$$

Combining the above with Eq. (A.5), we have

$$
\begin{aligned}
-\frac{1}{\bar{\rho}_{1o}}\nabla p_1 &\approx -\frac{\Delta\rho}{\bar{\rho}_{1o}}g\nabla h + \frac{g}{2\bar{\rho}_{1o}}h\nabla\rho_1 \\
&\approx -g'\nabla h + \frac{g}{2\bar{\rho}_{1o}}h\nabla\rho_1
\end{aligned}
\tag{A.7}
$$

APPENDIX B

DERIVATION OF THE CONTINOUS ADJOINT EQUATIONS

We now derive the continuous form of the adjoint equations from the continuous reduced gravity model [Eq. (3.21), Eq. (3.22), and Eq. (3.23)], using the calculus of variations (Courant and Hilbert, 1953 [20]) and forming a Lagrange function by adding the constraints multiplied by the Lagrange multipliers.

From [Eq. (3.39)], the associated Lagrange function is given by:

$$L(S, \Lambda, \rho) = \int_{\Sigma} \Lambda^T E(S, \mathbf{x}, t, \rho) d\sigma + J(T, \rho)$$

$$= \int_{\Sigma} \lambda_u \left\{ \frac{\partial U}{\partial t} + \frac{1}{a \cos \theta} \frac{\partial}{\partial \phi} \left(\frac{U^2}{h} \right) + \frac{1}{a} \frac{\partial}{\partial \theta} \left(\frac{UV}{h} \right) - \frac{2 \tan \theta}{a} \left(\frac{UV}{h} \right) \right.$$
$$- A \left[\Delta(U) + \frac{1 - \tan^2 \theta}{a^2} U - \frac{2 \tan \theta}{a^2 \cos \theta} \frac{\partial V}{\partial \phi} \right]$$
$$\left. - \frac{\tau^\phi}{\rho_o} + \frac{g}{2a \cos \theta \rho_o} \frac{\partial}{\partial \phi} \left[(\rho_2 - \rho_1(\phi, \theta)) h^2 \right] - 2\Omega \sin \theta V \right\} d\sigma$$

$$+ \int_{\Sigma} \lambda_v \left\{ \frac{\partial V}{\partial t} + \frac{1}{a \cos \theta} \frac{\partial}{\partial \phi} \left(\frac{UV}{h} \right) + \frac{1}{a} \frac{\partial}{\partial \theta} \left(\frac{V^2}{h} \right) + \frac{\tan \theta}{a} \left(\frac{U^2 - V^2}{h} \right) \right.$$
$$- A \left[\Delta(V) + \frac{1 - \tan^2 \theta}{a^2} V + \frac{2 \tan \theta}{a^2 \cos \theta} \frac{\partial U}{\partial \phi} \right]$$
$$\left. - \frac{\tau^\theta}{\rho_o} + \frac{g}{2a\rho_o} \frac{\partial}{\partial \theta} \left[(\rho_2 - \rho_1(\phi, \theta)) h^2 \right] + 2\Omega \sin \theta U \right\} d\sigma$$

$$+ \int_{\Sigma} \lambda_h \left\{ \frac{\partial h}{\partial t} + \frac{1}{a \cos \theta} \left[\frac{\partial U}{\partial \phi} + \frac{\partial}{\partial \theta} (V \cos \theta) \right] \right\} d\sigma$$

$$+ \frac{K_T}{2} \sum_i \int_0^\tau \left[\int_{\Sigma_i} \left(C_T (h - h_o) + [\frac{T_{i,j}^o - T_{io}}{\Gamma i}] \right) \Delta^i(\mathbf{x}) d\sigma \right]^2 dt$$

$$+\tau \int_{\Sigma_s} \frac{K_\rho}{2}[\rho(\mathbf{x}) - \tilde{\rho}(\mathbf{x})]^2 d\sigma \tag{B.1}$$

where $d\sigma = a^2 \cos\theta\, d\theta d\phi dt$, λ_u, λ_v and λ_h are the adjoint variables for the U, V and h equations.

At the minimum of J, L has a stationary point, and its first variation with respect to all of its arguments must vanish there. In order to find the adjoint equations, one has to take the first variations of the associated Lagrange function, L [see Eq. (B.1)]

$$\begin{aligned}
\frac{\partial}{\partial U} \int_\Sigma \lambda_u \frac{\partial U}{\partial t} d\sigma &= \frac{\partial}{\partial U}\Big[\int_\Sigma \frac{\partial}{\partial t}(\lambda_u U)d\sigma - \int_\Sigma \frac{\partial \lambda_u}{\partial t} U d\sigma\Big] \\
&= -\int_\Sigma \frac{\partial \lambda_u}{\partial t} d\sigma
\end{aligned} \tag{B.2}$$

where the initial conditions, $\lambda_u|_{t=\tau}$ and $U|_{t=0}$, are used. Similar calculations of the corresponding terms are as follows:

$$\frac{\partial}{\partial V} \int_\Sigma \lambda_v \frac{\partial V}{\partial t} d\sigma = -\int_\Sigma \frac{\partial \lambda_v}{\partial t} d\sigma \tag{B.3}$$

$$\frac{\partial}{\partial h} \int_\Sigma \lambda_h \frac{\partial h}{\partial t} d\sigma = -\int_\Sigma \frac{\partial \lambda_h}{\partial t} d\sigma \tag{B.4}$$

From the continuity equation [Eq. (3.23)] we have

$$\begin{aligned}
\frac{\partial}{\partial U} \int_\Sigma \frac{1}{a\cos\theta} \lambda_h \frac{\partial U}{\partial \phi} d\sigma &= \frac{\partial}{\partial U}\Big[\int_\Sigma \frac{1}{a\cos\theta}\Big(\frac{\partial}{\partial \phi}(\lambda_h U) - \frac{\partial \lambda_h}{\partial \phi} U\Big)d\sigma\Big] \\
&= -\int_\Sigma \frac{1}{a\cos\theta} \frac{\partial \lambda_h}{\partial \phi} d\sigma
\end{aligned} \tag{B.5}$$

where the no-slip boundary condition, $U = 0$, at the eastern boundary has been used. A discussion of the terms at the open boundaries, which are the northern, western and southern boundaries, will be postponed until the finite difference equations are derived. Similary we find

$$\frac{\partial}{\partial V} \int_\Sigma \frac{\lambda_v}{a\cos\theta} \frac{\partial}{\partial \theta}(V\cos\theta)d\sigma$$

$$= \frac{\partial}{\partial V} \int_t \int_\phi \int_\theta a \left[\frac{\partial}{\partial \theta} (\lambda_v V \cos \theta) - V \cos \theta \frac{\partial \lambda_h}{\partial \theta} \right] d\theta d\phi dt$$

$$= -\int_\Sigma \frac{1}{a} \frac{\partial \lambda_h}{\partial \theta} d\sigma \qquad (B.6)$$

The two integration terms from the pressure terms yield

$$\frac{\partial}{\partial h} \int_\Sigma \frac{g}{2a \cos \theta \rho_o} \lambda_u \frac{\partial}{\partial \phi} \left[(\rho_2 - \rho_1(\phi, \theta)) h^2 \right] d\sigma$$

$$= \frac{\partial}{\partial h} \int_t \int_\phi \int_\theta \frac{ag}{2\rho_o} \left\{ \frac{\partial}{\partial \phi} \left[\lambda_u (\rho_2 - \rho_1) h^2 \right] - (\rho_2 - \rho_1) h^2 \frac{\partial \lambda_u}{\partial \phi} \right\} d\theta d\phi dt$$

$$= -\int_\Sigma \frac{g(\rho_2 - \rho_1(\phi, \theta)) h}{a \cos \theta \rho_o} \frac{\partial \lambda_u}{\partial \phi} d\sigma \qquad (B.7)$$

and

$$\frac{\partial}{\partial h} \int_\Sigma \frac{g}{2a\rho_o} \lambda_v \frac{\partial}{\partial \theta} \left[(\rho_2 - \rho_1(\phi, \theta)) h^2 \right] d\sigma$$

$$= \frac{\partial}{\partial h} \int_t \int_\phi \int_\theta \frac{ag}{2\rho_o} \left\{ \frac{\partial}{\partial \theta} \left[\cos \theta \lambda_v (\rho_2 - \rho_1) h^2 \right] - \cos \theta (\rho_2 - \rho_1) h^2 \frac{\partial \lambda_v}{\partial \theta} \right\} d\theta d\phi dt$$

$$= -\int_\Sigma \frac{g(\rho_2 - \rho_1(\phi, \theta)) h}{a\rho_o} \frac{\partial \lambda_v}{\partial \theta} d\sigma \qquad (B.8)$$

where the no-slip boundary conditions, $\lambda_u = 0$ and $\lambda_v = 0$, are applied along the eastern coastline.

We decompose $\Delta(U)$ [Eq. (3.24)] into two terms:

$$A \frac{\partial}{\partial U} \int_\Sigma \lambda_u \Delta(U) d\sigma =$$

$$\frac{A}{a^2} \frac{\partial}{\partial U} \int_\Sigma \lambda_u \left[\underbrace{\frac{1}{\cos^2 \theta} \frac{\partial^2 U}{\partial \phi^2}}_{a} + \underbrace{\frac{\partial^2 U}{\partial \theta^2} - \tan \theta \frac{\partial U}{\partial \theta}}_{b} \right] d\sigma \qquad (B.9)$$

We find that term (a) is

$$\frac{A}{a^2} \frac{\partial}{\partial U} \int_\Sigma \frac{\lambda_u}{\cos^2 \theta} \frac{\partial^2 U}{\partial \phi^2} d\sigma$$

$$= \frac{A}{a^2}\frac{\partial}{\partial U}\int_{\Sigma}\frac{1}{\cos^2\theta}\left[\frac{\partial}{\partial\phi}(\lambda_u\frac{\partial U}{\partial\phi})(\Rightarrow 0) - \frac{\partial\lambda_u}{\partial\phi}\frac{\partial U}{\partial\phi}\right]d\sigma$$

$$= -\frac{A}{a^2}\frac{\partial}{\partial U}\int_{\Sigma}\frac{1}{\cos^2\theta}\left[\frac{\partial}{\partial\phi}(U\frac{\partial\lambda_u}{\partial\phi})(\Rightarrow 0) - U\frac{\partial^2 U}{\partial\phi^2}\right]d\sigma$$

$$= \frac{A}{a^2}\int_{\Sigma}\frac{1}{\cos^2\theta}\frac{\partial^2 U}{\partial\phi^2}d\sigma \tag{B.10}$$

and term (b):

$$\frac{\partial}{\partial U}\int_{\Sigma}\frac{A}{a^2}\lambda_u\left[\frac{\partial^2 U}{\partial\theta^2} - \tan\theta\frac{\partial U}{\partial\theta}\right]d\sigma$$

$$= A\frac{\partial}{\partial U}\int_t\int_{\phi}\int_{\theta}\lambda_u\left[\cos\theta\frac{\partial^2 U}{\partial\theta^2} - \sin\theta\frac{\partial U}{\partial\theta}\right]d\theta d\phi dt$$

$$= A\frac{\partial}{\partial U}\int_t\int_{\phi}\int_{\theta}\left\{\left[\frac{\partial}{\partial\theta}(\lambda_u\cos\theta\frac{\partial U}{\partial\theta})(\Rightarrow 0) - \frac{\partial\lambda_u}{\partial\theta}\cos\theta\frac{\partial U}{\partial\theta}\right.\right.$$

$$\left.\left. +\lambda_u\sin\theta\frac{\partial U}{\partial\theta}\right] - \lambda_u\sin\theta\frac{\partial U}{\partial\theta}\right\}d\theta d\phi dt$$

$$= -A\frac{\partial}{\partial U}\int_t\int_{\phi}\int_{\theta}\left[\frac{\partial}{\partial\theta}(\cos\theta U\frac{\partial\lambda_u}{\partial\theta})(\Rightarrow 0) - \cos\theta U\frac{\partial^2\lambda_u}{\partial\theta^2}\right.$$

$$\left. +\sin\theta U\frac{\partial\lambda_u}{\partial\theta}\right]d\theta d\phi dt$$

$$= \frac{\partial}{\partial U}\int_{\Sigma}\frac{A}{a^2}\left[\frac{\partial^2\lambda_u}{\partial\theta^2} - \tan\theta\frac{\partial\lambda_u}{\partial\theta}\right]d\sigma \tag{B.11}$$

Combining [Eq. (B.10)] and [Eq. (B.11)] yields [Eq. (B.9)]

$$A\frac{\partial}{\partial U}\int_{\Sigma}\lambda_u\Delta(U)d\sigma = A\int_{\Sigma}\Delta(\lambda_u)d\sigma \tag{B.12}$$

A similar integration of the corresponding term for V gives

$$A\frac{\partial}{\partial V}\int_{\Sigma}\lambda_v\Delta(V)d\sigma = A\int_{\Sigma}\Delta(\lambda_v)d\sigma \tag{B.13}$$

Meanwhile, the second to the last term in the diffusion for U is

$$\frac{A}{a^2}\frac{\partial}{\partial U}\int_{\Sigma}\lambda_u\frac{1-\tan^2\theta}{a^2}Ud\sigma = \frac{A}{a^2}\int_{\Sigma}\frac{1-\tan^2\theta}{a^2}\lambda_u d\sigma \tag{B.14}$$

and for V

$$\frac{A}{a^2}\frac{\partial}{\partial V}\int_\Sigma \lambda_v \frac{1-\tan^2\theta}{a^2}V d\sigma = \frac{A}{a^2}\int_\Sigma \frac{1-\tan^2\theta}{a^2}\lambda_v d\sigma \qquad (B.15)$$

The last term in the diffusion for U is

$$-A\frac{\partial}{\partial V}\int_\Sigma \lambda_u \frac{2\tan\theta}{a^2\cos\theta}\frac{\partial V}{\partial\phi}d\sigma$$

$$= -A\frac{\partial}{\partial V}\int_\Sigma \frac{2\tan\theta}{a^2\cos\theta}\left[\frac{\partial}{\partial\phi}(V\lambda_u)(\Rightarrow 0) - V\frac{\partial\lambda_u}{\partial\phi}\right]d\sigma$$

$$= A\int_\Sigma \frac{2\tan\theta}{a^2}\frac{\partial\lambda_u}{\partial\phi}d\sigma \qquad (B.16)$$

and similarly for V

$$A\frac{\partial}{\partial U}\int_\Sigma \lambda_v \frac{2\tan\theta}{a^2\cos\theta}\frac{\partial U}{\partial\phi}d\sigma$$

$$= A\frac{\partial}{\partial U}\int_\Sigma \frac{2\tan\theta}{a^2\cos\theta}\left[\frac{\partial}{\partial\phi}(U\lambda_v)(\Rightarrow 0) - U\frac{\partial\lambda_v}{\partial\phi}\right]d\sigma$$

$$= -A\int_\Sigma \frac{2\tan\theta}{a^2}\frac{\partial\lambda_v}{\partial\phi}d\sigma \qquad (B.17)$$

Using [Eq. (B.9) - Eq. (B.17)], we obtain the integration of the diffusion for U

$$\frac{\partial}{\partial U}\int_\Sigma A\lambda_u\left[\Delta(U) + \frac{1-\tan^2\theta}{a^2}U\right]d\sigma + \frac{\partial}{\partial U}\int_\Sigma A\lambda_v \frac{2\tan\theta}{a^2\cos\theta}\frac{\partial U}{\partial\phi}d\sigma$$

$$= \int_\Sigma A\left[\Delta(\lambda_u) + \frac{1-\tan^2\theta}{a^2}\lambda_u\right]d\sigma - \int_\Sigma A\frac{2\tan\theta}{a^2\cos\theta}\frac{\partial\lambda_v}{\partial\phi}d\sigma \qquad (B.18)$$

and for U

$$\frac{\partial}{\partial V}\int_\Sigma A\lambda_v\left[\Delta(V) + \frac{1-\tan^2\theta}{a^2}V\right]d\sigma - \frac{\partial}{\partial V}\int_\Sigma A\lambda_u \frac{2\tan\theta}{a^2\cos\theta}\frac{\partial V}{\partial\phi}d\sigma$$

$$= \int_\Sigma A\left[\Delta(\lambda_v) + \frac{1-\tan^2\theta}{a^2}\lambda_v\right]d\sigma + \int_\Sigma A\frac{2\tan\theta}{a^2\cos\theta}\frac{\partial\lambda_u}{\partial\phi}d\sigma \qquad (B.19)$$

It is easily seen that the following is true for the Coriolis terms

$$\frac{\partial}{\partial U}\int_\Sigma \lambda_v(2\Omega\sin\theta U)d\sigma = \int_\Sigma 2\Omega\sin\theta\lambda_v d\sigma \tag{B.20}$$

and

$$-\frac{\partial}{\partial V}\int_\Sigma \lambda_u(2\Omega\sin\theta V)d\sigma = -\int_\Sigma 2\Omega\sin\theta\lambda_u d\sigma \tag{B.21}$$

The integrations for the nonlinear terms by parts for both U and V yield

$$\frac{\partial}{\partial U}\int_\Sigma \lambda_u\left[\frac{1}{a\cos\theta}\frac{\partial}{\partial\phi}\left(\frac{U^2}{h}\right)\right]d\sigma$$

$$= \frac{\partial}{\partial U}\int_\Sigma \frac{1}{a\cos\theta}\left[\frac{\partial}{\partial\phi}\left(\lambda_u\frac{U^2}{h}\right)(\Rightarrow 0) - \frac{U^2}{h}\frac{\partial\lambda_u}{\partial\phi}\right]d\sigma$$

$$= -\int_\Sigma \frac{2U}{a\cos\theta h}\frac{\partial\lambda_u}{\partial\phi}d\sigma \tag{B.22}$$

$$\frac{\partial}{\partial V}\int_\Sigma \lambda_v\left[\frac{1}{a\cos\theta}\frac{\partial}{\partial\phi}\left(\frac{UV}{h}\right)\right]d\sigma = -\int_\Sigma \frac{U}{a\cos\theta h}\frac{\partial\lambda_v}{\partial\phi}d\sigma \tag{B.23}$$

$$\frac{\partial}{\partial U}\int_\Sigma \lambda_u\left[\frac{1}{a}\frac{\partial}{\partial\theta}\left(\frac{UV}{h}\right)\right]d\sigma$$

$$= \frac{\partial}{\partial U}\int_t\int_\phi\int_\theta a\left[\frac{\partial}{\partial\theta}\left(\frac{UV}{h}\lambda_u\cos\theta\right)(\Rightarrow 0) - \frac{UV}{h}\frac{\partial}{\partial\theta}\left(\lambda_u\cos\theta\right)\right]d\theta d\phi dt$$

$$= -\int_\Sigma \frac{V}{a\cos\theta h}\frac{\partial}{\partial\theta}\left(\lambda_u\cos\theta\right)d\sigma \tag{B.24}$$

$$\frac{\partial}{\partial V}\int_\Sigma \lambda_v\left[\frac{1}{a}\frac{\partial}{\partial\theta}\left(\frac{V^2}{h}\right)\right]d\sigma = -\int_\Sigma \frac{2V}{a\cos\theta h}\frac{\partial}{\partial\theta}\left(\lambda_v\cos\theta\right)d\sigma \tag{B.25}$$

$$\frac{\partial}{\partial U}\int_\Sigma \lambda_v\left[\frac{1}{a\cos\theta}\frac{\partial}{\partial\phi}\left(\frac{UV}{h}\right)\right]d\sigma$$

$$= \frac{\partial}{\partial U}\int_\Sigma \frac{1}{a\cos\theta}\left[\frac{\partial}{\partial\phi}\left(\lambda_v\frac{UV}{h}\right)(\Rightarrow 0) - \frac{UV}{h}\frac{\partial\lambda_v}{\partial\phi}\right]d\sigma$$

$$= -\int_\Sigma \frac{V}{a\cos\theta h}\frac{\partial\lambda_v}{\partial\phi}d\sigma \tag{B.26}$$

$$\frac{\partial}{\partial V} \int_{\Sigma} \lambda_u \left[\frac{1}{a} \frac{\partial}{\partial \theta} \left(\frac{UV}{h} \right) \right] d\sigma = - \int_{\Sigma} \frac{U}{a \cos \theta h} \frac{\partial}{\partial \theta} \left(\lambda_u \cos \theta \right) d\sigma \qquad (B.27)$$

$$-\frac{\partial}{\partial U} \int_{\Sigma} \lambda_u \left(\frac{2 \tan \theta}{a} \frac{UV}{h} \right) d\sigma = - \int_{\Sigma} \frac{2 \tan \theta V}{ah} \lambda_u d\sigma \qquad (B.28)$$

$$-\frac{\partial}{\partial V} \int_{\Sigma} \lambda_u \left(\frac{2 \tan \theta}{a} \frac{UV}{h} \right) d\sigma = - \int_{\Sigma} \frac{\dot{2} \tan \theta U}{ah} \lambda_u d\sigma \qquad (B.29)$$

$$-\frac{\partial}{\partial h} \int_{\Sigma} \lambda_u \left(\frac{2 \tan \theta}{a} \frac{UV}{h} \right) d\sigma = \int_{\Sigma} \frac{2 \tan \theta UV}{ah^2} \lambda_u d\sigma \qquad (B.30)$$

$$\frac{\partial}{\partial U} \int_{\Sigma} \lambda_v \left[\frac{\tan \theta}{a} \frac{U^2 - V^2}{h} \right] d\sigma = \int_{\Sigma} \frac{2 \tan \theta U}{ah} \lambda_v d\sigma \qquad (B.31)$$

$$\frac{\partial}{\partial V} \int_{\Sigma} \lambda_v \left[\frac{\tan \theta}{a} \frac{U^2 - V^2}{h} \right] d\sigma = - \int_{\Sigma} \frac{2 \tan \theta V}{ah} \lambda_v d\sigma \qquad (B.32)$$

$$\frac{\partial}{\partial h} \int_{\Sigma} \lambda_v \left[\frac{\tan \theta}{a} \frac{U^2 - V^2}{h} \right] d\sigma = - \int_{\Sigma} \frac{\tan \theta}{a} \left(\frac{U^2 - V^2}{h^2} \right) \lambda_v d\sigma \qquad (B.33)$$

$$\frac{\partial}{\partial h} \int_{\Sigma} \lambda_u \left[\frac{1}{a \cos \theta} \frac{\partial}{\partial \phi} \left(\frac{U^2}{h} \right) \right] d\sigma$$
$$= \frac{\partial}{\partial h} \int_{\Sigma} \frac{1}{a \cos \theta} \left[\frac{\partial}{\partial \phi} \left(\lambda_u \frac{U^2}{h} \right) (\Rightarrow 0) - \frac{U^2}{h} \frac{\partial \lambda_u}{\partial \phi} \right] d\sigma$$
$$= \int_{\Sigma} \frac{U^2}{a \cos \theta h^2} \frac{\partial \lambda_u}{\partial \phi} d\sigma \qquad (B.34)$$

$$\frac{\partial}{\partial h} \int_{\Sigma} \lambda_v \left[\frac{1}{a \cos \theta} \frac{\partial}{\partial \phi} \left(\frac{UV}{h} \right) \right] d\sigma = \int_{\Sigma} \frac{UV}{a \cos \theta h^2} \frac{\partial \lambda_v}{\partial \phi} d\sigma \qquad (B.35)$$

$$\frac{\partial}{\partial h} \int_{\Sigma} \lambda_u \left[\frac{1}{a} \frac{\partial}{\partial \theta} \left(\frac{UV}{h} \right) \right] d\sigma$$
$$= \frac{\partial}{\partial h} \int_t \int_\phi \int_\theta a \left[\frac{\partial}{\partial \theta} \left(\frac{UV}{h} \lambda_u \cos \theta \right) (\Rightarrow 0) - \frac{UV}{h} \frac{\partial}{\partial \theta} \left(\lambda_u \cos \theta \right) \right] d\theta d\phi dt$$
$$= \int_{\Sigma} \frac{UV}{a \cos \theta h^2} \frac{\partial}{\partial \theta} \left(\lambda_u \cos \theta \right) d\sigma \qquad (B.36)$$

$$\frac{\partial}{\partial h}\int_\Sigma \lambda_v\left[\frac{1}{a}\frac{\partial}{\partial\theta}\left(\frac{V^2}{h}\right)\right]d\sigma = \int_\Sigma \frac{V^2}{a\cos\theta h^2}\frac{\partial}{\partial\theta}\left(\lambda_v\cos\theta\right)d\sigma \qquad (B.37)$$

Combining [Eq. (B.24)] and [Eq. (B.28)] for U, we have

$$-\frac{V}{a\cos\theta h}\frac{\partial}{\partial\theta}\left(\lambda_u\cos\theta\right) - \frac{2\tan\theta V}{ah}\lambda_u = -\frac{V}{ah}\frac{\partial\lambda_u}{\partial\theta} - \frac{\tan\theta V}{ah}\lambda_u \qquad (B.38)$$

Similarly, with [Eq. (B.25)], [Eq. (B.27)], [Eq. (B.29)] and [Eq. (B.32)] for V we

obtain

$$-\frac{2V}{a\cos\theta h}\frac{\partial}{\partial\theta}\left(\lambda_v\cos\theta\right) - \frac{U}{a\cos\theta h}\frac{\partial}{\partial\theta}\left(\lambda_u\cos\theta\right) - \frac{2\tan\theta U}{ah}\lambda_u - \frac{2\tan\theta V}{ah}\lambda_v$$

$$= -\frac{2V}{ah}\frac{\partial\lambda_v}{\partial\theta} - \frac{U}{ah}\frac{\partial\lambda_u}{\partial\theta} - \frac{\tan\theta U}{ah}\lambda_u \qquad (B.39)$$

Again, combining [Eq. (B.30)], [Eq. (B.33)], [Eq. (B.37)] and [Eq. (B.38)] for h, we have

$$\frac{UV}{a\cos\theta h^2}\frac{\partial}{\partial\theta}\left(\lambda_u\cos\theta\right) + \frac{V^2}{a\cos\theta h^2}\frac{\partial}{\partial\theta}\left(\lambda_v\cos\theta\right)$$

$$+\frac{2\tan\theta UV}{ah^2}\lambda_u - \frac{\tan\theta}{a}\left(\frac{U^2-V^2}{h^2}\right)\lambda_v$$

$$= \frac{1}{ah^2}\left[V\left(U\frac{\partial\lambda_u}{\partial\theta} + V\frac{\partial\lambda_v}{\partial\theta}\right) + U\tan\theta\left(V\lambda_u - U\lambda_v\right)\right] \qquad (B.40)$$

In summary, the first order variation of L with respect to U, V and h leads to linear adjoint equations infering λ_u, λ_v, and λ_h, respectively:

$$-\frac{\partial\lambda_u}{\partial t} - \frac{1}{h}\left[\frac{2U}{a\cos\theta}\frac{\partial\lambda_u}{\partial\phi} + \frac{V}{a}\frac{\partial\lambda_u}{\partial\theta} + \frac{\tan\theta V}{a}\lambda_u - \frac{2\tan\theta U}{a}\lambda_v + \frac{V}{a\cos\theta}\frac{\partial\lambda_v}{\partial\phi}\right] + 2\Omega\sin\theta\lambda_v$$

$$= \frac{1}{a\cos\theta}\frac{\partial\lambda_h}{\partial\phi} + A\left[\Delta(\lambda_u) + \frac{1-\tan^2\theta}{a^2}\lambda_u - \frac{2\tan\theta}{a^2\cos\theta}\frac{\partial\lambda_v}{\partial\phi}\right]$$

$$(\text{B.41})$$

$$-\frac{\partial\lambda_v}{\partial t} - \frac{1}{h}\left[\frac{U}{a\cos\theta}\frac{\partial\lambda_v}{\partial\phi} + \frac{2V}{a}\frac{\partial\lambda_v}{\partial\theta} + \frac{U}{a}\frac{\partial\lambda_u}{\partial\theta} + \frac{\tan\theta U}{a}\lambda_u\right] - 2\Omega\sin\theta\lambda_u$$

$$= \frac{1}{a}\frac{\partial\lambda_h}{\partial\theta} + A\left[\Delta(\lambda_v) + \frac{1-\tan^2\theta}{a^2}\lambda_v + \frac{2\tan\theta}{a^2\cos\theta}\frac{\partial\lambda_u}{\partial\phi}\right]$$

$$(\text{B.42})$$

$$-\frac{\partial\lambda_h}{\partial t} + \frac{g(\rho_2 - \rho_1(\phi,\theta))h}{a\cos\theta\rho_o}\frac{\partial\lambda_u}{\partial\phi} + \frac{g(\rho_2 - \rho_1(\phi,\theta))h}{a\rho_o}\frac{\partial\lambda_v}{\partial\theta}$$

$$+\frac{1}{ah^2}\left[\frac{U}{\cos\theta}\left(U\frac{\partial\lambda_u}{\partial\phi} + V\frac{\partial\lambda_v}{\partial\phi}\right) + V\left(U\frac{\partial\lambda_u}{\partial\theta} + V\frac{\partial\lambda_v}{\partial\theta}\right) + U\tan\theta\left(V\lambda_u - U\lambda_v\right)\right]$$

$$= K_T C_T \sum_i\left[\left(C_T(h - h_o) + [\frac{T_i^o - T_{io}}{\Gamma i}]\right)\Delta^i(\mathbf{x})\right]$$

$$(\text{B.43})$$

APPENDIX C

MODEL IMPLEMENTATION OF THE FINITE DIFFERENCE

EQUATION

The model equations [Eq. (3.21),Eq. (3.22), and Eq. (3.23)] are:

$$\frac{\partial U}{\partial t} + \frac{1}{a\cos\theta}\frac{\partial}{\partial\phi}\left(\frac{U^2}{h}\right) + \frac{1}{a}\frac{\partial}{\partial\theta}\left(\frac{UV}{h}\right) - \frac{2\tan\theta}{a}(\frac{UV}{h})$$

$$-A\left[\Delta(U) + \frac{1-\tan^2\theta}{a^2}U - \frac{2\tan\theta}{a^2\cos\theta}\frac{\partial V}{\partial\phi}\right]$$

$$-\frac{\tau^\phi}{\rho_o} + \frac{g}{2a\cos\theta\rho_o}\frac{\partial}{\partial\phi}\left[(\rho_2 - \rho_1(\phi,\theta))h^2\right] - 2\Omega\sin\theta V = 0 \qquad (C.1)$$

$$\frac{\partial V}{\partial t} + \frac{1}{a\cos\theta}\frac{\partial}{\partial\phi}\left(\frac{UV}{h}\right) + \frac{1}{a}\frac{\partial}{\partial\theta}\left(\frac{V^2}{h}\right) + \frac{\tan\theta}{a}(\frac{U^2-V^2}{h})$$

$$-A\left[\Delta(V) + \frac{1-\tan^2\theta}{a^2}V + \frac{2\tan\theta}{a^2\cos\theta}\frac{\partial U}{\partial\phi}\right]$$

$$-\frac{\tau^\theta}{\rho_o} + \frac{g}{2a\rho_o}\frac{\partial}{\partial\theta}\left[(\rho_2 - \rho_1(\phi,\theta))h^2\right] + 2\Omega\sin\theta U = 0 \qquad (C.2)$$

$$\frac{\partial h}{\partial t} + \frac{1}{a\cos\theta}\left[\frac{\partial U}{\partial\phi} + \frac{\partial}{\partial\theta}(V\cos\theta)\right] = 0 \qquad (C.3)$$

where

$$A\Delta(\cdot) = \frac{A}{a^2}\left(\frac{\partial^2}{\partial\theta^2} + \frac{1}{\cos^2\theta}\frac{\partial^2}{\partial\phi^2} - \tan\theta\frac{\partial}{\partial\theta}\right) \qquad (C.4)$$

Assume F is a function of the independent variables ϕ, θ and t. Let $\Delta = \Delta\phi = \Delta\theta$, unit side, since the model domain equally spaced in latitude and longitude is formed in a system of a square meshes. Denote the value of F at the representative

73

mesh point $P(j\Delta, k\Delta)$ at the time $t = n\Delta t$ by

$$F(\phi, \theta, t) = F(j\Delta, k\Delta, n\Delta t) = F^n{}_{j,k}$$

For the numerical solution of the above equations, all variables are measured at discrete grid point locations using a staggered Arakawa C-grid. The distribution of the variables is shown below. The equations are integrated in time using a leapfrog time differencing scheme. A Dufort-Frankel scheme is used for the diffusive term.

$h_{j-1,k+1}$ $U_{j-1,k+1}$ $h_{j,k+1}$ $U_{j,k+1}$ $h_{j+1,k+1}$ $U_{j+1,k+1}$ $\longrightarrow$ $k+1$

$V_{j-1,k+1}$ $V_{j,k+1}$ $V_{j+1,k+1}$ $\longrightarrow$ $k+\frac{1}{2}$

$\Delta\phi$

$h_{j-1,k}$ $U_{j-1,k}$ $h_{j,k}$ $U_{j,k}$ $h_{j+1,k}$ $U_{j+1,k}$ $\longrightarrow$ k

$\Delta\theta$

$V_{j-1,k}$ $V_{j,k}$ $V_{j+1,k}$ $\longrightarrow$ $k-\frac{1}{2}$

$h_{j-1,k-1}$ $U_{j-1,k-1}$ $h_{j,k-1}$ $U_{j,k-1}$ $h_{j+1,k-1}$ $U_{j+1,k-1}$ $\longrightarrow$ $k-1$

$V_{j-1,k-1}$ $V_{j,k-1}$ $V_{j+1,k-1}$
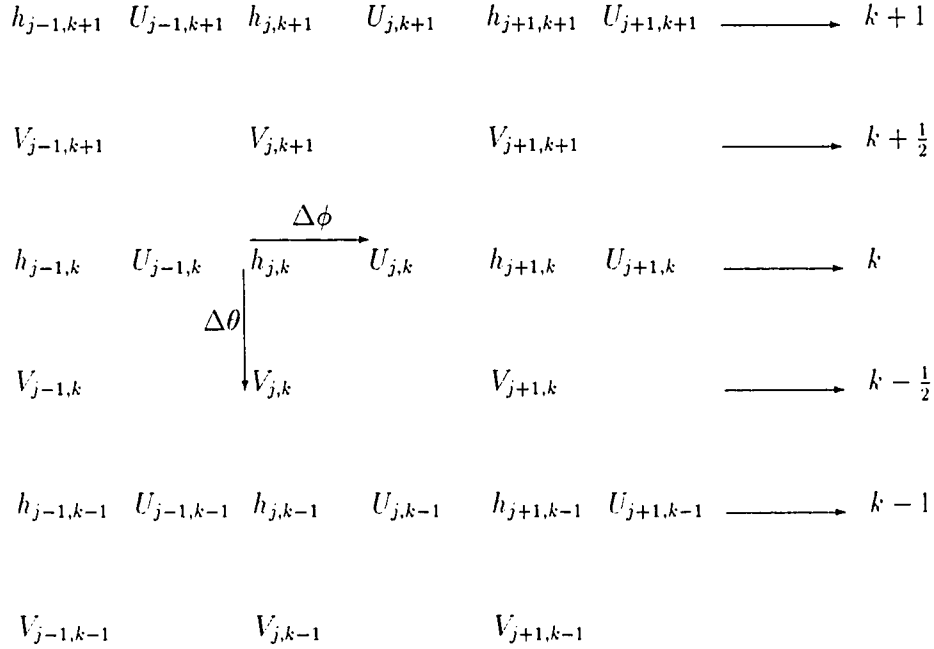
For time differencing in [Eq. (C.1), Eq. (C.2) and Eq. (C.3)], we have respectively

$$\frac{\partial U}{\partial t} \quad \Rightarrow \quad \frac{U_{j,k}^{n+1} - U_{j,k}^{n-1}}{2\Delta \tau}$$

$$\frac{\partial V}{\partial t} \quad \Rightarrow \quad \frac{V_{j,k}^{n+1} - V_{j,k}^{n-1}}{2\Delta \tau}$$

$$\frac{\partial h}{\partial t} \quad \Rightarrow \quad \frac{h_{j,k}^{n+1} - h_{j,k}^{n-1}}{2\Delta \tau}$$

where "$\Rightarrow$" denotes numerical approximation.

The finite-difference approximations of advective nonlinear terms in [Eq. (C.1)] are

$$\frac{1}{a\cos\theta}\frac{\partial}{\partial \phi}\left(\frac{U^2}{h}\right) \quad \Rightarrow \quad \frac{1}{8a\cos\theta_k\Delta\phi}\left[\frac{(U^n_{j,k} + U^n_{j+1,k})^2}{h^n_{j+1,k}} - \frac{(U^n_{j-1,k} + U^n_{j,k})^2}{h^n_{j,k}}\right]$$

$$\frac{1}{a}\frac{\partial}{\partial \theta}\left(\frac{UV}{h}\right) \quad \Rightarrow \quad \frac{1}{2a\Delta\theta}\left[\frac{(U^n_{j,k} + U^n_{j,k+1})(V^n_{j,k+1} + V^n_{j+1,k+1})}{h^n_{j,k} + h^n_{j,k+1} + h^n_{j+1,k} + h^n_{j+1,k+1}}\right.$$
$$\left. - \frac{(U^n_{j,k} + U^n_{j,k-1})(V^n_{j,k} + V^n_{j+1,k})}{h^n_{j,k} + h^n_{j,k-1} + h^n_{j+1,k} + h^n_{j+1,k-1}}\right]$$

$$-\frac{2\tan\theta}{a}\left(\frac{UV}{h}\right) \quad \Rightarrow \quad -\frac{2}{a}\tan\theta_k U^n_{j,k}\frac{V^n_{j,k} + V^n_{j,k+1} + V^n_{j+1,k} + V^n_{j+1,k+1}}{h^n_{j,k} + h^n_{j+1,k}}$$

similarly in [Eq. (C.2)]:

$$\frac{1}{a\cos\theta}\frac{\partial}{\partial \phi}\left(\frac{UV}{h}\right) \quad \Rightarrow \quad \frac{1}{2a\cos\theta_{k-\frac{1}{2}}\Delta\phi}\left[\frac{(U^n_{j,k-1} + U^n_{j,k})(V^n_{j,k} + V^n_{j+1,k})}{h^n_{j,k} + h^n_{j,k-1} + h^n_{j+1,k-1} + h^n_{j+1,k}}\right.$$
$$\left. - \frac{(U^n_{j-1,k-1} + U^n_{j-1,k})(V^n_{j,k} + V^n_{j-1,k})}{h^n_{j,k} + h^n_{j,k-1} + h^n_{j-1,k} + h^n_{j-1,k-1}}\right]$$

$$\frac{1}{a}\frac{\partial}{\partial \theta}\left(\frac{V^2}{h}\right) \quad \Rightarrow \quad \frac{1}{8a\Delta\theta}\left[\frac{(V^n_{j,k} + V^n_{j,k+1})^2}{h^n_{j,k}} - \frac{(V^n_{j,k-1} + V^n_{j,k})^2}{h^n_{j,k-1}}\right]$$

$$\frac{\tan\theta}{a}\left(\frac{U^2 - V^2}{h}\right) \quad \Rightarrow \quad \frac{\tan\theta_{k-\frac{1}{2}}}{8a}\left[\frac{(U^n_{j,k} + U^n_{j-1,k} + U^n_{j,k-1} + U^n_{j-1,k-1})^2 - 16(V^n_{j,k})^2}{h^n_{j,k} + h^n_{j,k-1}}\right]$$

The Coriolis terms are

$$-2\Omega \sin\theta V \quad \Rightarrow \quad -\frac{1}{2}\sin\theta_k \Omega\left(V^n_{j,k} + V^n_{j,k+1} + V^n_{j+1,k} + V^n_{j+1,k+1}\right)$$

$$2\Omega \sin\theta U \quad \Rightarrow \quad \frac{1}{2}\sin\theta_{k-\frac{1}{2}}\Omega\left(U^n_{j,k} + U^n_{j-1,k} + U^n_{j,k-1} + U^n_{j-1,k-1}\right)$$

With the Dufort-Frankel Scheme for a variable $F(\phi,\theta,t)$

$$F^n_{j,k} \Rightarrow \frac{F^{n+1}_{j,k} + F^{n-1}_{j,k}}{2} \qquad\qquad (C.5)$$

The horizontal viscous terms for the moment[Eq. (C.1)] are for

$$-\frac{A}{a^2}\frac{\partial^2 U}{\partial\theta^2} \quad \Rightarrow \quad -\frac{A}{a^2}\frac{U^n_{j,k+1} + U^n_{j,k-1} - 2U^n_{j,k}}{(2\Delta\theta)^2}$$

$$= \quad -\frac{A}{a^2}\frac{[U^n_{j,k+1} + U^n_{j,k-1} + 2U^n_{j,k} - 2(U^{n+1}_{j,k} + U^{n-1}_{j,k})]}{(2\Delta\theta)^2}$$

$$-\frac{A}{a^2\cos^2\theta}\frac{\partial^2 U}{\partial\phi^2} \quad \Rightarrow \quad -A\frac{[U^n_{j-1,k} + U^n_{j+1,k} + 2U^n_{j,k} - 2(U^{n+1}_{j,k} + U^{n-1}_{j,k})]}{a^2\cos^2\theta_k(2\Delta\phi)^2}$$

$$\frac{A\tan\theta}{a^2}\frac{\partial U}{\partial\theta} \quad \Rightarrow \quad \frac{A}{2a^2}\left[\tan\theta_{k+1}\frac{U^n_{j,k+1} - U^n_{j,k}}{2\Delta\theta} + \tan\theta_{k-1}\frac{U^n_{j,k} - U^n_{j,k-1}}{2\Delta\theta}\right]$$

$$-\frac{A}{a^2}(1 - \tan^2\theta) \quad \Rightarrow \quad -\frac{A}{a^2}(1 - \tan^2\theta_k)U^n_{j,k}$$

$$\frac{2A\tan\theta}{a^2\cos\theta}\frac{\partial V}{\partial\phi} \quad \Rightarrow \quad \frac{2A\tan\theta_k}{a^2\cos\theta_k}\frac{(V^n_{j+1,k} + V^n_{j+1,k+1}) - (V^n_{j,k} + V^n_{j,k+1})}{4\Delta\phi}$$

Similarly in [Eq. (C.2)]

$$-\frac{A}{a^2}\frac{\partial^2 V}{\partial\theta^2} \quad \Rightarrow \quad -\frac{A}{a^2}\frac{V^n_{j,k+1} + V^n_{j,k-1} - 2V^n_{j,k}}{(2\Delta\theta)^2}$$

$$= \quad -\frac{A}{a^2}\frac{[V^n_{j,k+1} + V^n_{j,k-1} + 2V^n_{j,k} - 2(V^{n+1}_{j,k} + V^{n-1}_{j,k})]}{(2\Delta\theta)^2}$$

$$-\frac{A}{a^2\cos^2\theta}\frac{\partial^2 V}{\partial\phi^2} \quad \Rightarrow \quad -A\frac{[V^n_{j-1,k} + V^n_{j+1,k} + 2V^n_{j,k} - 2(V^{n+1}_{j,k} + V^{n-1}_{j,k})]}{a^2\cos^2\theta_{k-\frac{1}{2}}(2\Delta\phi)^2}$$

$$\frac{A\tan\theta}{a^2}\frac{\partial V}{\partial\theta} \;\Rightarrow\; \frac{A}{2a^2}\left[\tan\theta_{k+\frac{1}{2}}\frac{V^n_{j,k+1}-V^n_{j,k}}{2\Delta\theta}+\tan\theta_{k-\frac{3}{2}}\frac{V^n_{j,k}-V^n_{j,k-1}}{2\Delta\theta}\right]$$

$$-\frac{A}{a^2}(1-\tan^2\theta) \;\Rightarrow\; -\frac{A}{a^2}(1-\tan^2\theta_{k-\frac{1}{2}})V^n_{j,k}$$

$$-\frac{2A\tan\theta}{a^2\cos\theta}\frac{\partial U}{\partial\phi} \;\Rightarrow\; -\frac{2A\tan\theta_{k-\frac{1}{2}}}{a^2\cos\theta_{k-\frac{1}{2}}}\frac{(U^n_{j,k}+U^n_{j,k-1})-(U^n_{j-1,k}+U^n_{j-1,k-1})}{4\Delta\phi}$$

The pressure gradient terms which also include thermohaline forcing are:

$$\frac{g}{2a\cos\theta\rho_o}\frac{\partial}{\partial\phi}\left[(\rho_2-\rho_1(\phi,\theta))h^2\right] \;\Rightarrow\; \frac{g}{2a\cos\theta\rho_o}\frac{(\rho_2-\rho_1{}^n_{j+1,k})h^n{}^2_{j+1,k}-(\rho_2-\rho_1{}^n_{j,k})h^n{}^2_{j,k}}{2\Delta\phi}$$

$$\frac{g}{2a\rho_o}\frac{\partial}{\partial\theta}\left[(\rho_2-\rho_1(\phi,\theta))h^2\right] \;\Rightarrow\; \frac{g}{2a\rho_o}\frac{(\rho_2-\rho_1{}^n_{j,k})h^n{}^2_{j,k}-(\rho_2-\rho_1{}^n_{j,k-1})h^n{}^2_{j,k-1}}{2\Delta\theta}$$

The divergence terms in the equation of continuity [Eq. (C.3)] are:

$$\frac{1}{a\cos\theta}\frac{\partial U}{\partial\phi} \;\Rightarrow\; \frac{1}{a\cos\theta_k}\frac{(U^n_{j,k}-U^n_{j-1,k})}{2\Delta\phi} \tag{C.6}$$

$$\frac{1}{a}\frac{\partial V}{\partial\theta} \;\Rightarrow\; \frac{1}{a}\frac{(V^n_{j,k+1}-V^n_{j,k})}{2\Delta\theta} \tag{C.7}$$

$$-\frac{\tan\theta}{a}V \;\Rightarrow\; -\frac{\tan\theta_k}{2a}(V^n_{j,k+1}+V^n_{j,k}) \tag{C.8}$$

Finally, the finite difference form of the horizontal momentum equations can then be written as:

$$U^{n+1}_{j,k}-U^{n-1}_{j,k}+\alpha\beta_k\left[\frac{(U^n_{j,k}+U^n_{j+1,k})^2}{h^n_{j+1,k}}-\frac{(U^n_{j-1,k}+U^n_{j,k})^2}{h^n_{j,k}}\right]$$

$$+\alpha\left[\frac{(U^n_{j,k}+U^n_{j,k+1})(V^n_{j,k+1}+V^n_{j+1,k+1})}{h^n_{j,k}+h^n_{j,k+1}+h^n_{j+1,k}+h^n_{j+1,k+1}}\right.$$

$$\left.-\frac{(U^n_{j,k}+U^n_{j,k-1})(V^n_{j,k}+V^n_{j+1,k})}{h^n_{j,k}+h^n_{j,k-1}+h^n_{j+1,k}+h^n_{j+1,k-1}}\right]$$

$$-Cl_k U^n{}_{j,k} \frac{(V^n{}_{j,k} + V^n{}_{j,k+1} + V^n{}_{j+1,k} + V^n{}_{j+1,k+1})}{h^n{}_{j,k} + h^n{}_{j+1,k}}$$

$$-Co_k\left(V^n{}_{j,k} + V^n{}_{j,k+1} + V^n{}_{j+1,k} + V^n{}_{j+1,k+1}\right)$$

$$-\alpha A^1\left[U^n{}_{j,k+1} + U^n{}_{j,k-1} + 2U^n{}_{j,k} - 2(U^{n+1}_{j,k} + U^{n-1}_{j,k})\right]$$

$$-\alpha A^2_k\left[U^n{}_{j-1,k} + U^n{}_{j+1,k} + 2U^n{}_{j,k} - 2(U^{n+1}_{j,k} + U^{n-1}_{j,k})\right]$$

$$+\alpha A^3\left[\tan\theta_{k+\frac{1}{2}}(U^n{}_{j,k+1} - U^n{}_{j,k}) + \tan\theta_{k-\frac{1}{2}}(U^n{}_{j,k} - U^n{}_{j,k-1})\right]$$

$$-A^4_k U^n{}_{j,k} + \alpha A^5_k\left[(V^n{}_{j+1,k} + V^n{}_{j+1,k+1}) - (V^n{}_{j,k} + V^n{}_{j,k+1})\right]$$

$$+\alpha\chi^u_k\left[(\rho_2 - \rho_1{}^n{}_{j+1,k})h^{n2}_{j+1,k} - (\rho_2 - \rho_1{}^n{}_{j,k})h^{n2}_{j,k}\right] = 0$$

(C.9)

and

$$V^{n+1}_{j,k} - V^{n-1}_{j,k} + \frac{\alpha}{4}\left[\frac{(V^n{}_{j,k} + V^n{}_{j,k+1})^2}{h^n{}_{j,k}} - \frac{(V^n{}_{j,k-1} + V^n{}_{j,k})^2}{h^n{}_{j,k-1}}\right]$$

$$+4\alpha\beta_{k-\frac{1}{2}}\left[\frac{(U^n{}_{j,k-1} + U^n{}_{j,k})(V^n{}_{j,k} + V^n{}_{j+1,k})}{h^n{}_{j,k} + h^n{}_{j,k-1} + h^n{}_{j+1,k-1} + h^n{}_{j+1,k}}\right.$$

$$\left.- \frac{(U^n{}_{j-1,k-1} + U^n{}_{j-1,k})(V^n{}_{j,k} + V^n{}_{j-1,k})}{h^n{}_{j,k} + h^n{}_{j,k-1} + h^n{}_{j-1,k} + h^n{}_{j-1,k-1}}\right]$$

$$+\frac{Cl_{k-\frac{1}{2}}}{8}\left[\frac{(U^n{}_{j,k} + U^n{}_{j-1,k} + U^n{}_{j,k-1} + U^n{}_{j-1,k-1})^2 - 16(V^n{}_{j,k})^2}{h^n{}_{j,k} + h^n{}_{j,k-1}}\right]$$

$$+Co_{k-\frac{1}{2}}\left(U^n{}_{j,k} + U^n{}_{j-1,k} + U^n{}_{j,k-1} + U^n{}_{j-1,k-1}\right)$$

$$-\alpha A^1\left[V^n{}_{j,k+1} + V^n{}_{j,k-1} + 2V^n{}_{j,k} - 2(V^{n+1}_{j,k} + V^{n-1}_{j,k})\right]$$

$$-\alpha A^2_{k-\frac{1}{2}}\left[V^n{}_{j-1,k} + V^n{}_{j+1,k} + 2V^n{}_{j,k} - 2(V^{n+1}_{j,k} + V^{n-1}_{j,k})\right]$$

$$+\alpha A^3\left[\tan\theta_k(V^n{}_{j,k+1} - V^n{}_{j,k}) + \tan\theta_{k-1}(V^n{}_{j,k} - V^n{}_{j,k-1})\right]$$

$$-A^4_{k-\frac{1}{2}}V^n{}_{j,k} - \alpha A^5_{k-\frac{1}{2}}\left[(U^n{}_{j,k} + U^n{}_{j,k-1}) - (U^n{}_{j-1,k} + U^n{}_{j-1,k-1})\right]$$

$$+\alpha\chi^v\left[(\rho_2 - \rho_1{}^n{}_{j,k})h^{n2}_{j,k} - (\rho_2 - \rho_1{}^n{}_{j,k-1})h^{n2}_{j,k-1}\right] = 0$$

(C.10)

where

$$\alpha \quad = \frac{2\Delta\tau}{2a\Delta}$$

$$\beta_k \quad = \frac{1}{4\cos\theta_k}$$

$$Cl_k \quad = \frac{2\tan\theta_k\Delta\tau}{a}$$

$$Co_k \quad = \Omega\sin\theta_k\Delta\tau$$

$$A^1 \quad = \frac{A}{2a\Delta}$$

$$A_k^2 \quad = \frac{A}{2a\Delta\cos^2\theta_k}$$

$$A^3 \quad = \frac{A}{2a}$$

$$A_k^4 \quad = \frac{2A\Delta\tau(1-\tan^2\theta_k)}{a^2}$$

$$A_k^5 \quad = \frac{A\tan\theta_k}{a\cos\theta_k}$$

$$\chi_k^u \quad = \frac{g}{2\cos\theta_k\rho_o}$$

$$\chi^v \quad = \frac{g}{2\rho_o}$$

(C.11)

The continuity equation [[Eq. (C.3)]] can be written in the form

$$h_{j,k}^{n+1} - h_{j,k}^{n-1} + 4\alpha\beta_k(U^n{}_{j,k} - U^n{}_{j-1,k})$$
$$+ \quad \alpha(V^n{}_{j,k+1} - V^n{}_{j,k}) - \frac{Cl_k}{2}(V^n{}_{j,k+1} + V^n{}_{j,k}) = 0$$

APPENDIX D

DERIVATION OF THE DISCRETIZED ADJOINT EQUATIONS

Now define a functional J as [Eq. (3.38)]

where $T^o_{i,j}$ is the observed value of travel time along ray i at time t_j. We have assumed that the observations are located on the same regular space/time grid as the model values.

The functinal J [Eq. (2.3)] is to be minimized subject to the constraints of the $F(U, X)$ [Eq. (2.4)]. The goal is to find ρ, the gradient of J, with respect to the density and then use it in an iterative descent large-scale minimization procedure as described in Chapter 2. To do this, define a new functional.

$$
\begin{aligned}
L = \quad & J \\
+ \quad & \sum_{j=1}^{J-1} \sum_{k=1}^{K-1} \sum_{n=1}^{N} \lambda_{u\,j,k}^{n} \left\{ U_{j,k}^{n+1} - U_{j,k}^{n-1} \right. \\
& + \alpha \beta_k \left[\frac{(U^n_{j,k} + U^n_{j+1,k})^2}{h^n_{j+1,k}} - \frac{(U^n_{j-1,k} + U^n_{j,k})^2}{h^n_{j,k}} \right] \\
& + \alpha \left[\frac{(U^n_{j,k} + U^n_{j,k+1})(V^n_{j,k+1} + V^n_{j+1,k+1})}{h^n_{j,k} + h^n_{j,k+1} + h^n_{j+1,k} + h^n_{j+1,k+1}} \right. \\
& \left. - \frac{(U^n_{j,k} + U^n_{j,k-1})(V^n_{j,k} + V^n_{j+1,k})}{h^n_{j,k} + h^n_{j,k-1} + h^n_{j+1,k} + h^n_{j+1,k-1}} \right] \\
& - C l_k U^n_{j,k} \frac{(V^n_{j,k} + V^n_{j,k+1} + V^n_{j+1,k} + V^n_{j+1,k+1})}{h^n_{j,k} + h^n_{j+1,k}} \\
& - C o_k (V^n_{j,k} + V^n_{j,k+1} + V^n_{j+1,k} + V^n_{j+1,k+1}) \\
& - \alpha A^1 [U^n_{j,k+1} + U^n_{j,k-1} + 2U^n_{j,k} - 2(U_{j,k}^{n+1} + U_{j,k}^{n-1})] \\
& - \alpha A_k^2 [U^n_{j-1,k} + U^n_{j+1,k} + 2U^n_{j,k} - 2(U_{j,k}^{n+1} + U_{j,k}^{n-1})] \\
& + \alpha A^3 [\tan \theta_{k+\frac{1}{2}} (U^n_{j,k+1} - U^n_{j,k}) + \tan \theta_{k-\frac{1}{2}} (U^n_{j,k} - U^n_{j,k-1})]
\end{aligned}
$$

$$-A_k^4 U^n{}_{j,k} + \alpha A_k^5[(V^n{}_{j+1,k} + V^n{}_{j+1,k+1}) - (V^n{}_{j,k} + V^n{}_{j,k+1})]$$

$$+\alpha\chi_k^u[(\rho_2 - \rho_1{}^n{}_{j+1,k})h^{n2}{}_{j+1,k} - (\rho_2 - \rho_1{}^n{}_{j,k})h^{n2}{}_{j,k}]\Big\}$$

$$+ \sum_{j=1}^J \sum_{k=1}^K \sum_{n=1}^N \lambda_{vj,k}^n \Big\{ V_{j,k}^{n+1} - V_{j,k}^{n-1} + \frac{\alpha}{4}\left[\frac{(V^n{}_{j,k} + V^n{}_{j,k+1})^2}{h^n{}_{j,k}} - \frac{(V^n{}_{j,k-1} + V^n{}_{j,k})^2}{h^n{}_{j,k-1}}\right]$$

$$+4\alpha\beta_{k-\frac{1}{2}}\left[\frac{(U^n{}_{j,k-1} + U^n{}_{j,k})(V^n{}_{j,k} + V^n{}_{j+1,k})}{h^n{}_{j,k} + h^n{}_{j,k-1} + h^n{}_{j+1,k-1} + h^n{}_{j+1,k}}\right.$$

$$\left.-\frac{(U^n{}_{j-1,k-1} + U^n{}_{j-1,k})(V^n{}_{j,k} + V^n{}_{j-1,k})}{h^n{}_{j,k} + h^n{}_{j,k-1} + h^n{}_{j-1,k} + h^n{}_{j-1,k-1}}\right]$$

$$+\frac{Cl_{k-\frac{1}{2}}}{8}\left[\frac{(U^n{}_{j,k} + U^n{}_{j-1,k} + U^n{}_{j,k-1} + U^n{}_{j-1,k-1})^2 - 16(V^n{}_{j,k})^2}{h^n{}_{j,k} + h^n{}_{j,k-1}}\right]$$

$$+Co_{k-\frac{1}{2}}(U^n{}_{j,k} + U^n{}_{j-1,k} + U^n{}_{j,k-1} + U^n{}_{j-1,k-1})$$

$$-\alpha A^1[V^n{}_{j,k+1} + V^n{}_{j,k-1} + 2V^n{}_{j,k} - 2(V_{j,k}^{n+1} + V_{j,k}^{n-1})]$$

$$-\alpha A_{k-\frac{1}{2}}^2[V^n{}_{j-1,k} + V^n{}_{j+1,k} + 2V^n{}_{j,k} - 2(V_{j,k}^{n+1} + V_{j,k}^{n-1})]$$

$$+\alpha A^3[\tan\theta_k(V^n{}_{j,k+1} - V^n{}_{j,k}) + \tan\theta_{k-1}(V^n{}_{j,k} - V^n{}_{j,k-1})]$$

$$-A_{k-\frac{1}{2}}^4 V^n{}_{j,k} - \alpha A_{k-\frac{1}{2}}^5[(U^n{}_{j,k} + U^n{}_{j,k-1}) - (U^n{}_{j-1,k} + U^n{}_{j-1,k-1})]$$

$$-\alpha\chi^v[(\rho_2 - \rho_1{}^n{}_{j,k})h^{n2}{}_{j,k} - (\rho_2 - \rho_1{}^n{}_{j,k-1})h^{n2}{}_{j,k-1}]\Big\}$$

$$+ \sum_{j=1}^J \sum_{k=1}^{K-1} \sum_{n=1}^N \lambda_{hj,k}^n \Big\{ h_{j,k}^{n+1} - h_{j,k}^{n-1} + 4\alpha\beta_k(U^n{}_{j,k} - U^n{}_{j-1,k})$$

$$+\alpha(V^n{}_{j,k+1} - V^n{}_{j,k}) - \frac{Cl_k}{2}(V^n{}_{j,k+1} + V^n{}_{j,k})\Big\}$$

(D.1)

where the $\lambda_{uj,k}^n, \lambda_{vj,k}^n, \lambda_{hj,k}^n$ are the undetermined Lagrange multipliers. Since the constraints in [Eq. (3.21), Eq. (3.22) and Eq. (3.23)] all equal to zero, the minimum of L is also a minimum of I. The minimum of L can be found by differentiating L with respect to each of the variables λs and model variables U, V, h and setting the results to zero:

$$\frac{\partial L}{\partial \lambda_u} = 0$$

$$\frac{\partial L}{\partial \lambda_v} = 0$$

$$\frac{\partial L}{\partial \lambda_h} = 0$$

$$\frac{\partial L}{\partial u} = 0$$

$$\frac{\partial L}{\partial v} = 0$$

$$\frac{\partial L}{\partial h} = 0$$

(D.2)

Equations simply return the model constraints [Eq. (3.21), Eq. (3.22) and Eq. (3.23)]

To determine the calculation of ρ, we first list all terms in L which contain $U^n_{j,k}$ and differentation with respect to $U^n_{j,k}$ yields:

$$
\begin{aligned}
\lambda_{u_{j,k}^n} \times & \left\{ 2\alpha\beta_k \left[\frac{U^n_{j,k} + U^n_{j+1,k}}{h^n_{j+1,k}} - \frac{U^n_{j-1,k} + U^n_{j,k}}{h^n_{j,k}} \right] + \right. \\
& \alpha \left[\frac{V^n_{j,k+1} + V^n_{j+1,k+1}}{h^n_{j,k+1} + h^n_{j,k} + h^n_{j+1,k+1} + h^n_{j+1,k}} - \right. \\
& \left. \frac{V^n_{j,k} + V^n_{j+1,k}}{h^n_{j,k-1} + h^n_{j,k} + h^n_{j+1,k-1} + h^n_{j+1,k}} \right] - \\
& Cl_k \frac{(V^n_{j,k} + V^n_{j,k+1} + V^n_{j+1,k} + V^n_{j+1,k+1})}{h^n_{j,k} + h^n_{j+1,k}} - \\
& \left. 2\alpha A^1 - 2\alpha A^2_k - \alpha A^3(\tan\theta_{k+\frac{1}{2}} - \tan\theta_{k-\frac{1}{2}}) - A^4_k \right\}
\end{aligned}
$$

$$+\lambda_{u_{j,k}^{n-1}} \times (1 + 2\alpha A^1 + 2\alpha A^2_k)$$

$$+\lambda_{u_{j,k}^{n+1}} \times (-1 + 2\alpha A^1 + 2\alpha A^2_k)$$

$$+\lambda_{u_{j,k+1}^n} \times \left\{ -\alpha \frac{V^n_{j,k+1} + V^n_{j+1,k+1}}{h^n_{j,k+1} + h^n_{j,k} + h^n_{j+1,k+1} + h^n_{j+1,k}} - \alpha A^1 - \alpha A^3 \tan\theta_{k+\frac{1}{2}} \right\}$$

$$+\lambda_{u_{j,k-1}^n} \times \left\{ \alpha \frac{V^n_{j,k} + V^n_{j+1,k}}{h^n_{j,k-1} + h^n_{j,k} + h^n_{j+1,k-1} + h^n_{j+1,k}} - \alpha A^1 + \alpha A^3 \tan\theta_{k-\frac{1}{2}} \right\}$$

$$+\lambda_{u_{j-1,k}^n} \times \left\{ 2\alpha\beta_k \frac{U^n_{j-1,k} + U^n_{j,k}}{h^n_{j,k}} - 2\alpha A^2_k \right\}$$

$$+\lambda_{u_{j+1,k}^n} \times \left\{ -2\alpha\beta_k \frac{U^n_{j,k} + U^n_{j+1,k}}{h^n_{j+1,k}} - 2\alpha A^2_k \right\}$$

$$
\begin{aligned}
+\lambda_{v_{j+1,k+1}^n} \times & \left\{ -4\alpha\beta_{k+\frac{1}{2}} \frac{V^n_{j,k+1} + V^n_{j+1,k+1}}{h^n_{j,k+1} + h^n_{j,k} + h^n_{j+1,k+1} + h^n_{j+1,k}} + \right. \\
& \frac{Cl_{k+\frac{1}{2}}}{4} \frac{(U^n_{j,k} + U^n_{j,k+1} + U^n_{j+1,k} + U^n_{j+1,k+1})}{h^n_{j+1,k} + h^n_{j+1,k+1}} + \\
& \left. Co_{k+\frac{1}{2}} + \alpha A^5_{k+\frac{1}{2}} \right\}
\end{aligned}
$$

$$+\lambda_{v\,j,k}^{n} \quad \times \quad \left\{ 4\alpha\beta_{k-\frac{1}{2}} \frac{V^{n}_{j,k} + V^{n}_{j+1,k}}{h^{n}_{j,k-1} + h^{n}_{j,k} + h^{n}_{j+1,k-1} + h^{n}_{j+1,k}} + \right.$$

$$\frac{Cl_{k-\frac{1}{2}}}{4} \frac{(U^{n}_{j,k} + U^{n}_{j-1,k} + U^{n}_{j,k-1} + U^{n}_{j-1,k-1})}{h^{n}_{j,k} + h^{n}_{j,k-1}} +$$

$$\left. Co_{k-\frac{1}{2}} - \alpha A^{5}_{k-\frac{1}{2}} \right\}$$

$$+\lambda_{v\,j+1,k}^{n} \quad \times \quad \left\{ -4\alpha\beta_{k-\frac{1}{2}} \frac{V^{n}_{j,k} + V^{n}_{j+1,k}}{h^{n}_{j,k-1} + h^{n}_{j,k} + h^{n}_{j+1,k-1} + h^{n}_{j+1,k}} + \right.$$

$$\frac{Cl_{k-\frac{1}{2}}}{4} \frac{(U^{n}_{j,k} + U^{n}_{j,k-1} + U^{n}_{j+1,k-1} + U^{n}_{j+1,k})}{h^{n}_{j+1,k-1} + h^{n}_{j+1,k}} +$$

$$\left. Co_{k-\frac{1}{2}} + \alpha A^{5}_{k-\frac{1}{2}} \right\}$$

$$+\lambda_{v\,j,k+1}^{n} \quad \times \quad \left\{ 4\alpha\beta_{k+\frac{1}{2}} \frac{V^{n}_{j,k+1} + V^{n}_{j+1,k+1}}{h^{n}_{j,k+1} + h^{n}_{j,k} + h^{n}_{j+1,k+1} + h^{n}_{j+1,k}} + \right.$$

$$\frac{Cl_{k+\frac{1}{2}}}{4} \frac{(U^{n}_{j,k} + U^{n}_{j,k+1} + U^{n}_{j-1,k} + U^{n}_{j-1,k+1})}{h^{n}_{j,k} + h^{n}_{j,k+1}} +$$

$$\left. Co_{k+\frac{1}{2}} - \alpha A^{5}_{k+\frac{1}{2}} \right\}$$

$$+\lambda_{h\,j,k}^{n} \quad \times \quad 4\alpha\beta_{4}$$

$$+\lambda_{h\,j+1,k}^{n} \quad \times \quad 4\alpha\beta_{4}$$

$$= \quad 0 \qquad\qquad\qquad (D.3)$$

Similarly, the differentation with respect to $V^{n}_{j,k}$ yields:

$$\lambda_{v\,j,k}^{n} \quad \times \quad \left\{ \frac{\alpha}{2} \left[\frac{V^{n}_{j,k} + V^{n}_{j,k+1}}{h^{n}_{j,k}} - \frac{V^{n}_{j,k-1} + V^{n}_{j,k}}{h^{n}_{j,k-1}} \right] + \right.$$

$$4\alpha\beta_{k-\frac{1}{2}} \left[\frac{U^{n}_{j,k-1} + U^{n}_{j,k}}{h^{n}_{j,k} + h^{n}_{j,k-1} + h^{n}_{j+1,k-1} + h^{n}_{j+1,k}} - \right.$$

$$\left. \frac{U^{n}_{j-1,k-1} + U^{n}_{j-1,k}}{h^{n}_{j,k} + h^{n}_{j,k-1} + h^{n}_{j-1,k} + h^{n}_{j-1,k-1}} \right] -$$

$$4Cl_{k-\frac{1}{2}} \frac{V^{n}_{j,k}}{h^{n}_{j,k} + h^{n}_{j,k-1}} - 2\alpha(A^{1} + A^{2}_{k-\frac{1}{2}}) +$$

$$\left. \alpha A^{3}(\tan\theta_{k-1} - \tan\theta k) - A^{4}_{k-\frac{1}{2}} \right\}$$

$$+\lambda_{v\,j,k}^{n-1} \quad \times \quad [2\alpha(A^{1} + A^{2}_{k-\frac{1}{2}}) + 1]$$

$$+\lambda_{v\,j,k}^{n+1} \quad \times \quad [2\alpha(A^{1} + A^{2}_{k-\frac{1}{2}}) - 1]$$

$$+\lambda_{v\,j,k+1}^{n} \quad \times \quad \left\{-\alpha(A^1 + A^3\tan\theta_k) - \frac{\alpha}{2}\frac{V^n_{j,k} + V^n_{j,k+1}}{h^n_{j,k}}\right\}$$

$$+\lambda_{v\,j,k-1}^{n} \quad \times \quad \left\{-\alpha(A^1 - A^3\tan\theta_{k-1}) + \frac{\alpha}{2}\frac{V^n_{j,k-1} + V^n_{j,k}}{h^n_{j,k-1}}\right\}$$

$$+\lambda_{v\,j-1,k}^{n} \quad \times \quad \left\{-\alpha A^2_{k-\frac{1}{2}} + 4\alpha\beta_{k-\frac{1}{2}}\frac{U^n_{j-1,k-1} + U^n_{j-1,k}}{h^n_{j,k} + h^n_{j,k-1} + h^n_{j-1,k} + h^n_{j-1,k-1}}\right\}$$

$$+\lambda_{v\,j+1,k}^{n} \quad \times \quad \left\{-\alpha A^2_{k-\frac{1}{2}} - 4\alpha\beta_{k-\frac{1}{2}}\frac{U^n_{j,k-1} + U^n_{j,k}}{h^n_{j,k} + h^n_{j,k-1} + h^n_{j+1,k-1} + h^n_{j+1,k}}\right\}$$

$$-\lambda_{u\,j,k}^{n} \quad \times \quad \left\{\alpha\frac{U^n_{j,k-1} + U^n_{j,k}}{h^n_{j,k} + h^n_{j,k-1} + h^n_{j+1,k-1} + h^n_{j+1,k}} + \right.$$
$$\left. Cl_k\frac{U^n_{j,k}}{h^n_{j,k} + h^n_{j+1,k}} + Co_k + \alpha A^5_k\right\}$$

$$-\lambda_{u\,j-1,k}^{n} \quad \times \quad \left\{\alpha\frac{U^n_{j-1,k-1} + U^n_{j-1,k}}{h^n_{j,k} + h^n_{j,k-1} + h^n_{j-1,k} + h^n_{j-1,k-1}} + \right.$$
$$\left. Cl_k\frac{U^n_{j-1,k}}{h^n_{j-1,k} + h^n_{j,k}} + Co_k - \alpha A^5_k\right\}$$

$$-\lambda_{u\,j,k-1}^{n} \quad \times \quad \left\{-\alpha\frac{U^n_{j,k-1} + U^n_{j,k}}{h^n_{j,k} + h^n_{j,k-1} + h^n_{j+1,k-1} + h^n_{j+1,k}} + \right.$$
$$\left. Cl_{k-1}\frac{U^n_{j,k-1}}{h^n_{j,k-1} + h^n_{j+1,k-1}} + Co_{k-1} + \alpha A^5_{k-1}\right\}$$

$$-\lambda_{u\,j-1,k-1}^{n} \quad \times \quad \left\{-\alpha\frac{U^n_{j-1,k-1} + U^n_{j-1,k}}{h^n_{j,k} + h^n_{j,k-1} + h^n_{j-1,k} + h^n_{j-1,k-1}} + \right.$$
$$\left. Cl_{k-1}\frac{U^n_{j-1,k-1}}{h^n_{j-1,k-1} + h^n_{j,k-1}} + Co_{k-1} - \alpha A^5_{k-1}\right\}$$

$$+\lambda_{h\,j,k}^{n} \quad \times \quad (\alpha - \frac{Cl_k}{2})$$

$$-\lambda_{h\,j,k-1}^{n} \quad \times \quad (\alpha - \frac{Cl_{k-1}}{2})$$

$$= \quad 0 \qquad\qquad\qquad\qquad\qquad (D.4)$$

and the differentation with respect to $h^n_{j,k}$ yields:

$$-\lambda_{h\,j,k}^{n+1}$$
$$+\lambda_{h\,j,k}^{n-1}$$
$$+\lambda_{u\,j,k}^{n} \quad \times \quad \left\{\alpha\beta_k\frac{(U^n_{j-1,k} + U^n_{j,k})^2}{h(^n_{j,k})^2} + \right.$$
$$Cl_kU^n_{j,k}\frac{(V^n_{j,k} + V^n_{j,k+1} + V^n_{j+1,k} + V^n_{j+1,k+1})}{(h^n_{j,k} + h^n_{j+1,k})^2} +$$

$$
\alpha\left[\frac{(U^n{}_{j,k}+U^n{}_{j,k-1})(V^n{}_{j,k}+V^n{}_{j+1,k})}{(h^n{}_{j,k}+h^n{}_{j,k-1}+h^n{}_{j+1,k}+h^n{}_{j+1,k-1})^2}-\right.
$$

$$
\left.\left.\frac{(U^n{}_{j,k}+U^n{}_{j,k+1})(V^n{}_{j,k+1}+V^n{}_{j+1,k+1})}{(h^n{}_{j,k}+h^n{}_{j,k+1}+h^n{}_{j+1,k}+h^n{}_{j+1,k+1})^2}\right]\right\}
$$

$$
+\lambda_{u}{}^n{}_{j-1,k}\quad\times\quad\left\{-\alpha\beta_k\frac{(U^n{}_{j-1,k}+U^n{}_{j,k})^2}{h(^n{}_{j,k})^2}+\right.
$$

$$
Cl_kU^n{}_{j-1,k}\frac{(V^n{}_{j,k}+V^n{}_{j,k+1}+V^n{}_{j-1,k}+V^n{}_{j-1,k+1})}{(h^n{}_{j,k}+h^n{}_{j-1,k})^2}+
$$

$$
\alpha\left[\frac{(U^n{}_{j-1,k}+U^n{}_{j-1,k-1})(V^n{}_{j,k}+V^n{}_{j-1,k})}{(h^n{}_{j,k}+h^n{}_{j,k-1}+h^n{}_{j-1,k}+h^n{}_{j-1,k-1})^2}-\right.
$$

$$
\left.\left.\frac{(U^n{}_{j-1,k}+U^n{}_{j-1,k+1})(V^n{}_{j,k+1}+V^n{}_{j-1,k+1})}{(h^n{}_{j,k}+h^n{}_{j,k+1}+h^n{}_{j-1,k}+h^n{}_{j-1,k+1})^2}\right]\right\}
$$

$$
+\lambda_{u}{}^n{}_{j,k+1}\quad\times\quad\alpha\frac{(U^n{}_{j,k+1}+U^n{}_{j,k})(V^n{}_{j,k+1}+V^n{}_{j+1,k+1})}{(h^n{}_{j,k+1}+h^n{}_{j,k}+h^n{}_{j+1,k+1}+h^n{}_{j+1,k})^2}
$$

$$
-\lambda_{u}{}^n{}_{j,k-1}\quad\times\quad\alpha\frac{(U^n{}_{j,k-1}+U^n{}_{j,k})(V^n{}_{j,k}+V^n{}_{j+1,k})}{(h^n{}_{j,k-1}+h^n{}_{j,k}+h^n{}_{j+1,k-1}+h^n{}_{j+1,k})^2}
$$

$$
+\lambda_{u}{}^n{}_{j-1,k+1}\quad\times\quad\alpha\frac{(U^n{}_{j-1,k+1}+U^n{}_{j-1,k})(V^n{}_{j-1,k+1}+V^n{}_{j,k+1})}{(h^n{}_{j-1,k+1}+h^n{}_{j,k}+h^n{}_{j-1,k}+h^n{}_{j,k+1})^2}
$$

$$
-\lambda_{u}{}^n{}_{j-1,k-1}\quad\times\quad\alpha\frac{(U^n{}_{j-1,k-1}+U^n{}_{j-1,k})(V^n{}_{j-1,k}+V^n{}_{j,k})}{(h^n{}_{j-1,k-1}+h^n{}_{j,k}+h^n{}_{j-1,k}+h^n{}_{j,k-1})^2}
$$

$$
+\lambda_{v}{}^n{}_{j,k}\quad\times\quad\left\{-\frac{\alpha}{4}\frac{(V^n{}_{j,k}+V^n{}_{j,k+1})^2}{(h^n{}_{j,k})^2}+\right.
$$

$$
4\alpha\beta_{k-\frac{1}{2}}\left[\frac{(U^n{}_{j-1,k-1}+U^n{}_{j-1,k})(V^n{}_{j,k}+V^n{}_{j-1,k})}{(h^n{}_{j,k}+h^n{}_{j,k-1}+h^n{}_{j-1,k}+h^n{}_{j-1,k-1})^2}-\right.
$$

$$
\left.\frac{(U^n{}_{j,k-1}+U^n{}_{j,k})(V^n{}_{j,k}+V^n{}_{j+1,k})}{(h^n{}_{j,k}+h^n{}_{j,k-1}+h^n{}_{j+1,k-1}+h^n{}_{j+1,k})^2}\right]-
$$

$$
\left.\left.\frac{Cl_{k-\frac{1}{2}}}{8}\left[\frac{(U^n{}_{j,k}+U^n{}_{j-1,k}+U^n{}_{j,k-1}+U^n{}_{j-1,k-1})^2-16(V^n{}_{j,k})^2}{(h^n{}_{j,k}+h^n{}_{j,k-1})^2}\right]\right\}\right.
$$

$$
+\lambda_{v}{}^n{}_{j,k+1}\quad\times\quad\left\{\frac{\alpha}{4}\frac{(V^n{}_{j,k}+V^n{}_{j,k+1})^2}{(h^n{}_{j,k})^2}+\right.
$$

$$
4\alpha\beta_{k+\frac{1}{2}}\left[\frac{(U^n{}_{j-1,k}+U^n{}_{j-1,k+1})(V^n{}_{j,k+1}+V^n{}_{j-1,k+1})}{(h^n{}_{j,k}+h^n{}_{j,k+1}+h^n{}_{j-1,k}+h^n{}_{j-1,k+1})^2}-\right.
$$

$$
\left.\frac{(U^n{}_{j,k}+U^n{}_{j,k+1})(V^n{}_{j,k+1}+V^n{}_{j+1,k+1})}{(h^n{}_{j,k}+h^n{}_{j,k+1}+h^n{}_{j+1,k}+h^n{}_{j+1,k+1})^2}\right]-
$$

$$
\left.\left.\frac{Cl_{k+\frac{1}{2}}}{8}\left[\frac{(U^n{}_{j,k}+U^n{}_{j-1,k}+U^n{}_{j,k+1}+U^n{}_{j-1,k+1})^2-16(V^n{}_{j,k+1})^2}{(h^n{}_{j,k}+h^n{}_{j,k+1})^2}\right]\right\}\right.
$$

$$
+\lambda_{v}{}^n{}_{j+1,k+1}\quad\times\quad4\alpha\beta_{k+\frac{1}{2}}\frac{(U^n{}_{j,k}+U^n{}_{j,k+1})(V^n{}_{j,k+1}+V^n{}_{j+1,k+1})}{(h^n{}_{j,k}+h^n{}_{j,k+1}+h^n{}_{j+1,k}+h^n{}_{j+1,k+1})^2}
$$

$$+\lambda_{v_{j+1,k}}^{n} \quad \times \quad 4\alpha\beta_{k-\frac{1}{2}} \frac{(U^{n}_{j,k-1} + U^{n}_{j,k})(V^{n}_{j,k} + V^{n}_{j+1,k})}{(h^{n}_{j,k} + h^{n}_{j,k-1} + h^{n}_{j+1,k-1} + h^{n}_{j+1,k})^{2}}$$

$$-\lambda_{v_{j-1,k+1}}^{n} \quad \times \quad 4\alpha\beta_{k+\frac{1}{2}} \frac{(U^{n}_{j-1,k} + U^{n}_{j-1,k+1})(V^{n}_{j,k+1} + V^{n}_{j-1,k+1})}{(h^{n}_{j,k} + h^{n}_{j,k+1} + h^{n}_{j-1,k} + h^{n}_{j-1,k+1})^{2}}$$

$$-\lambda_{v_{j-1,k}}^{n} \quad \times \quad 4\alpha\beta_{k-\frac{1}{2}} \frac{(U^{n}_{j-1,k-1} + U^{n}_{j-1,k})(V^{n}_{j,k} + V^{n}_{j-1,k})}{(h^{n}_{j,k} + h^{n}_{j,k-1} + h^{n}_{j-1,k} + h^{n}_{j-1,k-1})^{2}}$$

$$= \quad 0 \tag{D.5}$$

Rearranging [Eq. (D.3)] and putting it on the left hand side, and referring to [Eq. (B.41)] on the right hand side yield

$$-\underbrace{(\lambda_{u_{j,k}}^{n+1} - \lambda_{u_{j,k}}^{n-1})}_{a} \quad \Leftarrow \quad -\frac{\partial\lambda_{u}}{\partial t}$$

$$-2\alpha\beta_{k}\left\{\underbrace{\frac{U^{n}_{j,k} + U^{n}_{j+1,k}}{h^{n}_{j+1,k}}(\lambda_{u_{j+1,k}}^{n} - \lambda_{u_{j,k}}^{n})}_{b_{1}} + \right.$$

$$\left. \underbrace{\frac{U^{n}_{j-1,k} + U^{n}_{j,k}}{h^{n}_{j,k}}(\lambda_{u_{j,k}}^{n} - \lambda_{u_{j-1,k}}^{n})}_{b_{2}}\right\} \quad \Leftarrow \quad -\frac{2U}{ha\cos\theta}\frac{\partial\lambda_{u}}{\partial\phi}$$

$$-\alpha\left\{\underbrace{\frac{V^{n}_{j,k+1} + V^{n}_{j+1,k+1}}{h^{n}_{j,k+1} + h^{n}_{j,k} + h^{n}_{j+1,k+1} + h^{n}_{j+1,k}}(\lambda_{u_{j,k+1}}^{n} - \lambda_{u_{j,k}}^{n})}_{c_{1}} + \right.$$

$$\left. \underbrace{\frac{V^{n}_{j,k} + V^{n}_{j+1,k}}{h^{n}_{j,k-1} + h^{n}_{j,k} + h^{n}_{j+1,k-1} + h^{n}_{j+1,k}}(\lambda_{u_{j,k}}^{n} - \lambda_{u_{j,k-1}}^{n})}_{c_{2}}\right\} \quad \Leftarrow \quad -\frac{V}{ha}\frac{\partial\lambda_{u}}{\partial\theta}$$

$$-\underbrace{\frac{Cl_{k}}{2}\frac{(V^{n}_{j,k} + V^{n}_{j,k+1} + V^{n}_{j+1,k} + V^{n}_{j+1,k+1})}{h^{n}_{j,k} + h^{n}_{j+1,k}}\lambda_{u_{j,k}}^{n}}_{d} \quad \Leftarrow \quad -\frac{2\tan\theta U}{ha}\lambda_{v}$$

$$+\frac{1}{4}\left\{Cl_{k-\frac{1}{2}}\left[\underbrace{\frac{(U^{n}_{j,k} + U^{n}_{j,k-1} + U^{n}_{j+1,k-1} + U^{n}_{j+1,k})}{h^{n}_{j+1,k-1} + h^{n}_{j+1,k}}\lambda_{v_{j+1,k}}^{n}}_{e_{1}} + \right.\right.$$

$$\left.\underbrace{\frac{(U^{n}_{j,k} + U^{n}_{j-1,k} + U^{n}_{j,k-1} + U^{n}_{j-1,k-1})}{h^{n}_{j,k} + h^{n}_{j,k-1}}\lambda_{v_{j,k}}^{n}}_{e_{2}}\right] +$$

$$Cl_{k+\frac{1}{2}}\left[\underbrace{\frac{(U^{n}_{j,k} + U^{n}_{j,k+1} + U^{n}_{j+1,k} + U^{n}_{j+1,k+1})}{h^{n}_{j+1,k} + h^{n}_{j+1,k+1}}\lambda_{v_{j+1,k+1}}^{n}}_{e_{3}} + \right.$$

$$\left.\frac{(U^n{}_{j,k} + U^n{}_{j,k+1} + U^n{}_{j-1,k} + U^n{}_{j-1,k+1})}{h^n{}_{j,k} + h^n{}_{j,k+1}}\lambda_{v}{}^n_{j,k+1}\right]\right\} \quad \Leftarrow \quad -\frac{2\tan\theta U}{ha}\lambda_v$$

$$\underbrace{\hphantom{\frac{(U^n{}_{j,k} + U^n{}_{j,k+1} + U^n{}_{j-1,k} + U^n{}_{j-1,k+1})}{h^n{}_{j,k} + h^n{}_{j,k+1}}}}_{e_4}$$

$$-4\alpha\left\{\underbrace{\frac{\beta_{k-\frac{1}{2}}(V^n{}_{j,k} + V^n{}_{j+1,k})}{h^n{}_{j,k-1} + h^n{}_{j,k} + h^n{}_{j+1,k-1} + h^n{}_{j+1,k}}(\lambda_{v}{}^n_{j+1,k} - \lambda_{v}{}^n_{j,k}) +}_{f_1}\right.$$

$$\left.\underbrace{\frac{\beta_{k+\frac{1}{2}}(V^n{}_{j,k+1} + V^n{}_{j+1,k+1})}{h^n{}_{j,k+1} + h^n{}_{j,k} + h^n{}_{j+1,k+1} + h^n{}_{j+1,k}}(\lambda_{v}{}^n_{j+1,k+1} - \lambda_{v}{}^n_{j,k+1})}_{f_2}\right\} \quad \Leftarrow \quad -\frac{V}{ha\cos\theta}\frac{\partial\lambda_v}{\partial\phi}$$

$$+\underbrace{\left\{Co_{k-\frac{1}{2}}(\lambda_{v}{}^n_{j,k} + \lambda_{v}{}^n_{j+1,k}) + Co_{k+\frac{1}{2}}(\lambda_{v}{}^n_{j+1,k+1} + \lambda_{v}{}^n_{j,k+1})\right\}}_{g} \quad \Leftarrow \quad 2\Omega\sin\theta\lambda_v$$

$$-4\alpha\beta_k\underbrace{(\lambda_{h}{}^n_{j+1,k} - \lambda_{h}{}^n_{j,k})}_{h} \quad \Leftarrow \quad -\frac{1}{a\cos\theta}\frac{\partial\lambda_h}{\partial\phi}$$

$$-\alpha\left\{\underbrace{A^1\left[\lambda_{u}{}^n_{j,k+1} + \lambda_{u}{}^n_{j,k-1} + 2\lambda_{u}{}^n_{j,k} - 2(\lambda_{u}{}^{n+1}_{j,k} + \lambda_{u}{}^{n-1}_{j,k})\right] +}_{i_1}\right.$$

$$\underbrace{A^2_k\left[\lambda_{u}{}^n_{j,k+1} + \lambda_{u}{}^n_{j,k-1} + 2\lambda_{u}{}^n_{j,k} - 2(\lambda_{u}{}^{n+1}_{j,k} + \lambda_{u}{}^{n-1}_{j,k})\right] -}_{i_2}$$

$$\left.\underbrace{A^3\left[\tan\theta_{k+\frac{1}{2}}(\lambda_{u}{}^n_{j,k+1} - \lambda_{u}{}^n_{j,k}) + \tan\theta_{k-\frac{1}{2}}(\lambda_{u}{}^n_{j,k} - \lambda_{u}{}^n_{j,k-1})\right]}_{i_3}\right\} \quad \Leftarrow \quad -A\Delta(\lambda_u)$$

$$+\alpha\underbrace{\left\{A^5_{k-\frac{1}{2}}(\lambda_{v}{}^n_{j+1,k} - \lambda_{v}{}^n_{j,k}) + A^5_{k+\frac{1}{2}}(\lambda_{v}{}^n_{j+1,k+1} - \lambda_{v}{}^n_{j,k+1})\right\}}_{i_4} \quad \Leftarrow \quad A\frac{2\tan\theta}{a^2\cos\theta}\frac{\partial\lambda_v}{\partial\phi}$$

$$-\underbrace{A^4_k\lambda_{u}{}^n_{j,k}}_{i_5} \quad \Leftarrow \quad -A\frac{1-\tan^2\theta}{a^2}\lambda_u$$

$$= 0 \qquad\qquad (D.6)$$

Therefore, we have proven the identity between the discretization of the continuous adjoint equations and the adjoint equations which are from discretized model equations with the Arakawa C for the adjoint U equation.

For the adjoint V equation, the similar proof is as follows, rearranging [Eq. (D.4)] and refering to [Eq. (B.42)]

$$-\underbrace{(\lambda_{v\,j,k}^{n+1} - \lambda_{v\,j,k}^{n-1})}_{a} \quad \Leftarrow \quad -\frac{\partial \lambda_v}{\partial t}$$

$$-4\alpha\beta_{k-\frac{1}{2}}\left\{ \underbrace{\frac{U^n_{j,k-1} + U^n_{j,k}}{h^n_{j,k} + h^n_{j,k-1} + h^n_{j+1,k-1} + h^n_{j+1,k}}(\lambda_{v\,j+1,k}^n - \lambda_{v\,j,k}^n)}_{b_1} + \right.$$

$$\left. \underbrace{\frac{U^n_{j-1,k-1} + U^n_{j-1,k}}{h^n_{j,k} + h^n_{j,k-1} + h^n_{j-1,k} + h^n_{j-1,k-1}}(\lambda_{v\,j,k}^n - \lambda_{v\,j-1,k}^n)}_{b_2}\right\} \quad \Leftarrow \quad -\frac{U}{ha\cos\theta}\frac{\partial\lambda_v}{\partial\phi}$$

$$-\frac{\alpha}{2}\left\{ \underbrace{\frac{V^n_{j,k} + V^n_{j,k+1}}{h^n_{j,k}}(\lambda_{v\,j,k+1}^n - \lambda_{v\,j,k}^n)}_{c_1} + \right.$$

$$\left. \underbrace{\frac{V^n_{j,k-1} + V^n_{j,k}}{h^n_{j,k-1}}(\lambda_{v\,j,k}^n - \lambda_{v\,j,k-1}^n)}_{c_2}\right\} \quad \Leftarrow \quad -\frac{2V}{ha}\frac{\partial\lambda_v}{\partial\theta}$$

$$-\alpha\left\{ \underbrace{\frac{U^n_{j,k-1} + U^n_{j,k}}{h^n_{j,k} + h^n_{j,k-1} + h^n_{j+1,k-1} + h^n_{j+1,k}}(\lambda_{u\,j,k}^n - \lambda_{u\,j,k-1}^n)}_{d_1} + \right.$$

$$\left. \underbrace{\frac{U^n_{j-1,k-1} + U^n_{j-1,k}}{h^n_{j,k} + h^n_{j,k-1} + h^n_{j-1,k} + h^n_{j-1,k-1}}(\lambda_{u\,j-1,k}^n - \lambda_{u\,j-1,k-1}^n)}_{d_2}\right\} \quad \Leftarrow \quad -\frac{U}{ha}\frac{\partial\lambda_u}{\partial\theta}$$

$$-\frac{1}{2}\left\{ \underbrace{C'l_{k-1}\frac{U^n_{j-1,k-1}\lambda_{u\,j-1,k-1}^n}{h^n_{j-1,k-1} + h^n_{j,k-1}} + \frac{U^n_{j,k-1}\lambda_{u\,j,k-1}^n}{h^n_{j,k-1} + h^n_{j+1,k-1}}}_{e_1} + \right.$$

$$\left. \underbrace{Cl_k\frac{U^n_{j-1,k}\lambda_{u\,j-1,k}^n}{h^n_{j-1,k} + h^n_{j,k}} + \frac{U^n_{j,k}\lambda_{u\,j,k}^n}{h^n_{j,k} + h^n_{j+1,k}}}_{e_2}\right\} \quad \Leftarrow \quad -\frac{\tan\theta U}{ha}\lambda_u$$

$$-4C'l_{k-\frac{1}{2}}\underbrace{\frac{V^n_{j,k}}{h^n_{j,k} + h^n_{j,k-1}}\lambda_{v\,j,k}^n}_{d}$$

$$-\underbrace{\left\{ C'o_{k-1}(\lambda_{u\,j-1,k-1}^n + \lambda_{u\,j,k-1}^n) + Co_k(\lambda_{u\,j-1,k}^n + \lambda_{u\,j,k}^n)\right\}}_{f} \quad \Leftarrow \quad -2\Omega\sin\theta\lambda_u$$

$$-\underbrace{\alpha(\lambda_{h\,j,k}^n - \lambda_{h\,j,k-1}^n)}_{g} \quad \Leftarrow \quad -\frac{1}{a}\frac{\partial\lambda_h}{\partial\theta}$$

$$-\alpha\Bigg\{\underbrace{A^1\Big[\lambda_{vj,k+1}^n + \lambda_{vj,k-1}^n + 2\lambda_{vj,k}^n - 2(\lambda_{vj,k}^{n+1} + \lambda_{vj,k}^{n-1})\Big]}_{i_1} +$$

$$\underbrace{A_{k-\frac{1}{2}}^2\Big[\lambda_{vj,k+1}^n + \lambda_{vj,k-1}^n + 2\lambda_{vj,k}^n - 2(\lambda_{vj,k}^{n+1} + \lambda_{vj,k}^{n-1})\Big]}_{i_2} -$$

$$\underbrace{A^3\Big[\tan\theta_k(\lambda_{vj,k+1}^n - \lambda_{vj,k}^n) + \tan\theta_{k-1}(\lambda_{vj,k}^n - \lambda_{vj,k-1}^n)\Big]}_{i_3}\Bigg\} \quad \Leftarrow \quad -A\Delta(\lambda_v)$$

$$-\underbrace{A_{k-\frac{1}{2}}^4\lambda_{vj,k}^n}_{i_4} \quad \Leftarrow \quad -A\frac{1-\tan^2\theta}{a^2}\lambda_v$$

$$-\alpha\underbrace{\Big\{A_{k-1}^5(\lambda_{uj,k-1}^n - \lambda_{uj-1,k-1}^n) + A_k^5(\lambda_{uj,k}^n - \lambda_{uj-1,k}^n)\Big\}}_{i_5} \quad \Leftarrow \quad -A\frac{2\tan\theta}{a^2\cos\theta}\frac{\partial\lambda_u}{\partial\phi}$$

$$= 0 \qquad\qquad (D.7)$$

Finally the adjoint h equation, rearranging [Eq. (D.5)] and refering to [Eq. (B.43)

$$-\underbrace{(\lambda_{hj,k}^{n+1} - \lambda_{hj,k}^{n-1})}_{a} \quad \Leftarrow \quad -\frac{\partial\lambda_h}{\partial t}$$

$$+\underbrace{\alpha\beta_k\frac{(U_{j-1,k}^n + U_{j,k}^n)^2}{h(_{j,k}^n)^2}(\lambda_{uj,k}^n - \lambda_{uj-1,k}^n)}_{b} \quad \Leftarrow \quad \frac{U^2}{ah^2\cos\theta}\frac{\partial\lambda_u}{\partial\phi}$$

$$+4\alpha\Bigg\{\beta_{k+\frac{1}{2}}\Bigg[\underbrace{\frac{(U_{j,k}^n + U_{j,k+1}^n)(V_{j,k+1}^n + V_{j+1,k+1}^n)}{(h_{j,k}^n + h_{j,k+1}^n + h_{j+1,k}^n + h_{j+1,k+1}^n)^2}(\lambda_{vj+1,k+1}^n - \lambda_{vj,k+1}^n)}_{c_1} +$$

$$\underbrace{\frac{(U_{j-1,k}^n + U_{j-1,k+1}^n)(V_{j,k+1}^n + V_{j-1,k+1}^n)}{(h_{j,k}^n + h_{j,k+1}^n + h_{j-1,k}^n + h_{j-1,k+1}^n)^2}(\lambda_{vj,k+1}^n - \lambda_{vj-1,k+1}^n)}_{c_2}\Bigg] +$$

$$\beta_{k-\frac{1}{2}}\Bigg[\underbrace{\frac{(U_{j,k-1}^n + U_{j,k}^n)(V_{j,k}^n + V_{j+1,k}^n)}{(h_{j,k}^n + h_{j,k-1}^n + h_{j+1,k-1}^n + h_{j+1,k}^n)^2}(\lambda_{vj+1,k}^n - \lambda_{vj,k}^n)}_{c_3} +$$

$$\underbrace{\frac{(U_{j-1,k-1}^n + U_{j-1,k}^n)(V_{j,k}^n + V_{j-1,k}^n)}{(h_{j,k}^n + h_{j,k-1}^n + h_{j-1,k}^n + h_{j-1,k-1}^n)^2}(\lambda_{vj,k}^n - \lambda_{vj-1,k}^n)}_{c_4}\Bigg]\Bigg\} \quad \Leftarrow \quad \frac{UV}{ah^2\cos\theta}\frac{\partial\lambda_v}{\partial\phi}$$

$$+\alpha\left\{\underbrace{\frac{(U^n_{j,k+1}+U^n_{j,k})(V^n_{j,k+1}+V^n_{j+1,k+1})}{(h^n_{j,k+1}+h^n_{j,k}+h^n_{j+1,k+1}+h^n_{j+1,k})^2}(\lambda_{u\,j,k+1}^{\,n}-\lambda_{u\,j,k}^{\,n})+}_{d_1}\right.$$

$$\underbrace{\frac{(U^n_{j,k}+U^n_{j,k-1})(V^n_{j,k}+V^n_{j+1,k})}{(h^n_{j,k}+h^n_{j,k-1}+h^n_{j+1,k}+h^n_{j+1,k-1})^2}(\lambda_{u\,j,k}^{\,n}-\lambda_{u\,j,k-1}^{\,n})+}_{d_2}$$

$$\underbrace{\frac{(U^n_{j-1,k}+U^n_{j-1,k-1})(V^n_{j,k}+V^n_{j-1,k})}{(h^n_{j,k}+h^n_{j,k-1}+h^n_{j-1,k}+h^n_{j-1,k-1})^2}(\lambda_{u\,j-1,k}^{\,n}-\lambda_{u\,j-1,k-1}^{\,n})+}_{d_3}$$

$$\left.\underbrace{\frac{(U^n_{j-1,k-1}+U^n_{j-1,k})(V^n_{j-1,k}+V^n_{j,k})}{(h^n_{j-1,k-1}+h^n_{j,k}+h^n_{j-1,k}+h^n_{j,k-1})^2}(\lambda_{u\,j-1,k+1}^{\,n}-\lambda_{u\,j-1,k}^{\,n})}_{d_4}\right\}\quad\Leftarrow\quad\frac{UV}{ah^2}\frac{\partial\lambda_u}{\partial\theta}$$

$$+\underbrace{\frac{\alpha}{4}\frac{(V^n_{j,k}+V^n_{j,k+1})^2}{(h^n_{j,k})^2}(\lambda_{v\,j,k+1}^{\,n}-\lambda_{v\,j,k}^{\,n})}_{e}\quad\Leftarrow\quad\frac{V^2}{ah^2}\frac{\partial\lambda_v}{\partial\theta}$$

$$+\frac{Cl_k}{2}\left\{\underbrace{U^n_{j,k}\frac{(V^n_{j,k}+V^n_{j,k+1}+V^n_{j+1,k}+V^n_{j+1,k+1})}{(h^n_{j,k}+h^n_{j+1,k})^2}\lambda_{u\,j,k}^{\,n}+}_{f_1}\right.$$

$$\left.\underbrace{U^n_{j-1,k}\frac{(V^n_{j,k}+V^n_{j,k+1}+V^n_{j-1,k}+V^n_{j-1,k+1})}{(h^n_{j,k}+h^n_{j-1,k})^2}\lambda_{u\,j-1,k}^{\,n}}_{f_2}\right\}\quad\Leftarrow\quad\frac{UV\tan\theta}{ah^2}\lambda_u$$

$$-\frac{1}{8}\left\{\underbrace{Cl_{k-\frac{1}{2}}\frac{(U^n_{j,k}+U^n_{j-1,k}+U^n_{j,k-1}+U^n_{j-1,k-1})^2}{(h^n_{j,k}+h^n_{j,k-1})^2}\lambda_{v\,j,k}^{\,n}+}_{g_1}\right.$$

$$\left.\underbrace{Cl_{k+\frac{1}{2}}\frac{(U^n_{j,k}+U^n_{j-1,k}+U^n_{j,k+1}+U^n_{j-1,k+1})^2}{(h^n_{j,k}+h^n_{j,k+1})^2}\lambda_{v\,j,k+1}^{\,n}}_{g_2}\right\}\quad\Leftarrow\quad\frac{U^2\tan\theta}{ah^2}\lambda_v$$

$$=0\qquad\qquad\text{(D.8)}$$

BIBLIOGRAPHY

[1] Anderson, D. L. T., 1991: Data assimilation in ocean models. *Strategies for future climate research*, M. Latif, Ed., Max-Plank-Institut für Meteorologie, Hamburg, Germany, 193-225.

[2] Anthes, R. A., 1974: Data assimilation and initialization of hurricane prediction models. *J. Atmos. Sci.*, **31**, 702-719.

[3] Barth, N. and C. Wunsch, 1992: Oceanographic experiment design by simulated annealing. *J. Phys. Oceanogr.*, **20**, 1249-1263.

[4] Banks, H. T. and K. Kunisch, 1989: *Estimation techniques for distributed parameter systems.* Birkhauser, Boston (Systems & Control: Formulations & Applications), Vol. 11, 315 pp.

[5] Bennett, A. F., 1992: *Inverse Methods in Physical Oceanography.* Cambridge University Press, 346 pp.

[6] Bergthorsson, P., and B. Doos, 1955: Numerical weather map analysis. *Tellus*, **7**, 329-340

[7] Bertsekas, D. P. 1982: *Constrained optimization and Lagrange multiplier methods.* Addison-Wesley, 4,91 pp.

[8] Buckley, A. G. and A. Lenir, 1983: QN-like variable storage conjugate gradients. *Math. Prog.*, **27**, 155-175.

[9] Burger, J., J. L. Brizaut and M. Pogu, 1992: Comparison of two methods for the calculation of the gradient and of the Hessian of the cost functions associated

with differential systems. *Mathematics and Computers in Simulation*, **34**, 551-562.

[10] Bus, J. C. P., 1977: Convergence of Newton-like methods for solving systems of nonlinear equations. *Numerische Mathematik*, **27**, 271-281.

[11] Cacuci, D. G., 1981: Sensitivity theory for nonlinear systems. I: Nonlinear functional analysis approach. *J. Math. Phy.* **22** (12),2794-2803.

[12] Cacuci, D. G., 1981: Sensitivity theory for nonlinear systems. II. Extensions to additional classes of responses. *J. Math. Phy.* **22** (12), 2803-2812.

[13] Cacuci, D. G., 1988: The forward and adjoint methods of sensitivity analysis. 71-144. In: *Uncertainty Analysis*, Yigal Ronen, CRC Press, Inc., pp 282.

[14] Camerlengo, A. L. and J. J. O'Brien, 1980: Open boundary conditions in rotating fluids. *J. Comp. Phys.*, **35**, 12-35.

[15] Carrera, J. and P. S. Neuman, 1986: Estimation of aquifer parameters under transient and steady state conditions, 1: Maximum likelihood method method incorporating prior information. *Water Resources Research*, **22** (2), 199-210.

[16] Carrera, J. and P. S. Neuman, 1986: Estimation of aquifer parameters under transient and steady state conditions, 2: Uniqueness, stability and solution algorithms. *Water Resources Research*, **22** (2), 211-227.

[17] Carrera, J. and P. S. Neuman, 1986: Estimation of aquifer parameters under transient and steady state conditions, 3: Application to synthetic and field data. *Water Resources Research*, **22** (2), 228-242.

[18] Chao W. C. and L. Chang, 1991: Development of a 4-dimensional analysis system using the adjoint method at GLA. part 1: dynamics. *Mon. Wea. Rev.*, **120**, 1661-1673.

[19] Cohn, S. E., 1982: *Methods of sequential estimation for determining initial data in numerical weather prediction.* Ph.D Thesis, New York University, 183 pp.

[20] Courant, R. and D. Hilbert, 1953: *Methods of Mathematical Physics*, vol. **1**. New York: Wiley Interscience, 560 pp.

[21] Courant, R. and D. Hilbert, 1962: *Methods of Mathematical Physics*, vol. **2**. New York: Wiley Interscience, 830 pp.

[22] Courtier, P. and O.Talagrand, 1987: Variational assimilation of meteorological observations with the adjoint equations Part 2. Numerical results.*Q. J. R. Meteorol. Soc.*, **113**, 1329-1347.

[23] Courtier, P. and O.Talagrand, 1990: Variational assimilation of meteorological observations with direct and adjoint shallow-water equations. *Tellus.*, **42A**, 531-549.

[24] Cressman, G., 1959: An operational objective analysis system. *Mon. Wea. Rev.*, **87**, 367-374.

[25] Daley, R., 1991: *Atmospheric data analysis.* Cambridge University Press, Cambridge, 457 pp.

[26] Daley, R, 1993: Estimating observation error statistics for atmospheric data assimilation. *Ann. Geophysicae*, **11**, 634-647.

[27] Daley. R, and R. Menard, 1993: Evaluation of assimilation systems. Notes for three lectures at the international summer school on assimilation of meteorological and oceanographic observations. La Garde, France, August 2-27.

[28] Das, S. K. and R. W. Lardner, 1992: Variational parameter estimation for a two-dimensional numerical tidal model. *International Journal for Numerical Methods in Fluids*, **15**, 313-327.

[29] Derber, J. C.,1985: *The variational four dimensional assimilation of analysis using filtered models as constraints.* Ph.D. Thesis, Univ. of Wisconsin-Madison, 141 pp.

[30] Derber, J. C.,1987: Variational four dimensional analysis using the quasi-geostrophic constraint. *Mon. Wea. Rev.*, **115**, 998-1008.

[31] Derber, J. C., 1989: A variational continuous assimilation technique. *Mon. Wea. Rev.*, **117**, 2437-2446.

[32] Fletcher, R., 1980: *Practical methods of optimization. Vol. 2: Constrained optimization.* John Wiley and Sons, New York, 224 pp.

[33] Fletcher, R., 1987: *Practical methods of optimization. Volume 1. 2nd ed.*, John Wiley and Sons, Chichester, New York, 431 pp.

[34] Gandin, L. S., 1963: *Objective analysis of meteorological fields.* Gidrometeorol. Izd. Leningrad (in Russian), English Translation by Israel Program for Scientific Translations, Jerusalem, 1965, 242 pp.

[35] Ghil, M., J. Tavantzis, K. Bube, and E. Isaacson, 1981: Application of estimation theory to numerical weather prediction. In: Dynamic Meteorology: Data Assimilation Methods, Bengtsson et al. (ed) Springer-Vergag, 139-224.

[36] Ghil, M., 1986: Sequential estimation and satellite data assimilation in meteorology and oceanography. Y. K. Sasaki, T. Gal-Chen, L. White, M. M. Zaman, C. Zieler, L. P. Chang and D. J. Rusk (ed.), *Variational Methods in Geosciences*, Elsevier, Amsterdam, 91-100.

[37] Ghil, M. and P. Malonotte-Rizzoli, 1991: Data assimilation in meteorology and oceanography. *Adv. Geophys.*, **33**, 141-266.

[38] Gill, P. E. and W. Murray, 1981: *Practical optimization.* Academic Press, 401 pp.

[39] Grammeltvedt, A., 1969: A survey of finite-difference schemes for the primitive equations for a barotropic fluid. *Mon. Wea. Rev.*, **97**, 387-404.

[40] Hao, Z., 1994: Data assimilation for interannual climate-change prediction. Ph.D dissertation, Department of atmospheric sciences, Univerisity of California, Los Angeles, 224 pp.

[41] Johnson, M. A. and J. J. O'Brien, 1989: The northeast Pacific Ocean response to the 1982-1983 El Niño. *J. Geophys. Res.*, **95**, 7155-7166.

[42] Kalman, R. E., 1960: A new approach to linear filtering and prediction problems. *trans. ASME, J. Basic Eng.*, **82D**, 35-45.

[43] Kalman, R. E. and R. S. Bucy, 1961: New results in linear filtering and prediction theory. Trans. ASME, *J. Basic Eng.*, **82** 35-45.

[44] Kamachi, M. and J. J. O'Brien, 1995: Continuous data assimilation of drifting buoy trajectory into an equatorial Pacific Ocean model. *J. Mar. Systems*, **6**, 159-178.

[45] Kitamura, S. and S.Nakagiri, 1977: Identifiability of spatially varying and constant parameters in distributed systems of parabolic type. *SIAM, Journal on Control and Optimization*, **15**, 785-802.

[46] Knox, R. A., 1989: Ocean acoustic tomography: a primer. Ocean Circulation Model: *Combining Data and Dynamics.* D. L. T. Anderson and J. Willebrand, Ed., D. Reidel Publishing Company, Dordrecht, 141-188.

[47] Lardner, R. W., A. H. Al-Rabeh and N. Gunay, 1993: Optimal estimation of parameters for a two-dimensional hydrodynamical model of the Arabian Gulf.

Personal communication. Water Resource and Environment Division, Research Institute, King Fahd University of Petroleum and Minerals, Dhahran, Saudi Arabia.

[48] Le Dimet, F. X., 1982: A general formalism of variational analysis. *CIMMS Report*, Norman, OK 73091, 22, 1-34 pp.

[49] Le Dimet, F. X. and O. Talagrand, 1986: Variational algorithms for analysis and assimilation of meteorological observations: Theoretical aspects. *Tellus*, **38A**, 97-110.

[50] Le Dimet, F. X. and I. M. Navon, 1988: Variational and optimization methods in meteorology: a review. *Tech. Rep. FSU-SCRI-88-144*, Florida State University, Tallahassee, Florida, 83 pp.

[51] Le Dimet, F. X. and H. E. Ngodock, 1994: Sensitivity analysis in variational data assimilation. Submitted to *Tellus*.

[52] Legler, D. M., I. M. Navon and J. J. O'Brien, 1989: Objective analysis and assimilation of meteorological observations: theoretical aspects. *Mon. Wea. Rev.*, **117**, 709-720.

[53] Legler, D. M. and I. M. Navon, 1991: VARIATM–A Fortran code for objective analysis of pseudo-stress with large-scale conjugate-gradient minimization. *Computers and Geosciences*, **17** (1), 1-21.

[54] Lewis, J. M. and J. C. Derber, 1985: The use of adjoint equations to solve a variational adjustment problem with advective constraints. *Tellus*, **37A**, 309-322.

[55] Li, Y., I. M. Navon, W. Y. Yang, X. L. Zou, J. R. Bates, S. Moorthi and R. W. Higgins, 1994: 4-D assimilation experiments with a multilevel semi-Lagrangian semi-implicit GCM. In press *Mon. Wea. Rev..*

[56] Lions J. L., 1971: *Optimal control of systems governed by partial differential equations.* Translated by S. K. Mitter, Springer-Verlag, Berlin-Heidelberg, 404 pp.

[57] Liu, D. C and Jorge Nocedal, 1989: On the limited memory BFGS method for large scale minimization. *Math. Prog.*, **45**, 503-528.

[58] Liu, M. and J. J. O'Brien, 1993: Preferential oceanic eddy generation sites off Pacific north America due to topography *In preparation.*

[59] Lorenc, A. C., 1981: A global three-dimensional multivariate statistical interpolation scheme. *Mon. Wea. Rev.*, **109**, 701-721

[60] Lorenc, A. C., 1988: Optimal nonlinear objective analysis. *Q. J. R. Meteorol. Soc.*, **114**, 205 -240.

[61] Luenberger, David G.,1984: *Linear and nonlinear programming.* 2nd edition, Addison-Wesley Inc., Reading, MA, 491 pp.

[62] Menke, W., 1984: *Geophysical Data Analysis: Discrete Inverse Theory.* Academic Press, London, 260 pp.

[63] S.D. Meyers, M. A. Johnson, M. Liu, J.J O'Brien and J.L. Spiesberger, 1995: Interdecadal variability in a numerical model of the northeast Pacific Ocean. 1970-1989. Submitted to *J. Phys. Oceanogr.*

[64] Mikolajewicz, U and E. Maier-Reimer, 1993: Acoustic detection of greenhouse-induced climate changes in the presence of slow fluctuation of the thermohaline circulation. *J. Phys. Oceanogr.*, **23**, 1099-1109.

[65] Moore, A. M, and B. F. Farrell, 1993: Rapid perturbation growth on spatially and temporally varying oceanic flows determined using adjoint method: application to the gulf stream. *J. Phys. Oceanogr.*, **23**, 1682-1702.

[66] Munk, W. and A. M. G. Forbes, 1989: Global ocean warming: An acoustic measure? *J. Phys. Oceanogr.*, **19**, 1765-1778.

[67] Munk, W. and C. Wunsch, 1979: Ocean acoustic tomography: a scheme for large scale monitoring. *Deep-Sea Res.*, **26A**, 123-161.

[68] Navon, I. M. and R. de Villiers, 1983: Combined penalty multiplier optimization methods to enforce integral invariants conservation. *Mon. Wea. Rev.*, **111**, 1228-1243.

[69] Navon, I. M., 1986: A review of variational and optimization methods in meteorology. Festive Volume of the International Symposium on Variational Methods in Geosciences (Y.K. Sasaki, Ed.), Elsevier Science Pub. Co. Developments in Geo-mathematics, *Vol. 5*, 29-34.

[70] Navon, I. M. and D. M. Legler, 1987: Conjugate gradient methods for large scale minimization in meteorology. *Mon. Wea. Rev.*, **115**, 1479-1502.

[71] Navon, I. M., X. L. Zou, J. Derber and J. Sela, 1992: Variational data assimilation with an adiabatic version of the NMC Spectral Model. *Mon. Wea. Rev.*,**122**, 1433-1446.

[72] Navon, I. M., 1995: Estimation theory and applications. Tokyo Conference.

[73] Neittaanmaki, P. and D. Tiba, 1994: *Optimal control of nonlinear parabolic systems*: Theory, algorithms, and applications. Marcel Dekker, Inc. 399 pp.

[74] Nocedal, J., 1980: Updating quasi-Newton matrices with limited storage. *Mathematics of Computation*, **35**, 773-782.

[75] Ocean Tomography Group, 1982: A demonstration of ocean acoustic tomography.*Nature*, **299**, 121-125.

[76] O'Brien, J. J., Ed., 1986: *Advanced Physical Oceanographic Numerical Modeling*. D. Reidel Publishing Company, Dordrecht. 608 pp.

[77] Panchang, V. G. and J. J. O'Brien, 1989: On the determination of hydraulic model parameters using the strong constraint formulation. in *Modeling Marine Systems*, I. Ed. A. M. Davies. CRC Press, Inc, 5-18 pp.

[78] Pares-Sierra, A. and J. J. O'Brien, 1989: The seasonal and interannual variability of the California Current system: A numerical model. *J. Geophys. Res.*, **94**, 3159-3180.

[79] Powell, M. J. D., 1982: *Nonlinear optimization 1981*. Academic Press, London, 298 pp.

[80] Robertson, A. W, 1992: the investigation of regional climate anomalies with a linear barotropic model and an adjoint technique. *Q. J. R. Meteorol. Soc.*, **118**, 1187-1209.

[81] Sasaki, Y. K., 1955: A functional study of the numerical prediction based on the variational principle. *J. Meteor. Soc. Japan*, **33**, 262-275.

[82] Sasaki, Y. K., 1958: An objective analysis based on the variational method. *J. Meteor. Soc. Japan*, **36**, 77-88.

[83] Sasaki, Y. K., 1969: Proposed inclusion of time-variation terms, observational and theoretical in numerical variational objective analysis. *J. Meteor. Soc. Japan*, **47**, 115-203.

[84] Sasaki, Y. K., 1970: Some basic formalisms in numerical variational analysis. *Mon. Wea. Rev.*, **98**, 857-883.

[85] Sasaki, Y. K., 1970: Numerical variational analysis formulated under the constraints as determined by long-wave equations as a low-pass filter. *Mon. Wea. Rev.*, **98**, 884-898.

[86] Sasaki, Y. K., 1970: Numerical variational analysis with weak constrain and application to the surface analysis as a low-pass filter. *Mon. Wea. Rev.*, **98**, 899-910.

[87] Sasaki, Y. K., Editor, 1986: *Variational methods in geosciences*. Elsevier.

[88] Schlitzer. R., 1993: Determining the mean, large-scale circulation of the atlantic with the adjoint method. *J. Phys. Oceanogr.* **23**, 1935-1952.

[89] Shanno, D. F. and K. H. Phua, 1980: Remark on algorithm 500 – a variable method subroutine for unconstrained nonlinear minimization. *ACMTOMS*, **6**, 618-622.

[90] Shriver, J. F., M. A. Johnson, and J. J. O'Brien, 1991: Analysis of remotely forced oceanic Rossby waves off California. *J. Geophys. Res.*, **96**, 749-757.

[91] Smedstad, O. M. and J. J. O'Brien, 1991: Variational data assimilation and parameter estimation in an equatorial Pacific Ocean model. *Prog. Oceanogr.*, **26**, 1250-1277.

[92] Spiegel, E. and G. Veronis, 1960: On the Boussinesq approximation for a compressible fluid. *Astrophys. J.*, **131**, 442-447.

[93] Spiesberger, J. L., T. G. Birdsall, and K. Metzger, 1983: Acoustic thermometer. Office of Naval Research Contract N00014-82-C-0019.

[94] Spiesberger, J. L. and K. Metzger, 1991: Basin-scale tomography: a new tool for studying weather and climate. *J. Geophys. Res.*, **96**, 4869-4889.

[95] Stensrud, D. J. and J. W. Bao, 1992: Behaviors of variational and nudging assimilation techniques with a chaotic low-order model. *Mon. Wea. Rev.*, **120**, 3016-3028.

[96] Stephens, J. J., 1966: *A variational approach to numerical weather analysis and prediction.* Ph.D. Thesis, Texas A&M University, College-Station, TX, 77863, Rep. 3, 243 pp.

[97] Stephens, J. J., 1968: Variational resolution of wind components. *Mon. Wea. Rev.*, **96** 229-231.

[98] Stephens, J. J., 1970: Variational initialization with the balance equation. *J. Appl. Meteor.*, **9**, 732-739.

[99] Sykes, J. F., J. L. Wilson and R. W. Andrews, 1985: Sensitivity analysis for steady state groundwater flow using adjoint operators. *Water Resources Research*, Vol. **21**, No. 3, 359-371.

[100] Talagrand, O. and P. Courtier, 1987: Variational assimilation of meteorological observations with the adjoint vorticity equation-Part 1. Theory. *Q. J. R. Meteorol. Soc.*, **113**, 1311-1328.

[101] Tarantola, A., 1987: *Inverse problem theory. methods for data fitting and model parameter estimation.* Elsevier, Amsterdam, 613 pp.

[102] Thacker, W. C. and R. B. Long,1988: Fitting dynamics to data. *J. Geophys. Res.*, **93**, 1227-1240.

[103] Thacker, W. C., 1989: The role of Hessian matrix in fitting models to measurements. *J. Geophys. Res.*, **94**, 6177-6196.

[104] Thacker, W. C., 1992: Oceanographic inverse problems. *Physica D*, **60**, 16-37.

[105] Thépaut, J. N. and P. Courtier, 1991: Four-dimensional variational assimilation using the adjoint of a multilevel primitive-equation model. *Q. J. R. Meteorol. Soc.*, **117**, 1225-1254.

[106] Thiebaux, H. J. and M. A. Pedder, 1987: Spatial Objective Analysis. Academic Press, pp 299.

[107] Wang, Z., 1993: *Variational data assimilation with 2-D shallow water equations and 3-d FSU global spectral models.* Ph.D. dissertation, Florida State University, 235 pp.

[108] Wang, Z., I. M. Navon, F. X. Le Dimet and X. Zou, 1992: The second order adjoint analysis: Theory and application. *Meteorol. and Atmos. Phy.*, **50**, 3-20.

[109] Wang, Z., I. M. Navon and X. Zou, 1993: The adjoint truncated Newton algorithm for large-scale unconstrained optimization. *Tech. Rep. FSU-SCRI-92-170,* Florida State University, Tallahassee, Florida, 44 pp.

[110] Wang, Z., I. M. Navon, X. Zou and F. X. Le Dimet, 1995: A truncated Newton optimization algorithm in meteorology applications with analytic Hessian/vector products. Accepted for publication *Computational Optimization and Application.* Vol 4, 241-263.

[111] Wunsch C., 1989: Tracer inverse problems. In *Oceanic Circulation Models: Combining Data and Dynamics*, D. L. T. Anderson and J. Willebrand (Eds.), Kluwer, pp. 1-79.

[112] Yang, W., I. M. Navon and Courtier, P., 1995: A new Hessian Preconditioning method applied to variational data assimilation experiments using adiabatic version of NASA/GEOS-1 GCM. Submitted to *Mon. Wea. Rev.*

[113] Yu, L, 1993: *Determining the surface heat flux distribution over the tropical Pacific ocean by the adjoint method.* Ph.D. dissertation, Florida State University, 167 pp.

[114] Yu, L., and J. J. O'Brien, 1992: On the initial condition in parameter estimation. *J. Phys. Oceanogr.*, **22**, 1361-1364

[115] Yu, L., and J. J. O'Brien, 1991: Variational estimation of the wind stress drag coefficient and the oceanic eddy viscosity profile. *J. Phys. Oceanogr.*, **21**, 709-719.

[116] Zou, X., I. M. Navon and F. X. Le Dimet, 1992: Incomplete observations and control of gravity waves in variational data assimilation. *Tellus*, **44A**, 273-296.

[117] Zou, X., I. M. Navon and F. X. Le Dimet, 1992: An optimal nudging data assimilation scheme using parameter estimation. *Q. J. R. Meteorol. Soc.,* **118**, 1163-1186.

[118] Zou, X., I. M. Navon and J. Sela, 1993: Variational data assimilation with threshold processes using the NMC multilevel primitive-equation model. *Tellus,* **45A**, 370-387.

[119] Zou, X., A. Barcilon, I. M. Navon, J. Whitaker, and D. G. Caccuci, 1993: An adjoint sensitivity study of blocking in a two-layer isentropic model. *Mon. Wea. Rev.*, **121**, 2833-2857.

[120] Zou, X., I. M. Navon, M. Berger, Paul K. H. Phua, T. Schlick and F. X. Le Dimet, 1993: Numerical experience with limited-memory quasi-Newton methods and truncated Newton methods. *SIAM Jour. on Numerical Optimization* **3**, 582-608.

[121] Zou, J. P. and G. Holloway, 1995: Improving steady-state fit of dynamics to data using adjoint equation for gradient preconditioning. *Mon. Wea. Rev.*, **123**, 199-211.

BIOGRAPHICAL SKETCH

MING LIU

EDUCATION

9/91-7/95   Doctor of Philosophy in Physical Oceanography

Florida State University, Tallahassee, FL 32306, USA.

9/86-12/90   Master of Science in Physical Oceanography

University of Rhode Island, Narragansett, RI 02882, USA.

9/79-7/83   Bachelor of Science in Applied Mathematics

Shandong College of Oceanography, Qingdao, P.R. China.

PUBLICATIONS

1   Ming Liu, 1995: Variational assimilation of acoustic tomography. Ph. D. dissertation.

2   S.D. Meyers, M.A. Johnson, M. Liu, J.J O'Brien and J.L. Spiesberger, 1995: Interdecadal variability in a numerical model of the northeast Pacific Ocean. 1970-1989. Submitted to *Journal of Physical Oceanography*.

3   Ming Liu and J. J. O'Brien, 1995: Preferential oceanic eddy generation sites off Pacific north America due to topography. Submitted to *Journal of Physical Oceanography*.

4   Ming Liu and T. Rossby, 1993: Observations of the velocity and vorticity structure of Gulf Stream meanders. *Journal of Physical Oceanography*, **23**, No. 2, 330-345.

5   Ming Liu, 1990: The upper ocean velocity in Gulf Stream meanders – an application of ADCP, M. S. thesis, University of Rhode Island.

6   Hummon, J., T. Rossby, E. Carter, J. Lillibridge III, M. Liu, K. Schultz Tokos, and A. Mariano, 1991: The anatomy of Gulf Stream meanders, Vol. **I, II**, *URI-Tech.- Rep. 91-4*, University of Rhode Island, 286 pp.

PRESENTATIONS

1/95   "Variational assimilation of acoustic tomography" at Colombia University, New York City, NY; at University of Miami, Fl; at GSFC/NASA and NMC/NOAA, MD; GAMOT Ocean Modeling Meeting, Mississippi State Univerisity, MS.

12/94   "Data Assimilation and Its Application on Acoustic Tomography", Tomography Meeting, San Francisco, CA

8/94   "Variational Assimilation of Acoustic Tomography", GAMOT Ocean Modeling Meeting, Pennsylvania State University, State College, PA

2/94   "Preferential oceanic eddy generation sites off Pacific north America due to topography", 94 Ocean Sciences Meeting, San Diego, CA

6/90   "Vorticity and transport in the Gulf Stream meanders", SYNOP workshop, NCAR, Boulder, CO

2/90   "Velocity structure of the Gulf Stream with ADCP", 90 Ocean Sciences Meeting, New Orleans, LA